SERVICE LIFE PREDICTION FOR DIFFERENT TYPES OF CONCRETE USING CHLORIDE DIFFUSION COEFFICIENTS

MD. JIHAN HASAN

MASTER OF SCIENCE IN CIVIL ENGINEERING (STRUCTURAL)
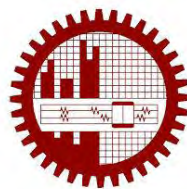
DEPARTMENT OF CIVIL ENGINEEIRG
BANGLADESH UNIVERSITY OF ENGINEERING & TECHNOLOGY, DHAKA

SEPTEMBER, 2018

SERVICE LIFE PREDICTION FOR DIFFERENT TYPES OF CONCRETE USING CHLORIDE DIFFUSION COEFFICIENTS

by

MD. JIHAN HASAN

A thesis submitted to Department of Civil Engineering, Bangladesh University of Engineering and Technology, Dhaka in partial fulfilment of the requirement for the degree of Master of Science in Civil Engineering (Structural)

DEPARTMENT OF CIVIL ENGINEEIRG

BANGLADESH UNIVERSITY OF ENGINEERING & TECHNOLOGY, DHAKA

SEPTEMBER, 2018

The thesis titled "Service Life Prediction for Different Types of Concrete Using Chloride Diffusion Coefficients" submitted by Md. Jihan Hasan, Roll No.:0417042330, Session: April, 2017 has been accepted as satisfactory in partial fulfilment of the requirement for the degree of Master of Science in Civil Engineering (Structural) on September 22, 2018.

BOARD OF EXAMINERS

(1)   Dr. Tanvir Manzur,   Chairman
Professor,   (Supervisor)
Dept. of Civil Engineering, BUET

(2)   Dr. Ahsanul Kabir,   Member
Professor & Head of the Dept.   (Ex-Officio)
Dept. of Civil Engineering, BUET

(3)   Dr. Ishtiaque Ahmed,   Member
Professor,
Dept. of Civil Engineering, BUET

(4)   Dr. Eqramul Hoque,   Member
Professor,
Dept. of Civil Engineering, BUET

(5)   Dr. Major Mohammed Russedul Islam,   Member (External)
Assistant Professor,
Dept. of Civil Engineering, MIST, Mirpur
Cantonment, Dhaka-1216

i

Declaration

It is hereby declared that the studies embodied in this thesis are the results of experiments carried out by the author under the supervision of Dr. Tanvir Manzur, Professor, Department of Civil Engineering, BUET except where specified by reference to other works. Neither the thesis nor any part of it has been submitted elsewhere for any other purposes.

Md. Jihan Hasan
Student ID: 0417042330
Date: 22.09.2018

Dedicated to

My Parents

Acknowledgement

Abstract

Concrete durability has emerged as a significant design consideration for reinforced concrete (RC) structures in recent years. This design consideration includes the measure of the level of serviceability degradation of a RC structure due to various adverse phenomena and the countermeasures adopted to rectify the deteriorating situation throughout its service life. However, the prevalent construction practices of Bangladesh overlook the durability aspects and focus mainly on the strength gaining objectives. One of the major phenomena that affects the durability of RC structures is corrosion induced by the chloride ion ingress which in turn depends on the concrete mix quality. Therefore, it is crucial to observe and quantify the effects of different concrete mixes and design parameters of a RC element on the resistance to chloride ion ingress and thus on its service life. Hence, a study has been carried out to evaluate service life of RC elements, prepared following local construction practices and using commonly available material. The experimental program involved determination of concrete resistance to chloride ion ingress in terms of diffusion coefficient values. Consequently, the service life evaluation of the concrete mixes was based on chloride induced corrosion damage only. The other effects like carbonation were not considered for determination of service life. The observations show high resistance of stone aggregate concrete against chloride intrusion as compared to brick aggregate concrete. Furthermore, usage of PCC as alternative to OPC and inclusion of water reducing admixture improves the permeability of concrete to a great extent. These observed patterns were further validated by electrical resistivity values of the mixes considered and correlations between resistivity and diffusion coefficient values were established. Based on the diffusion coefficient data, the corrosion initiation time of the considered mix variations were evaluated for different exposure classes and concrete cover values. The mixes with high coefficients, such as brick with OPC and mix proportion of 1:2:4, yield least value of corrosion initiation time because of its lower resistance to chloride attack. On the other hand, usage of stone aggregate, PCC and admixture with low w/c ratio seems to yield higher corrosion initiation time. Besides, higher value of concrete cover slows down the chloride ingress to rebar level and thus improves the initiation time. However, in case of OPC, significantly higher cover has been observed to be required when the structure is exposed to severe environment. A similar impact pattern can be observed in the ultimate service life of the various mixes considered. The corrosion initiation time is followed by the time required to severe crack to occur which is summation of the crack initiation and crack propagation time. The attained values of service life of different mixes follow a similar pattern of variation as that of corrosion initiation time with changes in parameters. Based on these observed patterns, it has been found that usage of stone and PCC in concrete mixes for severe environmental exposure would result in satisfactory service life of 75 to 100 years for chloride induced corrosion. Any concrete mix with OPC and with typical cover results in significantly less service life under severe marine environment. However, for normal exposure category, the service life of OPC concrete mixes with the typically used cover do not appear to be adversely affected. The inclusion of water reducing admixture with low w/c ratio also proves to be effective in improvement of service life, especially under severe exposure conditions.

Table of Content

List of Tables

List of Figures

1.1 General

Durability has become one of the prime concerns for civil engineers around the globe as a dominant contributor to the serviceability issues of reinforced concrete structures. One of the alarming causes accountable to the serviceability concerns of reinforced structures is corrosion due to ingress of chloride ions. The corrosion of embedded reinforcements in a RC structure, particularly in coastal areas, accounts to a premature dilapidation of structures before attaining the expected service life. The poor construction practices and negligence towards durability issues prevalent in developing countries further aggravate the aforementioned threats in RC structures. The deterioration of service life due to corrosion is accompanied by a gradual progress of activities including crack initiation, development of cracks followed up by propagation of cracks towards a level when the serviceability of the structure has plunged below the acceptable standard. Despite the astonishing significance of chloride induced corrosion on service life of RC structures, there have been limited studies regarding a proper quantitative evaluation of service lives of structures in the country subjected to the harsh environments. However, in today's construction domain, where the concern towards assurance of durable infrastructures is at its brisk, the necessity of prediction of service life in a multitude of corrosion prone environments is substantial. Hence, a study has been undertaken to evaluate the degree of resistance of concrete structures towards chloride ion permeability and to perform a subsequent service life prediction based on the degree of diffusion vulnerability. Meanwhile, the effect of different parameters of concrete structures (aggregate type, aggregate gradation, mix proportion, water-cement ratio, and concrete cover etc.) on their service lives has also been analyzed in this study. Section 1.2 provides an overview of the existing pattern of serviceability concerns of reinforced concrete structures and the urge of such study for predicting service lives of structures. Section 1.3 reflects the objectives of this study towards determining the effect of different parameters of concrete mixes on predicted ultimate service life of structures in terms of chloride induced corrosion susceptibility. Section 1.4 and Section 1.5 describes the scope of this research endeavor and the organization of this thesis, respectively.

1.2 Background

Concrete durability can be referred to its capability to resist weathering action, chemical attack, abrasion and crack formation while maintaining its desired engineering properties. Depending upon the service property required and surrounding environment it is exposed to, different concrete structures entail different degrees of durability. Concrete, as a structural material, features strong, ductile and durable behaviour when subjected to nonaggressive environmental conditions (Palumbo, 1991). Despite the recent developments and advances in the area of concrete durability, concrete technology has congregated a significant concern in the aspect of serviceability owing to its high permeability.

One of the severe and costly deterioration mechanisms hampering serviceability of reinforced concrete structures is chloride-ion induced corrosion of steel reinforcement (Samson et al., 2003; Lizarazo-Marriga and Claisse, 2009; Alonso et al., 2000). The high permeability of concrete structures, accounts to an intolerable level of chloride ion ingress, particularly in saline environment, leading to corrosion of embedded reinforcements. This can cause disfigurement on a small scale and yet, can lead to structural problems and occasional catastrophes on a large scale. The ultimate effect of this structural depreciation is diverse while reducing the service life of structures significantly and curtailing the performance much below than expected. The usual range of service life considered for reinforced concrete structures averages to around 50-60 years (Rasheeduzzafar et al., 1992) while escalating to around 100 years in some cases (Rumman et al., 2015). However, due to the detrimental conditions, reinforced-concrete structures often need costly and extensive repairs. Moreover, the indirect costs associated with traffic delays and lost productivity in case of corrosion in highway bridges are almost 10 times the direct costs associated with this form of structural damages as obtained in life cycle analysis (Yunovich et al. 2002). The reduction of service life due to corrosion is also an important problem for the nuclear industry (Sindelar et al. 2011). Since 1986, there have been more than 32 reported occurrences of corrosion in steel containments (Zhou et al., 2015).

The significance of this structural deterioration is at its brisk in case of developing countries like Bangladesh, where there has been an infrastructural boom coherent to the persistent recent economic outbursts. However, the construction practices in these regions often lags behind the rapid expansion due to inadequate available techniques and personnel (Afroz et al, 2015). Moreover, the poor quality control prevalent in these regions is also accompanied by ignorance to the durability and serviceability issues associated with reinforced concrete structures.

Consequently, this often results in early degradation and distress in serviceability of structures, particularly in southern coastal areas where the RC structures are exposed to harsh marine environment. However, the number of studies on the effect of chloride ion induced corrosion phenomenon on service lives of structures in Bangladesh is limited. Although the quantitative evaluation of the degree of corrosion for various aspects of concrete mixes by means of half-cell corrosion potential has been performed by the author in previous cases (Baten and Hasan, 2017), there has been seldom any quantitative study correlating the effect of these parameters on the service life reduction of structures. Hence, a research endeavour has been designed to evaluate the effect of different parameters of concrete mixes on corrosion susceptibility of concrete specimens, by means of diffusion coefficients, and subsequent effect on service lives of RC structures.

Corrosion of steel rebar is a very common situation since the iron in steel often tends to form a more stable iron oxide, commonly known as rust under aggressive environment (Smith, 1977). In a well compacted and properly cured concrete, reinforcement steel is unlikely to corrode even if sufficient moisture and oxygen are available. This is owing to a firmly adhering passive oxide film (Elsener, 2002), formed through oxidation of $Fe(OH)_2$ to γ-ferric hydroxide, under a high alkaline condition with pH>12.5 (Rosenberg et al, 1989) which can impede ingress of corrosion inducing agents (Verma et al, 2014). Such ideal conditions are usually difficult to ensure in real life situations and therefore, result in intrusion of corrosion inducing agents which abolishes the passive oxide film at low pH and forms porous oxide layer (Moreno et al, 2004; Mindess et al, 2003). The developed corrosion product produces an expansive force which the surrounding concrete cannot bear due to its lower tensile capacity and consequently results in crack formation and spalling of concrete (Etman, 2012; Pradhan and Bhattacharjee, 2009). According to Tuutti (1980) and Browne (1980), two distinct phases are associated in corrosion mechanism that impose a significant effect on service life of structures, namely, the initiation period (t_a) and the propagation period (t_f). The initiation time usually refers to the instant at which the chloride content at the rebar surface reaches to a critical level adequate to depassivate the protective layer around the embedded rebar (Wang et al., 2010; FIB Bulletin 34, 2006). The research project DuraCrete (1998) portrays a full design approach regarding the modelling of chloride induced corrosion in uncracked concrete which has further revised in the research project DARTS (2004). The crack initiation time has been referred to as the time duration required from the instant of corrosion initiation upto the point when the first crack has developed (Wang et al., 2010) and has been detailed in the model suggested by El Maaddawy

and Soudki (2007). Time to severe cracking corresponds to the summation of the crack initiation time and the crack propagation time.

Based on the high cost associated with the maintenance and repair of damaged structure, it is obligatory to have an estimation of the extent of deterioration that a structure can incur before being considered failed on serviceability grounds. Service life modelling relies on durability parameters such as chloride migration coefficients to determine service life of concrete structures (MottMcdonald, 2018; Wang et al., 2010). Some examples of such models include Duracrete (1998), LNEC E465 (2005) which have implemented several empirical data on the chloride ion penetration in concrete, migration coefficient of concrete, threshold chloride content to initiate corrosion of concrete, concrete cover and influence of blended cements to evaluate the predicted time of corrosion initiation. Development of reliable service models can assist engineers in enhancing the service life of structures through proper selection of different parameters of concrete mixes affecting corrosion susceptibility. The models also have considerable potentials in planning for rehabilitation and maintenance program of reinforced concrete structures. Combined with life cycle analysis of reinforced structures, the estimation of service life of structures can aid in predicting the direct and indirect associated with a prone structure. (Clifton, 1993).A proper development of service life prediction mode possesses an immense potential in developing durability based design standards for reinforced concrete structures.

1.3 Objectives

The overall objective of the research work is to predict service life for different RC structures prepared using common mix proportions of the country. The specific objectives of this research are:

i. To determine chloride diffusion coefficients for commonly used concrete mixes and observe its variation for different concrete mixes.

ii. To study the effect of mix variation (mix ratio, w/c ratio, cement type and aggregate type) on critical chloride level and the time to reach this critical value.

iii. To examine the changes in corrosion initiation time for varying mix proportion, w/c ratio, cement type and aggregate type.

iv. To investigate the effects of cover and diameter of embedded rebar and concrete compressive strength on crack initiation and propagation within concrete.

v. To evaluate probable service life of RC structures based on corrosion initiation, crack initiation and crack propagation time.

1.4 Scope of the Study

Scope of this study was limited to the following:

i. Two durability parameters-chloride diffusion coefficients and electrical resistivity, was measured as a basis to determine the resistance to chloride ingress of concrete.

ii. The diffusion coefficient was measured from the non-steady state migration test, performed as per the code specifications of NT Build 492 (1999) after 45 days of lime water curing.

iii. The tests were performed on laboratory cast cylindrical specimen of concrete, prepared using mainly two types of commonly used and available aggregate variations – stone and brick. In case of brick aggregate specimen, the aggregate gradation was limited to the ¾ inch (19mm) downgraded particle size. However, in case of stone aggregate three different gradation types were selected – 100% -¾ inch downgraded, 60% -¾ inch downgraded + 40% -½ inch downgraded and 100%-½ inch downgraded.

iv. The concrete mixes incorporated single type fine aggregate variation which is in this case 100% of Sylhet sand.

v. Two types of cement which are most widely used in the construction industry of Bangladesh – Ordinary Portland cement and Portland Composite cement were chosen for concrete mix preparations.

vi. The mix ratios considered in this study were limited to 1:1.5:3 in case stone aggregate concrete and both 1:1.5:3 and 1:2:4 in case of brick aggregate concrete.

vii. A wide range of w/c ratio from 0.33 to 0.55 was considered during mix preparations of stone aggregate concrete whereas brick aggregate concrete were prepared for w/c ratio ranging between 0.42 to 0.5.

viii. Water reducing admixture was used in case of stone aggregate concrete with low w/c ratio (0.33-0.38) with the intention of attaining proper workability.

ix. A varying range of admixture dosage (0.8L~1.2L /100Kg of cement) for concrete mixes with w/c ratio 0.35was used to obtain varying range of slump value and a number mixes

were prepared using higher water and cement content to obtain similar slump variation situation for the same w/c ratio without using admixture.

x. The chloride initiation time for different concrete mixes considered were evaluated using their respective diffusion coefficient values using the model suggested by Duracrete (1998) as specified in FIB Bulletin 34 (2006). The critical chloride value required to quantify the initiation time was considered invariant with changes in concrete property as per the Duracrete (1998) model.

xi. In order study the effect of bar diameter variation on crack initiation time and crack propagation time four types bar diameter variation were chosen-12mm, 16mm, 18mm and 20mm. The rebar were considered to be deformed steel bar.

xii. The total service life for all mixes considered were determined from the summation of their respective corrosion initiation, crack initiation and crack propagation time considering four exposure classes, five concrete cover parameter (25mm, 37.5mm, 50mm, 62.5mm and 75mm) and a single bar diameter variation of 16mm.

xiii. The service life evaluation was made based on the assumptions that chloride ingresses into concrete specimen through diffusion and the corrosion is induced by chloride ions only. Effect of carbonation was not considered in this study.

1.5 Organization of the Thesis

The thesis has been presented in seven distinct sections where the key aspects of the entire research are being reflected separately.

Chapter 1 refers to an introductory overview of the basics of the research. This also includes the potential objectives of the research and the implications of the outcomes in the respective domains of Civil Engineering.

A detailed synopsis of the corrosion phenomenon and its impacts on the serviceability of concrete structures has been covered in Chapter 2. The fundamental basics of this process and the related dependents have been clearly described in this section. It also outlines the significance of diffusion coefficients and resistivity in portraying the corrosion susceptibility of concrete. This chapter also reflects the implications of these parameters in predicting the service lives of structures.

Chapter 3 outlines the raw materials used in the entire research program. Abiding by the prevalent construction practices in Bangladesh, both stone and brick aggregates were used in constructing the samples. This chapter also describes the different material properties of the raw materials used in accordance to the specific procedures as per the standard codes.

A detailed outline of the designed experimental setup has been vividly represented in Chapter 4. This chapter describes the sample dimensions and the experimental sampling plan incorporating all the predetermined variants. All the necessary connections and the experimental arrangements for achieving the Rapid Migration Tests (RMT) and the resistivity tests have also been depicted in this chapter. This chapter also elaborates the necessary precautions while arranging the setup and taking measurements, abiding by the standard codes, aided by respective figures and schematic diagrams. A detailed mix design used in the experimental procedures has also been incorporated in this chapter along with the procedures of determining the general parameters (compressive strength, slump, workability etc.) of the concrete mixes.

Chapter 5 highlights the results obtained from all of the measurements during the entire research. This includes the calculated values of the diffusion coefficients from code specified equations based on chloride penetration depths. The obtained coefficients and resistivity values have been presented in graphical forms that make it easier to view any existing patterns with any respective variables. The illustrations also reflects any prevalent correlation the diffusion coefficients and resistivity parameters of the concrete mixes.

Chapter 6 consists of a detailed procedure of measurement of corrosion initiation time based on the diffusion coefficients of different concrete mixes. It also includes the estimation of time of crack initiation and crack propagation time based on compressive strength outcomes and values of different concrete mix parameters. The consequent estimation of the overall service life of different concrete specimens based on a cumulative estimations of the obtained times has also been represented in this chapter.

The possible conclusions that can be inferred from the obtained results are broadly entailed in Chapter 7. Hence, this chapter substantiates the significance of conducting the entire research and its possible implications in achieving the targets for which it was intended and designed. This chapter also highlights any recommendations to ensure a better future reproducibility of the research.

2.1 General

Literature review of previous research works on a particular subject aids in understanding the basic concept related to the topic. Furthermore, it is deemed essential to perform these reviews for the purpose of establishing advanced research objectives and designing an improved and successful experimental methodology. Considering these aspects, brief descriptions on previous research conducted on areas that are relevant to assessment of corrosion damage and service life prediction are presented in this chapter. The chapter summarizes some relevant concept such as corrosion, corrosion potential, chloride permeability and chloride induced corrosion, Service life models, diffusion coefficients etc.

2.2 Durability of Concrete Structures

According to Cooper (1994) and Ervine (2010), durability means "the ability of a product to perform its required function over a lengthy period under normal conditions of use without excessive expenditure on maintenance or repair". Criteria to measure durability may be service life, operational cycles, costs etc. Concrete durability can be referred to its capability to resist weathering action, chemical attack, abrasion and crack formation while maintaining its desired engineering properties. Depending upon the service property required and surrounding environment it is exposed to, different concrete entail different degrees of durability. According to American Concrete Institute the capability of concrete to resist weathering action, chemical attack and abrasion while maintaining its desired engineering properties is durability. Different concretes require different degrees of durability depending on the exposure environment and properties desired. For example, concrete exposed to tidal seawater will have different requirements than indoor concrete. The production of building materials depletes natural resources and can produce air and water pollution. Factors affecting durability of concrete can be:

- Cement content
- Compaction
- Curing

- Cover
- Permeability

The reasons of concrete deteriorations were classified in to three categories by Li (2011) and they are mechanical, physical and chemical. One of the main chemical reasons of concrete durability degradation is corrosion of reinforcement within.

2.3 Corrosion of Reinforced Concrete

Concrete is alkaline in nature with a pore solution pH of 12–13 that naturally passivizes embedded reinforcing bars (rebar). The passivation of steel is broken down by the presence of chloride ions or a reduction in alkalinity of concrete caused by carbonation (Almusallam et al., 1996). While chloride-induced corrosion is generally more pernicious and more expensive to repair, carbonation-induced corrosion of rebar may affect a wider range of RC structures at a larger scale. Both mechanisms of corrosion may result in significant reduction in the load-bearing capacity of the structure by reducing the cross sectional area of steel rebar, degrading steel elongation capacity and causing severe cracking to concrete. Corrosion types can be defined as general corrosion, localized corrosion, and pitting.

Corrosion of reinforcing steel and other embedded metals is the leading cause of deterioration in concrete. When steel corrodes, the resulting rust occupies a greater volume than the steel. This expansion creates tensile stresses in the concrete, which can eventually cause cracking, delamination, and spalling (Figure 2.1). Steel corrodes because it is not a naturally occurring material. Rather, iron ore is smelted and refined to produce steel. The production steps that transform iron ore into steel add energy to the metal. Steel, like most metals except gold and platinum, is thermodynamically unstable under normal atmospheric conditions and will release energy and revert back to its natural state—iron oxide, or rust. This process is called corrosion. For corrosion to occur, four elements must be present: There must be at least two metals (or two locations on a single metal) at different energy levels, an electrolyte, and a metallic connection.

In reinforced concrete, the rebar may have many separate areas at different energy levels. Concrete acts as the electrolyte, and the metallic connection is provided by wire ties, chair supports, or the rebar itself.
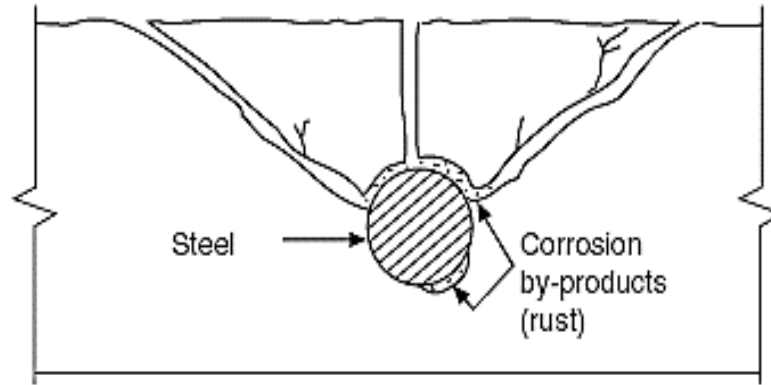
Figure 2.1: The expansion of corroding steel creates tensile stresses in the concrete, which can cause cracking, delamination, and spalling.

Corrosion is an electrochemical process involving the flow of charges (electrons and ions). Figure 2.2 shows a corroding steel bar embedded in concrete. At active sites on the bar, called anodes, iron atoms lose electrons and move into the surrounding concrete as ferrous ions.
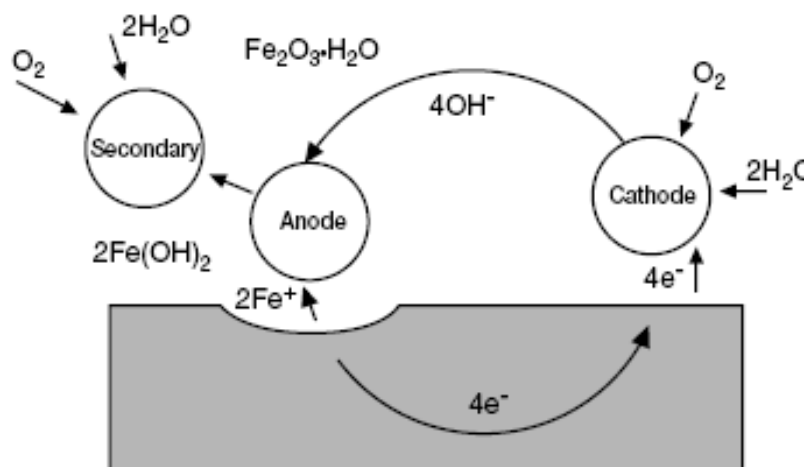
Figure 2.2: When reinforcing steel corrodes, electrons flow through the bar and ions flow through the concrete

This process is called a half-cell oxidation reaction, or the anodic reaction, and is represented as:

$2Fe \rightarrow 2Fe^{2+} + 4e^-$
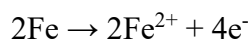
The electrons remain in the bar and flow to sites called cathodes, where they combine with water and oxygen in the concrete. The reaction at the cathode is called a reduction reaction. A common reduction reaction is:

$$2H_2O + O_2 + 4e^- \rightarrow 4OH^-$$
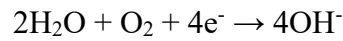
To maintain electrical neutrality, the ferrous ions migrate through the concrete pore water to these cathodic sites where they combine to form iron hydroxides, or rust:

$$2Fe^{2+} + 4OH^- \rightarrow 2\ Fe(OH)_2$$
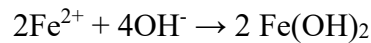
This initial precipitated hydroxide tends to react further with oxygen to form higher oxides. The increases in volume as the reaction products react further with dissolved oxygen leads to internal stress within the concrete that may be sufficient to cause cracking and spalling of the concrete cover.

2.4 Mechanical Degradation in RC Structures Due to Corrosion

Corrosion, induced by both carbonation and chloride, causes degradation in the mechanical properties of RC structures. While the corrosion damage was found not to significantly impact the ductility of RC members (Stanish, 1997; Altoubat et al., 2016), it results in concrete spalling and cracking, reduction in rebar properties, and interfacial bond loss, which are discussed in detail in the following:

2.4.1 Cracking and Spalling of Concrete

Cracking of concrete occurs because corrosion products (oxides) have a higher volume than basic metal. These cracks reduce the load-bearing capacity, shorten the service life, and increase the rate of ingress of aggressive elements (Alonso et al. 1998). Cracking in the compression region had no effect on the flexural behavior of the corroded beams; however, significant changes to the service behavior were observed due to degradations in the tensile zone, namely, loss of bending stiffness and asymmetrical behavior (due to asymmetrical distribution of the cracking pattern). The phenomenon of cracking and spalling due to corrosion of reinforcement is illustrated in the following Figure 2.3:
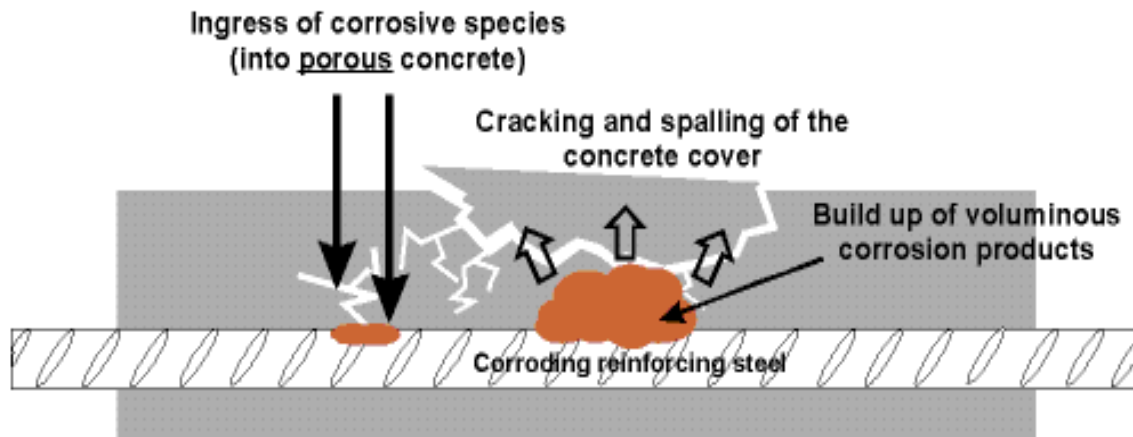
Figure 2.3: Cracking and spalling of concrete induced by reinforcement corrosion (Zhou et al., 2015)

It has been noted that (Zhou et al., 2015) rebar area reduction and bond strength loss are coupled. However, the global flexural behavior of the beams seems to be greatly affected when the rebar area reduction and bond strength loss are coupled because of the local increase in the steel stresses due to the reduction in the steel cross section and due to no contribution of concrete to tensile resistance. Use of groups of rebar (bundled rebar) to replace a rebar of larger diameter (by conserving total area) is not recommended if there is a chance of corrosion because bundled rebar generate higher stresses over the concrete due to the larger perimeter, thus a larger surface susceptible to corrosion.

2.4.2 Loss of Rebar Property

Rebar area loss is a direct result of corrosion and it is usually quantified in terms of mass loss. It was found that the yield and ultimate stress and strain at ultimate stress of rebar deteriorated, and the yield plateau became narrower or even disappeared with the development of corrosion (Webster, 2000). These reductions could lead to a premature fracture of the rebar before yielding is observed.

The inelastic constitutive behavior of corroded rebar was investigated by Kashani et al. (2013). It was found that a corrosion level above 15% mass loss significantly affected the ductility and plastic deformation of rebar in tension. Additionally, corrosion changed the buckling mechanism of the rebar in compression from classical inelastic buckling to inelastic buckling with unsymmetrical plastic hinges or inelastic buckling with multiple intermediate plastic hinges. The distribution of the corrosion pits along the length of corroded rebar was found to

be the most important parameter affecting the stress-strain response in both tension and compression. The reduction in reinforcement size, and hence reinforcement mass, is represented in the following Figure 2.4:

Figure 2.4: Loss of rebar diameter and mass due to corrosion

2.4.3 Loss in Interfacial Bond Strength

Corrosion significantly influences the interface bond behavior between concrete and rebar. It was found that the bond strength first increases and then decreases with increasing level of corrosion (Al-Sulaimani et al. 1990; Bajaj 2012). Al-Sulaimani et al. (1990) observed a sharp jump in the value of the free-end slip with the opening of a longitudinal crack indicating a sudden loss of rebar confinement in the rebar pullout tests. It was found by Almusallam et al. (1996) that in the pre-cracking stage (0–4% corrosion, measured as gravimetric loss in weight of rebar) the ultimate bond stress increases, whereas the slip at the ultimate bond stress decreases with increasing corrosion level. The degradation of bond results from the crushing of the concrete near the lugs of the rebar. When reinforcement corrosion is in the range of 4–6%, the bond failure occurs suddenly at a very low free-end slip. At this level of corrosion, a large slip was noted as the ultimate failure of the bond, occurring due to the splitting of the specimens. Beyond 6% rebar corrosion, the bond failure resulted from a continuous slippage of the rebar. The ultimate bond stress initially increased with an increase in the degree of corrosion until the corrosion reached a maximum value of 4%, after which there was a sharp reduction in the ultimate bond stress up to 6% rebar corrosion. Beyond the 6% rebar corrosion level, the ultimate bond stress did not vary much, even up to 80% corrosion. Bajaj (2012)

confirmed that the bond strength increases with an increase in the corrosion level up to a critical percentage (2% for plain concrete, 3.5% for concrete with polypropylene fiber as an additive, and 4.5% for concrete with basalt fiber as an additive) and then decreases.
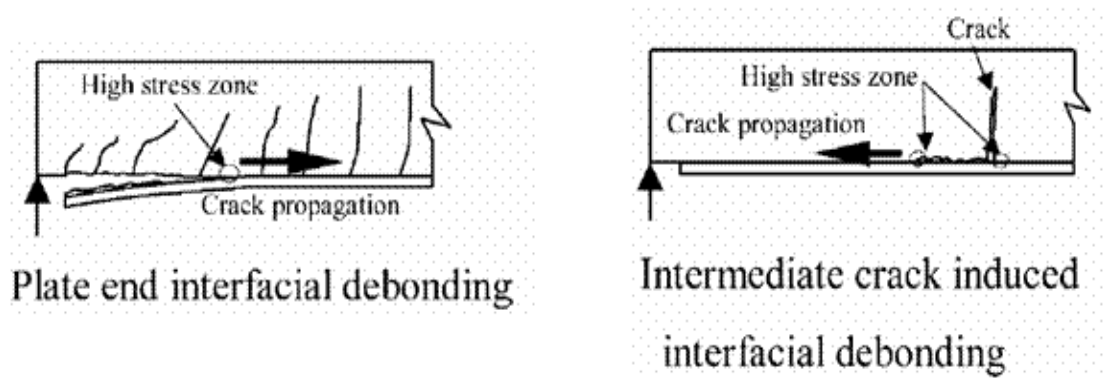
Figure 2.5: Effect on interfacial bonding of reinforcement bars due to corrosion

Corrosion had no substantial influence on the bond strength (Zhou et al., 2015) of deformed rebar in confined concrete. For smooth rebar in unconfined concrete when the corrosion level was low, bond strength increased as corrosion level increased, with the ultimate bond strength being as much as 2.5 times that of non-corroded rebar; while the bond strength decreased rapidly at higher corrosion levels. For smooth rebar in confined concrete, bond strength increased as corrosion level increased, up to a relatively high degree of corrosion

2.5 Service Life of RC Structures Subjected to Corrosion

Most of the published service life models associated with corrosion of reinforcing steel in concrete have followed a simplified model that was first introduced by Tuutti (1982), wherein the mechanism of corrosion is considered as a two-stage process (Martin-Perez, 1999):

a. Initiation Period: during which the steel remains in a passive state. The onset of corrosion corresponds to reinforcement depassivation due to either carbonation of the concrete cover or accumulation of chloride ions at the reinforcing steel layer.

b. Propagation Period: during which the structure deteriorates as a result of loss of reinforcing steel cross-sectional area and accumulation of corrosion products around the bar surface. This phase lasts until an unacceptable degree of corrosion damage has occurred.

2.6 Corrosion Initiation in Concrete

The highly alkaline de-passivating layer around the reinforcements is disrupted as the pH of the surrounding media is being lowered (Miyazato and Otsuki, 2010). This exposes the reinforcement to elements of corrosion that induces the slow degradation of the steel rebars and finally leading to the structural failure of the reinforced concrete structures. The corrosion phenomenon can be classified on the basis of the elements that induce the de-passivation of the highly alkaline protective layer into:

a) Corrosion induced by carbonation.
b) Corrosion induced by chlorination.

2.6.1 Corrosion Induced by Carbonation

Fresh concrete is highly alkaline because of hydration products such as calcium hydroxide. This environment protects the steel reinforcement bars from corrosion. The high alkalinity of cement paste is primarily due to the high calcium hydroxide content (lime) the product of cement hydration. Calcium silicate compounds (CS) contained in Portland cement, when mixed with water react and form hydrated calcium silicates (CSH) and Calcium Hydroxide (lime). Lime and other oxides of alkali earth elements, such Sodium (Na) and Potassium (K) create the highly alkaline environment of fresh or "young" concrete (Gemite, 2005). However, carbon dioxide and moisture at the surface of the concrete can react with these products to produce calcium carbonate.

Carbonation of concrete has started to attract more attention recently as a result of climate change (Yoon et al., 2007). This type of corrosion occurs naturally in RC structures at a rather slow yet invasive rate. The process of carbonation of concrete is presented in the following form by Leber and Blakey (1956):

$$Ca\,(OH)_2 \rightarrow Ca^{2+}\,(aq) + 2OH^-\,(aq) \tag{1}$$

$$Ca^{2+}\,(aq) + 2OH^-\,(aq) + CO_2 \rightarrow CaCO3 + H_2 \tag{2}$$

$$3CaO \cdot 2SiO_2 \cdot 3H_2O + 3CO_2 \rightarrow 3CaCO_3 \cdot 2SiO_2 \cdot 3H_2O. \tag{3}$$

$$3CaO \cdot SiO_2 + \mu H_2O + 3CO_2 \rightarrow 3CaCO_3 + SiO_2 \cdot \mu H_2O \tag{4}$$

$$3CaO \cdot SiO_2 + \mu H_2O + 3CO_2 \rightarrow 2CaCO_3 + SiO_2 \cdot \mu H_2O \tag{5}$$

Carbonation of concrete is the chemical reaction of portlandite, Ca (OH)$_2$, in the cement matrix with carbon dioxide (CO$_2$) gas leading to calcite (CaCO$_3$), as shown in the aforementioned equations. Carbonation takes place as a result of the interaction of carbon dioxide with the calcium hydroxide in concrete. The carbon dioxide gas dissolves in water to form carbonic acid (H$_2$CO$_3$), which reacts with calcium hydroxide and precipitates mainly as calcium carbonate (CaCO$_3$), which lines the pores. Depletion of hydroxyl ions (OH^{-1}) lowers the pore water pH from above 12.5 to below 9.0 where the passive layer becomes unstable, allowing general corrosion to occur if sufficient oxygen and water are present in the vicinity of the rebar (Heiyantuduwa et al. 2006; Zhou et al., 2015).

The following Figure 2.6 shows the pH scale and the associated three areas, according to steel corrosion occurrence, which shows the effect of carbonation on inducing corrosion in embedded reinforcement:
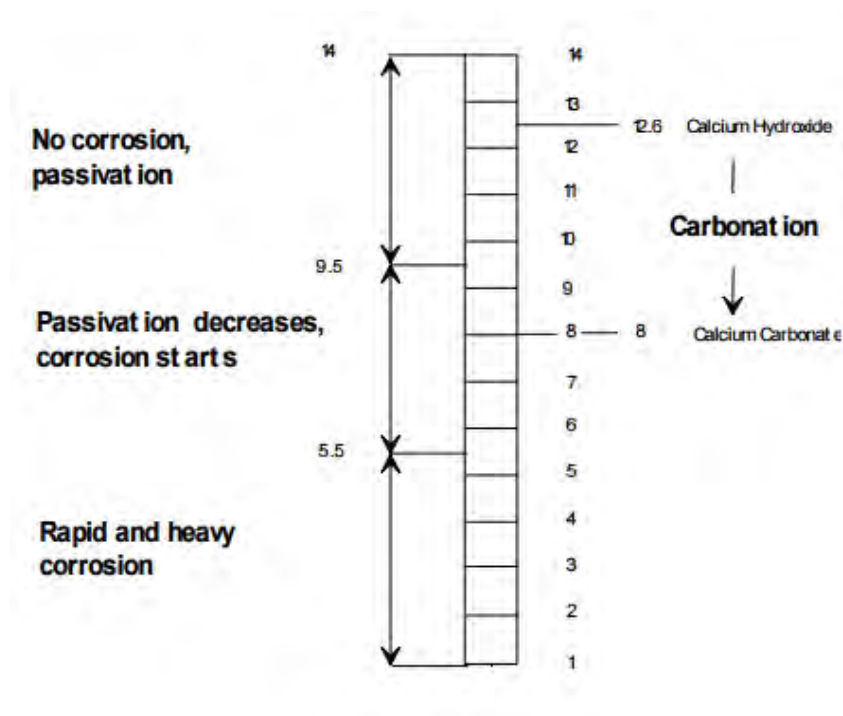
Figure 2.6: pH Scale

The statistical analysis by Das et al. (2012) showed that the carbonation potential of concrete decreases with an increase in the compressive strength of the concrete. The results indicated that using a decrease in the charge passed through concrete as a measure of carbonation could lead to misleading results in evaluation of the service life of concrete structures. It was also observed that a low water-to-cement ratio concrete with portland pozzolana cement has higher

resistance to carbonation and rapid chloride ion permeability compared with ordinary portland cement. (Zhou et al., 2015)

A variety of interrelated factors influence the carbonation depth in concrete, including cover thickness, carbonation resistivity, effective CO_2 diffusion coefficient, binding capacity for CO_2, curing condition, age, cement type, cement composition, calcium oxide (CaO) content in cement, surface concentration of carbon dioxide, time of wetness, ambient temperature, and relative humidity. Environmental conditions, such as sheltered versus exposed and underground versus atmospheric, also have an important impact on concrete carbonation process (Zhou et al., 2015).

2.6.2 Corrosion Induced by Chlorination

The highly alkaline passive protective layer can also be breached due to lowering of pH that results from a high ingress of Chloride ions. Chloride ions destroy the film and, in the presence of water and oxygen, corrosion occurs. Chloride ions were described by Verback (1975) as "a specific and unique destroyer" (Neville, 1995). Chloride-induced corrosion is a concern for RC structures that are located in a marine environment or subjected to deicing chemicals. The process of chloride-induced corrosion is described by the following reactions:

$$Fe^{2+} + 2Cl^- \rightarrow FeCl_2 \quad\quad\quad\quad (6)$$

$$Fe \rightarrow Fe^{2+} + 2e^- \quad\quad\quad\quad (7)$$

$$O_2 + 2H_2O + 4e^- \rightarrow 4OH^- \quad\quad\quad\quad (8)$$

$$Fe2^+ + 2OH^- \rightarrow Fe\,(OH)_2 \quad\quad\quad\quad (9)$$

$$2Fe(OH)_2 + \tfrac{1}{2}\,O_2 + H_2O \rightarrow 2Fe(OH)_3 \rightarrow Fe_2O_3 \cdot 3H_2O. \quad\quad (10)$$
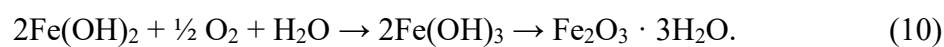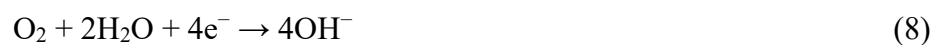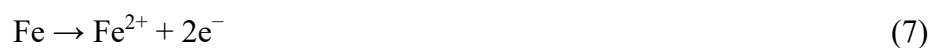
The products given by the reactions in (7)~(9) combine together to produce a stable film that passivizes the rebar. The stability of this film depends on the oxygen (O_2) availability and the pH of the interstitial solution at the interface between rebar and concrete (Montemor et al. 2003). The reactions shown in (6) and (10), the passivized film can be disrupted and the corrosion process is initiated at the presence of sufficient chloride ions (Cl^-), oxygen (O_2), and water (Zhou et al., 2015). However, provided that the surface of the reinforcing steel is free from loose rust, the presence of rust at the time the steel is embedded in concrete does not influence corrosion (Neville, 1995).

In the case of chloride intrusion, chloride ions have only a small influence on the pH of the pore solution. However, they can destroy the passive layer when the chloride content in the pore solution exceeds a critical value (chloride threshold). However it has proved rather difficult to establish a threshold chloride concentration below which there is no risk of corrosion as it depends on numerous factors including (Bertolini et al, 1996):

1- pH of concrete i.e. the concentration of hydroxyl ions in the pore solution. Corrosion can take place only above a critical ratio of chloride and hydroxyl ions. 0.6 can be referred to as the critical ratio. The hydroxyl ion concentration in the pore solution mainly depends on the type of cement and additives.

2- Presence of voids at the steel/concrete interface which depends on the workability of fresh concrete and the compacting procedure. Voids may weaken the layer of cement hydration products deposited at the steel/ concrete interface and thus favor local acidification which is required for corrosion to continue.

As discussed previously, similar to carbonation depth, a variety of material and environmental related factors influence the chloride concentration around reinforcement, including cover thickness, chloride resistivity, and chloride binding capacity of concrete, water-binder ratio of the concrete mixture, curing conditions, age of concrete, cement type, cement composition, surface chloride concentration, ambient temperature, and relative humidity. The geographic environment of the structure, such as inland zone, coastal region, or marine, also has a significant impact (Zhou et al., 2015).

2.7 Chloride Ion Ingress and Threshold Chloride Value

Chloride ions are present in seawater, groundwater, and deicing salts. The RC elements exposed to these sources can have the chlorides migrating from external environments into structural concrete. While the chloride ingress into concrete will not necessarily compromise the concrete properties, the chlorides can seriously destroy the electrochemical stability of the embedded reinforcement steel bars, inducing electrochemical corrosion. Actually, the deterioration of RC elements by chloride ingress has become one of the major concerns for durability of concrete structures. In addition, harsh winters and thus heavy use of deicing salts present a risk of chloride induced corrosion also inland. Those elements of structures exposed to cyclic wetting and drying have proven to be the most vulnerable to corrosion damage.

Those elements of structure which are exposed to cyclic wetting and drying have proven to be the most vulnerable to corrosion damage. In concretes exposed to wet/dry cycles, it is believed that chloride will enter the concrete initially by absorption and produce a reservoir of chloride ions a relatively short distance from the concrete surface from which diffusion can occur. This reservoir will be topped up by periodic absorption events. If the concrete dries out to a greater depth, subsequent wettings carry the chlorides deeper into the concrete (Hong & Hooton, 1999). Therefore, diffusion of chloride ions through pore liquid and absorption, whereby bulk solution containing chloride ions is sucked into concrete pores, are the two main transport mechanisms involved in chloride ingress in concrete. Diffusion occurs due to the chloride concentration gradient and is a relatively slow process and continuous, once some chloride has entered the concrete, provided the pore liquid does not completely evaporate.

Penetration of chloride in concrete exposed to wet/dry environments occurs by diffusion and absorption. Diffusion is a relatively slow and quite well understood process. However, absorption is a relatively rapid transport mechanism and there is a lack of understanding of the role of this mechanism on chloride ingress as studies on chloride penetration in concrete exposed to wet/dry cycles ignore the effect of this mechanism on chloride ingress. In addition, chloride penetration prediction models are mostly based on Fick's laws of diffusion, ignoring the effect of absorption on chloride ingress.

Chlorides can also be deposited on the surface of concrete in the form of airborne very fine droplets of sea water (raised from the sea by turbulence and carried by the wind) or of airborne dust which subsequently becomes wetted by dew. Although being a rare occurrence, chloride ions can ingress into concrete from conflagration of organic materials containing chlorides.

According to Tutti's model (1980), service life of reinforced concrete structures consists of two stages: 1) time to corrosion initiation (T_i) and 2) time of corrosion propagation (T_p) as shown in Figure 2.7. During T_i, diffusivity determines the time it takes for the chloride ions to reach at the rebar surface to initiate corrosion. Once, corrosion has initiated during T_p, resistivity and moisture content controls the available amount of water and/or O_2 which affects the corrosion rate (Presuel-Moreno, 2013).
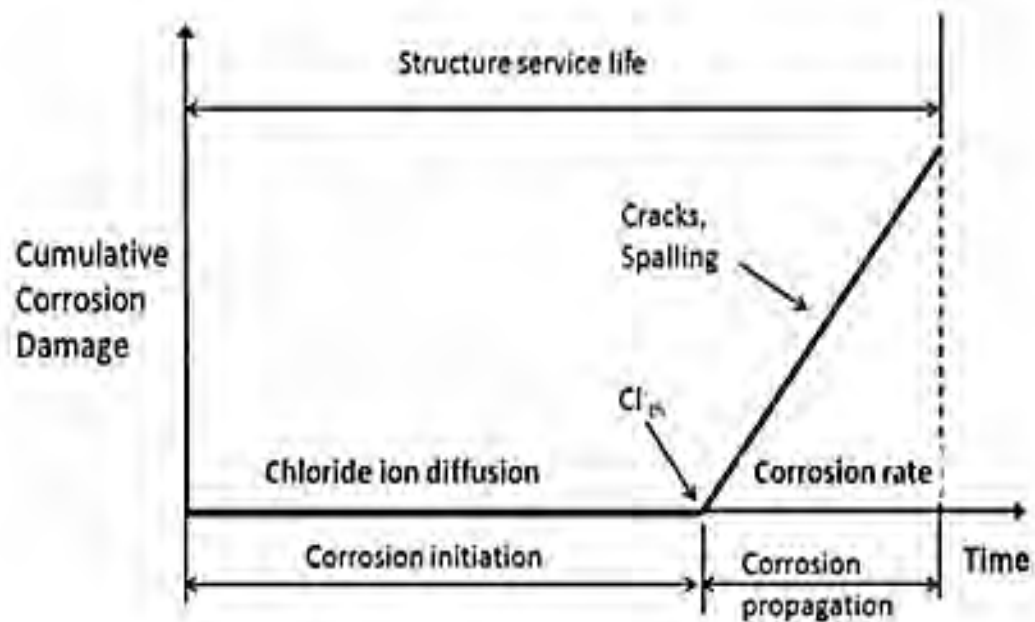
Figure 2.7: Schematic Illustration of the initiation and propagation stage in reinforced concrete (Presuel-Moreno, 2013)

Chloride induced reinforcement corrosion is widely accepted to be the most frequent mechanism causing premature degradation of reinforced concrete structures. Condition assessment and service life prediction is based on comparing the chloride content in the concrete at the steel depth – either measured in the field or computed by means of theoretical modelling – with the chloride content that is believed to be tolerable before corrosion starts. The latter is commonly referred to as critical chloride content or chloride threshold value. Owing to the considerable statistical variation of the parameters involved in service life considerations, probabilistic approaches are preferentially used since these aim at taking into account the uncertainties inherent to all parameters – at least on a theoretical basis (Angst, 2011).

A review on the critical chloride content has shown that this parameter scatters significantly in the literature and that the published data does not offer a basis to improve service life predictions. The reported values are not consistent, particularly regarding non-traditional binder types. This was, at least partly, explained by the wide variety of experimental methods and the pronounced effect of certain experimental parameters. It was concluded that there is a strong need for a generally accepted, practice-related test setup for the critical chloride content (Angst, 2011).

The threshold depends on an array of factors, many of which are still imperfectly understood. Moreover, the distribution of chlorides within the hardened cement paste is not uniform, as found in chloride profiles in actual structures. While, under any given circumstances, there may be a threshold chloride content for corrosion to be initiated, its progress depends on the resistivity of the hardened cement paste, which varies with humidity and on the availability of oxygen, which is affected by the immersion of concrete (Neville, 1995).

2.8 Chloride Diffusion

Provided that concrete is in a saturated state, chloride ions enter the concrete by ionic diffusion due to the existing concentration gradient between the exposed surface and the pore solution of the cement matrix (diffusion driving force). This process is mathematically described by Fick's 1st law of diffusion, according to which the rate of transfer of diffusing chlorides through a plane perpendicular to the direction of diffusion is proportional to the concentration gradient.

For the simple case where chloride binding is neglected Fick's 2nd law of diffusion, which in one-dimension is given by:

$$\frac{\partial C_{fc}}{\partial t} = \frac{\partial}{\partial x}\left(D_c \cdot \frac{\partial C_{fc}}{\partial x}\right) \text{---} (2.1)$$

2.9 Chloride Diffusion Coefficient

Experimental evidence has shown that the rate of chloride diffusion in concrete, usually defined by the chloride diffusion coefficient Dc, depends on internal material parameters such as temperature, porosity, cement type, cation type associated with Cl− ions, moisture content, and curing conditions.

2.10   Chloride Diffusion Coefficient Measurement

The calculation of the time to steel reinforcement depassivation is becoming an urgent need due to the engineering demand of prediction of the service life of concrete structures. The initiation time of steel corrosion is composed of two steps: the time taken by the aggressive (chlorides in present case) to reach the reinforcement in a certain amount and the depassivation stage itself. Due to the uncertainties on the chloride threshold value, it is simply assumed to be a fixed value, and the majority of calculation methods of the initiation period are based in characterising the chloride diffusion coefficient, D. However, it is often neglected the fact that

at least two kind of coefficients can be obtained: one of them from steady-state experiments using the so-called diffusion or migration cell (Ollivier et al., 1997), and the other from nonstationary experiments (Alonso et al., 2000). These coefficients are called in literature reversibly as effective, Deff, or apparent, Dapp, respectively. In order to avoid any confusion, in the present literature they will be named as Ds =stationary value of diffusion coefficient and Dns =nonstationary value.

Ds encounters only the ionic transport while Dns also takes into account binding of chlorides with cement phases. This difference concerning the consideration of chloride binding is very important when trying to use these values for prediction of the initiation period of rebar corrosion and when comparing different testing methods. Thus, any calculation of Ds from resistivity values leads to a value which cannot be directly used to predict service life or duration of the initiation period because it does not take into account chloride reaction. On the opposite, Dns obtained from experiments that explicitly do take into account binding, might be used for predicting purposes, only provided that other factors such as concrete ageing or chloride external concentration had been taken into account.

In order to determine the Ds, the device used is the classical two compartments cell, where one of the chambers is filled with a chloride solution while the other contains a free chloride solution. Periodically along the experiment, Cl- concentration in both compartments has to be monitored in order to determine the flux of chlorides throughout the specimen. Two disadvantages are mainly attributed to this type of test: The first one is the fact that it is time consuming since getting the values of diffusion coefficients takes a very long time. On the other hand, since it is necessary to take liquid samples for the chlorides to be analysed, this kind of test is laborious as well as expensive. The first disadvantage has been overcome by the application of an electrical field that accelerates the movement of chloride ions in the way that the time of testing can be shortened from several months to a few days. However, the second inconvenience has not been solved yet. In order to make this test less expensive and time consuming in steady-state conditions, in this paper, chloride concentration in the anolyte during a migration test has been correlated to the conductivity of the anodic solution.

NT BUILD 355 (1997) – Steady state migration test was developed in the beginning of the 1980's and revised in the middle of the 1990's. This is a steady state migration test. The test procedure according to the revised version involves: – Coating the curved surface of the specimen with, for example, epoxy resin; – Saturating the specimen by immersion in saturated

lime water until the weight changes by not more than 0.1% per day; – Mounting the specimen between the migration cells and filling the upstream cell with 5% NaCl solution and the downstream cell with 0.3 N NaOH solution; – Applying an external potential of 12 V DC between the two cells and measuring the actual potential drop across the specimen by using two reference electrodes; – Qualitatively checking the downstream cell for chlorides by using slightly acidified 1 M AgNO3 solution until a white precipitate can be observed; – Quantitatively determining chloride contents in the downstream cell at least once a day over at least seven days by using a standardised method; – Performing linear regression analysis of at least five points of the linear part of the c-t (concentration-time) curve until a linear correlation coefficient of at least 0.9 is obtained; – Calculating the chloride flux J from the slope of the linear regression.

Non-Steady State Migration Test standard NT BUILD 492 (1999) test procedure involves: – vacuum-saturating the specimen by using a procedure similar to AASHTO; – mounting the specimen in the migration cell (a silicon rubber tube) and filling the downstream cell with 0.3 N NaOH solution (anolyte); – p lacing the cell in the upstream reservoir (a plastic box) containing 10% NaCl solution (catholyte); – Applying an external potential of 30 V DC between the two electrodes and adjusting the potential (in a range of 10 to 60 V DC) according to the initial current so as to keep the power consumption of the specimen in most cases less than 2 W; – After a specified test duration (in most cases, 24 hours), axially splitting the specimen into two pieces; – Spraying 0.1 M AgNO3 solution on one of the freshly split surfaces of the specimen and, when the white silver chloride precipitation on the split surface is clearly visible (about 15 minutes), measuring the penetration depths across the split surface at intervals of 10 mm to obtain 5 to 7 valid depth readings; – Optionally, determining the surface chloride content in the other piece of the specimen by using a standardised method. The chloride diffusion coefficient, D_{rcm}, is then calculated using the following equation 2.2:

$$D_{rcm} = \frac{RTL}{zF\Delta E} \cdot \frac{x_d - \alpha\sqrt{x_d}}{t} \text{---}(2.2)$$

Where, xd is the average value of the penetration depths, t is the test duration, T is average temperature, z is ion valence, L is thickness of specimen, E is the absolute value of voltage applied and α can be taken as a laboratory constant

$$\alpha = [\frac{2}{\sqrt{a}} \cdot erf^{-1}\left(1 - \frac{2c_d}{c_0}\right) \text{---}(2.3)$$

2.11 Service Life Models

Various service life models like Duracrete (1998; 2015), LNEC E465 (2005) etc. were developed to predict the time of corrosion initiation using large amounts of empirical data on the chloride ion penetration in concrete, migration coefficient of concrete, threshold chloride content to initiate corrosion of concrete, concrete cover and influence of blended cements on corrosion of reinforcement. There are also some well-established methods for example-Mullard and Stewart (2009) to forecast the time for severe damage.

Considering these cover range and exposure categories, service life for different types of concrete were predicted in terms of corrosion initiation time, crack initiation time and crack propagation time. The relevant equations and affecting parameters with their corresponding values are given below:

In case of chloride induced corrosion, the corrosion of the rebar is initiated after the chloride content at rebar layer reaches a critical value required to depassivate the protective layer around the embedded rebar. The time required for the accumulation of the chloride ions inside the concrete to the critical level is defined as the corrosion initiation time (Wang et al., 2010; FIB Bulletin 34, 2006).

A full design approach for the modelling of chloride induced corrosion in uncracked concrete has been developed within the research project DuraCrete (1998) and slightly revised in the research project DARTS (2004). It is based on the limit-state equation 2.4, in which the critical chloride concentration C_{crit} is compared to the actual chloride concentration at the depth of the reinforcing steel at a time t C(x = a, t).

$$Ccrit = Co + (Cs, \Delta x - Co)\left[1 - \text{erf}\left(\frac{x - \Delta x}{2.\sqrt{Ke.Kt.(\frac{to}{t})^{a}.Drcm(to).t}}\right)\right] \text{-------------------------(2.4)}$$

Time to crack initiation is usually considered to be the time from corrosion initiation by depassivation of protective layer to the initiation of first crack (Wang et al., 2010). For this research venture, crack initiation time was calculated based on the model suggested by El Maaddawy and Soudki (2007).

$$t_{1st} = \left[\frac{7117.5(D + 2\delta)(1 + \nu + \Psi)}{365.icorr.Eef}\right]\left[\frac{2CFt}{D} + \frac{2\delta.Eef}{(D + 2\delta)(1 + \nu + \Psi)}\right] \text{--------------------------(2.5)}$$

Concrete tensile strength, F_t (MPa) = 0.53 (compressive strength)$^{1/2}$ ----------------------(2.6)

Effective Elastic Modulus, E_{ef}=(Elastic Modulus/1+Φ_{cr})----------------------------------(2.7)

Crack propagation time was calculated based on the model developed by Mullerd and Stewart (2009):

$$T_{sev}= Kr.\left[\frac{w-0.05}{Kc.ME.r(crack)}\right]\left[\frac{0.0114}{icorr.20}\right]$$--(2.8)

Cover Cracking Parameter, Ψ = (C/D.F_t)--(2.9)

Cracking rate, r (crack) (mm/hr) = $0.0008. e^{-1.7\Psi}$--(2.10)

$$Kr = 0.95 \left[\exp\left(\frac{-0.3 icorr.exp}{icorr,20}\right) - \frac{icorr,exp}{2500.icorr,20} + 0.3\right]$$------------------------------------(2.11)

2.12   Effect of Concrete Cover

If the measurement of absolute potentials or relative potential mapping indicates that active corrosion is likely to be occurring, then a measurement of concrete resistivity may be used to assess the probable maximum rate of corrosion and hence the potential severity of the problem. The electrical resistance of the concrete regulates the ionic flow current between anodic and cathodic areas of the reinforcement. The higher the concrete resistivity, the lower the current flowing between anodic and cathodic areas, and therefore the lower the corrosion rate.

The electrical resistivity or conductivity of concrete indicates the resistance of concrete against the flow of electrical current. (Presuel-Moreno, 2013). Concrete resistivity is the electrical resistance of concrete, which controls the ease with which ions migrate through the concrete between the anionic and cathodic sites. Electrical resistance, in turn, depends on the microstructure of the paste and the moisture content of the concrete. Thus, measurement of resistivity of the concrete is useful in conjunction with a half-cell potential survey.

It is well known that concrete resistivity affects the corrosion rate of steel reinforcement. In concrete with low resistivity potential distribution on surface represents potential at steel concrete interface. For better results interpretation of potential readings can be done in accordance with resistivity (Verma et al., 2014)

With respect to half-cell potential tests, as the resistivity of concrete increases, the detection of corrosion becomes harder (Elsener 2002). Figure 2.8 illustrates the effect of concrete resistivity on the potential distribution at the steel/concrete interface and on the surface of concrete.
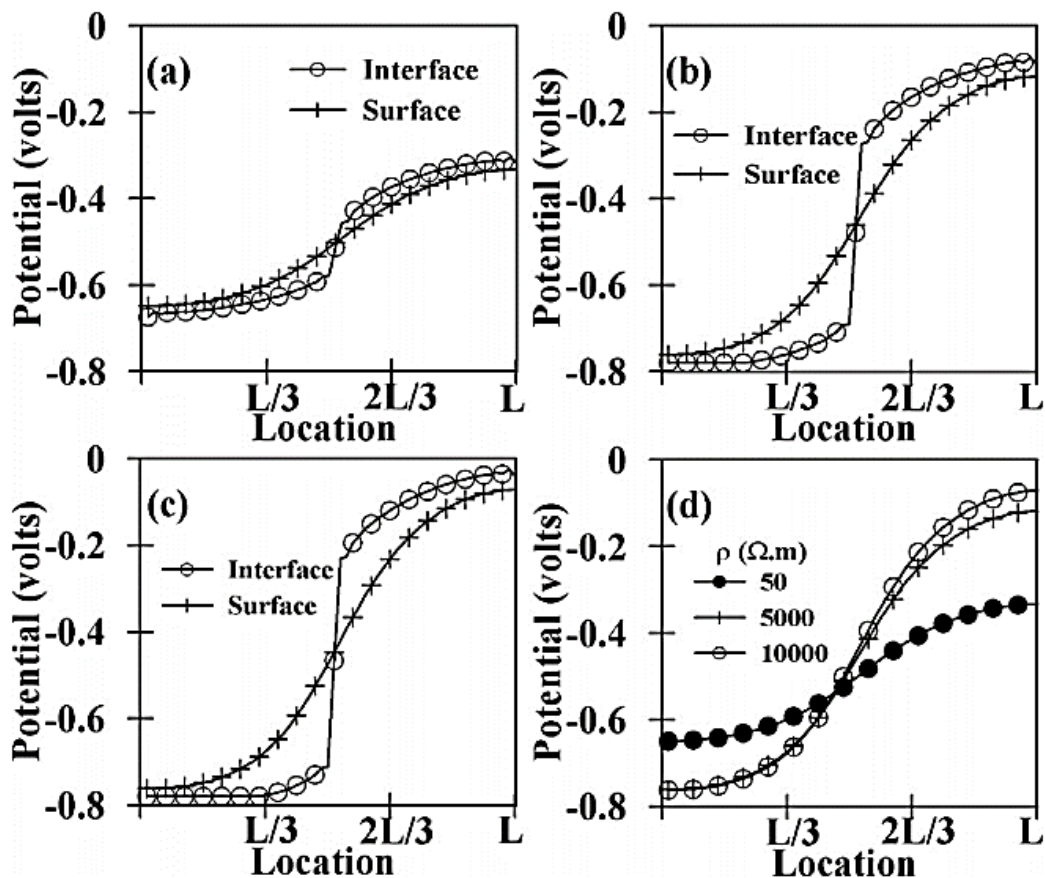
Figure 2.8: Potential distributions at the surface of concrete and at the steel/concrete interface

As it can be seen in the plots, the increase of resistivity shifts the potential of the anodic sites to more negative values and the potential of cathodic sites to more positive values. In low resistivity concrete, as illustrated in Figure 2.8.a, the potential distribution along the surface of the concrete closely represents the potential distribution at the interface of steel/concrete. As the resistivity of concrete increases, as shown in Figure 2.8.b and Figure 2.8.c the potential distribution at concrete surface tends to part noticeably from that of the steel/concrete interface. This difference is the more significant at sections close to the transition zone between the anode and the cathode.

Figure 2.8.d illustrates the potential distribution on the surface of the concrete to demonstrate that the shift in potential distribution curves with increasing concrete resistivity is not the same

for anodic and cathodic surfaces: increase in resistivity affects the cathodic sites more than the anodic sites. At high resistivities, the change in resistivity does not affect the potential distribution of the anodic sites; however, the cathodic potentials continue increasing to more positive values, signifying smaller cathodic polarization. Figure 2.8.d also suggests that with increasing resistivity, the potential difference between the anodic and cathodic sites increases. Thermodynamically, the tendency to corrode increases with larger potential difference; however, the corrosion rate is inversely related to concrete resistivity by Ohm's law. This implies that while carrying out half-cell measurements, potential readings should be interpreted in accordance with the resistivity of the system. Otherwise, the results can be misleading. For the same corrosion rate, one can measure different potentials at the surface of concrete, corresponding to different resistivities, and thus have more than one probability for the same state of corrosion.

Thickness of concrete cover positively affects both the protection of the steel against corrosion and the safe transmission of bond forces. On the other hand it affects Crack control inversely, larger concrete cover causes larger crack width, and as a result it yields reduction in the protection of the steel against corrosion (Farhat, 2010).

The depth of the concrete cover plays an important role in protection of reinforcement in concrete. The cover thickness has a remarkable effect on rebar corrosion due to penetration of chloride or carbonation (Zhou et al., 2015). Neville (1995) show that the effect of increase in cover thickness was less important for the severe corrosion level. This is probably that the thinner cover thickness, seawater solution is easy to arrive at embedded steel compared to other thicker cover thickness, so, its steel bar may be easily corroded due to chloride ion, which is resulted in shifting corrosion potential to negative direction, decreasing polarization resistance (Lee, 2013).

The effect of cover thickness on the potential mapping and corrosion rates in simulated half-cell tests was investigated by varying the cover thickness between 20 and 140 mm. Fig. 3 illustrates the potential distribution at the interface of steel/concrete and on the concrete surface for d= 20 mm and d= 140 mm.
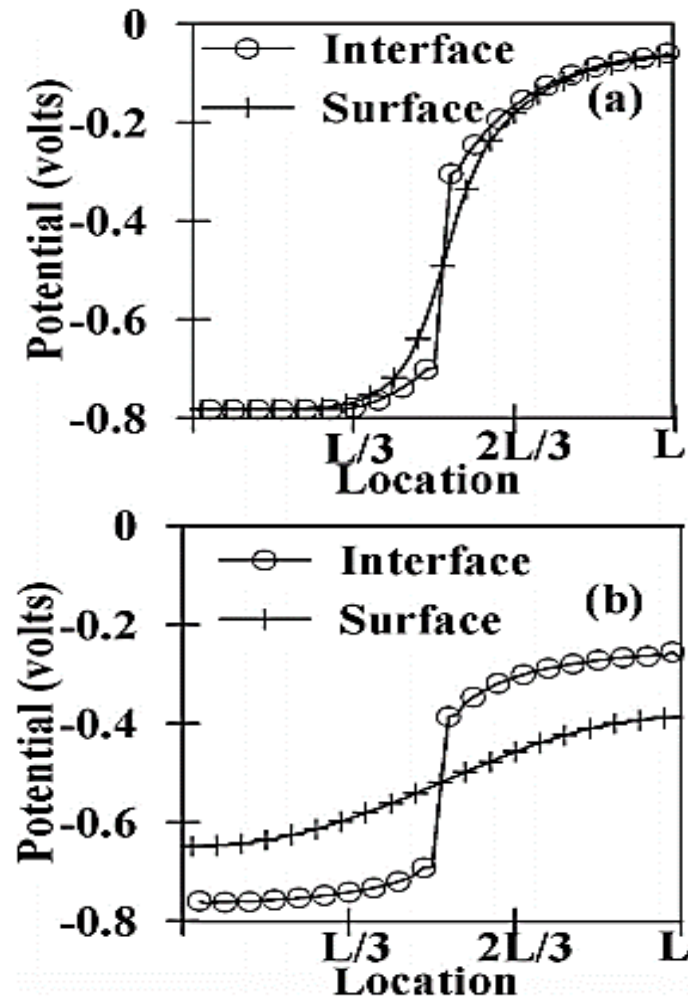
Figure 2.9: Potential distributions at the surface of concrete and at the steel/concrete interface: a) d= 20 mm; b) d= 140 mm

If the cover thickness is small e.g., 20 mm, as shown in Figure 2.9.a the potential distribution on the surface of concrete is almost the same as potential distribution at the interface of steel/concrete. However, such a small cover thickness is not practical, and usually thicker covers are used in practice. As cover thickness increases, the potential of the surface differs from that of interface significantly, as illustrated in Figure 2.9.b. At these large values of cover thickness, the potential distribution on the concrete surface does not provide accurate information about the potential distribution at the steel/concrete interface. As a result of these numerical observations, in half-cell potential measurements, one should also consider the effect of cover thickness on the potential distribution.

2.13 Effect of Oxygen Availibility:

Oxygen is one of the prime ingredients for inducing corrosion in embedded reinforcements subjected to corrosion prone environments. Hence oxygen concentration is also a key consideration while evaluating the half-cell corrosion potential of the reinforced concrete samples. An increase in oxygen concentration usually results in an increase in corrosion rate and subsequent corrosion potential, except in critical conditions. Figure 2.10 illustrates three cases of oxygen availability to the rebar (0.002, 0.02, and 0.2 A/m2) corresponding to low, moderate and high oxygen contents, respectively.
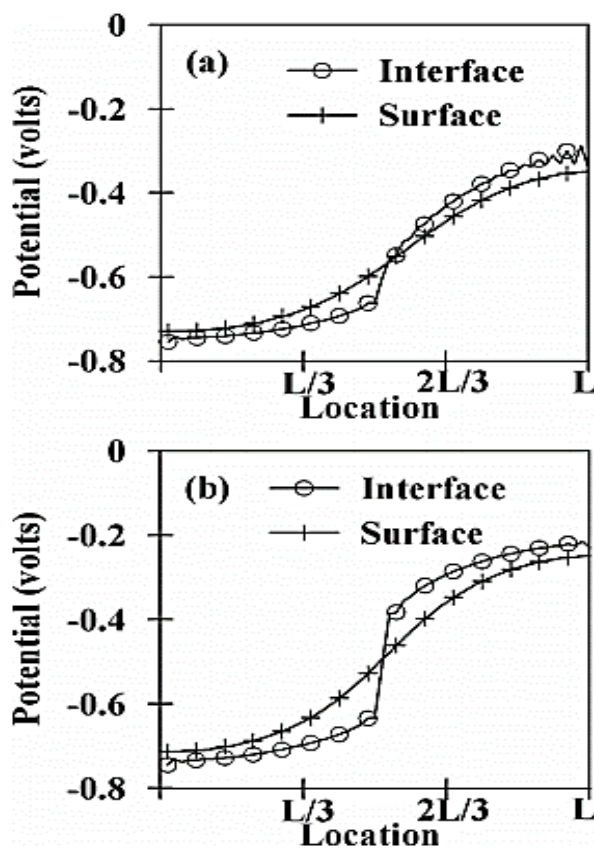
Figure 2.10: Potential distributions at the surface of concrete and at the steel/concrete interface: (a) low oxygen content (0.002 A/m2); (b) moderate (b) 0.02 A/m2 and high (0.2 A/m2) oxygen contents.

It should be noted that the plots for iL = 0.02 A/m2 and iL= 0.2 A/m2 were exactly the same as they were plotted in Figure 2.10. As it can be observed in Figure 2.10, as oxygen availability increases from 0.002 to 0.2 A/m^2, the potential of cathodic sites slightly approaches to more positive values, and potential distribution of the anodic sites is almost not affected with oxygen availability. These observations suggest that oxygen availability is not a significant factor affecting half-cell potential measurements if the concrete is not completely deprived of oxygen.

2.14 Concrete Resistivity Measurement

The electrical resistivity of concrete is an important parameter concerning determination of intensity of the initiated corrosion process. After a bar loses its passivity, the corrosion rate depends on the availability of oxygen for the cathodic reaction. It also depends on the electrical resistance of the concrete, which controls the ease with which ions migrate through the concrete between anodic and cathodic sites.

Electrical resistance, in turn, depends on the microstructure of the paste and the moisture content of the concrete. Thus, measurement of the resistivity of the concrete is useful in conjunction with a half-cell potential survey. The resistivity is numerically equal to the electrical resistance of a unit cube of a material and has units of resistance (in ohms) times length (Millard et al. 1989).

2.14.1 Principles

Two different techniques, namely AC and DC measurements are used for determination of electrical resistivity. In these measurements both surface and embedded probes are applied. Applying a constant electric field between the two embedded electrodes and measuring the resulting current as a voltage drop over a small resistance accomplish the DC measurements.

The AC measurements can be conducted both by means of two and four-pin methods. The most common surface mounted probe is known as the Wenner array. An alternating current is passed between the outer electrodes and the potential between the inner electrodes is measured. There is no ASTM test method for measuring the in-place resistivity of concrete. One technique that has been used successfully is shown in Figure 2.11 (Millard et al. 1989). This is based on the classical four-electrode system described by Wenner (1915).

The four, equally spaced electrodes are electrically connected to the concrete surface by using, for example, a conducting cream (Millard et al. 1990). The outer electrodes are connected to a source of alternating current, and the inner electrodes are connected to a voltmeter. The apparent resistivity ρ is given by the following expression (Wenner 1915; Millard et al. 1990):

$\rho = 2\,\pi\,s\,R$; where, resistance, R = V/I

Where, s = probe spacing; V = measured voltage between the inner electrodes; and I = current between the outer electrodes.

The method was developed under the assumptions (Wenner, 1915) that:

a) Material is semi-infinite and homogeneous
b) Applied electrodes are well bound to the concrete and the spacing between them is adjusted to the dimensions of test sample (Song and Saraswathy, 2007)
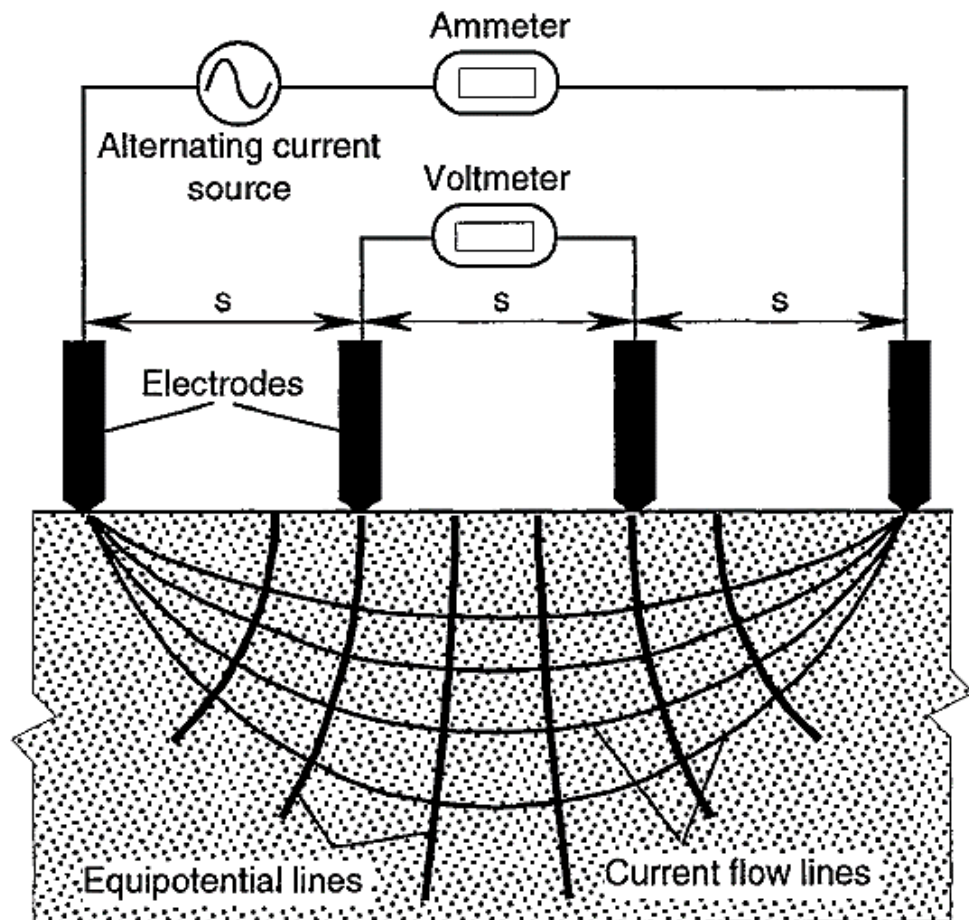
Figure 2.11: Four-Probe Resistivity Test (Carino, 1999)

The electrical resistivity of concrete is being increasingly used indirectly to evaluate concrete characteristics such as the chloride ion diffusivity, the degree of concrete saturation and its aggressiveness (Song and Saraswathy, 2007). This parameter may also provide useful information regarding the rebar corrosion performance in concrete (Millard et al., 1989). As indicated by Feliu and coworkers (1989), the electrical resistivity of concrete is inversely proportional to the corrosion rate. When the influence of concrete resistivity on the rebar corrosion rate is evident, there are important differences (Table 2.1) in the threshold values of ρ proposed by several authors in order to evaluate the degree of rebar corrosion.

Table 2.1: Comparison of Relationships between Concrete Resistivity and Corrosion Risk (Carino, 1999)

Resistivity (kΩ.cm)	Corrosion Risk
(a) Feliu´ et al., 1996	
100-200	Negligible Corrosion
50-100	Low Corrosion Rate
10-50	Moderate to High Corrosion Rate
<10	Resistivity does not control corrosion rate, Very High
b) Bungey 1989 (nonsaturated concrete)	
>20	Low
10-20	Low/Moderate
5-10	High
<5	Very High

3.1 General

One of the significant modern discoveries in the sector of civil engineering is concrete, especially reinforced concrete. Concrete can be defined to be a composite material, containing mixture of coarse and fine aggregates, bonded together with a cementitious material-fluid cement, asphalt cement etc. that gets hardened over time. Reinforced concrete is that composite version of concrete in which reinforcement (usually steel) is embedded passively before the concrete sets. When aggregates are mixed together with dry Portland cement and water, cement reacts chemically with the water and other ingredients to form a fluid mass. This mass eventually hardened, binding all materials together into a stone-like durable material (Li, 2011). Sometimes to enhance concrete slump value water reducing admixture is used. This chapter includes the information regarding the materials used for preparing test samples. Section 3.2 presents details about type of cement used, its composition and its noteworthy properties. Latter sections 3.3 and 3.4 provides descriptions of type and properties of coarse and fine aggregates used respectively. Last section (3.5) includes some basic information related to the chemical admixture used to increase workability of concrete cylinders with low w/c ratio.

3.2 Cement

Cement is a binding material. It can be referred to as a substance used during construction that forms a fluid mass when mixed with water. This fluid mass eventually sets and hardens binding together other materials. The most important use of cement in the production of mortar in masonry and of concrete. Cement is usually manufactured from calcareous material (compounds of calcium and magnesium) and in many respects possesses hydraulic properties far better than hydraulic lime. There are numerous types of cement available, classified based on their components, properties and the purposes they serve. For this research, two types of cement – Ordinary Portland Cement (OPC) and Portland Composite Cement (PCC) were used to prepare sample.

In this study, the Portland cement used conforms to BDS EN 197-1:2003, CEM I/ 52.5N and ASTM C-150, Type – I cement specifications. It contains 95-100% of clinker and 0-5% of

Gypsum. The composite cement used is of type that conforms to BDS EN 197-1:2003, CEM II/ B-M (S-V-L) 52.5N and ASTM C-595. It contains 80-94% clinker, 6-20% slag-fly ash-limestone and 0-5% Gypsum.

3.3 Coarse Aggregates

Construction aggregate, or simply "aggregate", is a broad category of granular material used in construction, including sand, gravel, crushed stone, slag, recycled concrete and geosynthetic aggregates. As an essential element, aggregates both coarse and fine usually occupy about 60-85 percent of concrete's total volume.

Coarse aggregates are particles greater than 4.75mm, but generally range between 9.5mm to 37.5mm in diameter. They can either be from Primary, Secondary or Recycled sources. Primary aggregates are either Land- or Marine-Won. Gravel is a coarse marine-won aggregate; land-won coarse aggregates include gravel and crushed rock, stone etc. Secondary aggregates are materials which are the by-products of extractive operations and are derived from a very wide range of materials (for example brick). Recycled concrete is a viable source of aggregate and can be classified into Recycled Aggregate (RA) or Recycled Concrete Aggregate (RCA).

For this particular project work locally available stone (Figure 3.1.a and b) and brick chips (Figure 3.1.c) were chosen as coarse aggregates. To ensure homogeneity, all the samples were prepared using both stone and brick aggregates, collected from a single source. The size of the aggregates was ensured to be **19 mm (¾ inch) downgraded, in case of brick aggregate**. For this study, three different combinations of stone (coarse) aggregates (SCA) were considered – SCA mix type 1[100% of ¾ inch (19mm) downgraded], SCA mix type 2 [60% of ¾ inch (19mm) downgraded + 40% of ½ inch (12.5mm) downgraded] and SCA mix type 3 [100% of ½ inch (12.5mm) downgraded].

<div align="center">(a)</div>

<div align="center">(b)</div>

<div align="center">(c)</div>

<div align="center">Figure 3.1: a) and b) Stone Chips and b) Brick Chips</div>

3.3.1   Properties of Stone Aggregates

3.3.1.1 Sieve Analysis and Fineness Modulus

Sieve analysis or sometimes known as Gradation test can be defined to be a process to divide a batch of aggregates into several fraction each having a specified particle size limit. This is done to assess the particle size distribution (known as gradation) within a lot of granular material and its fineness modulus.

For the purpose of determining gradation and fineness modulus, stone aggregate batch used was subjected to sieve analysis as per the specification of ASTM C136 (2006). The gradation curve of stone aggregates is shown in following Figure 3.2:
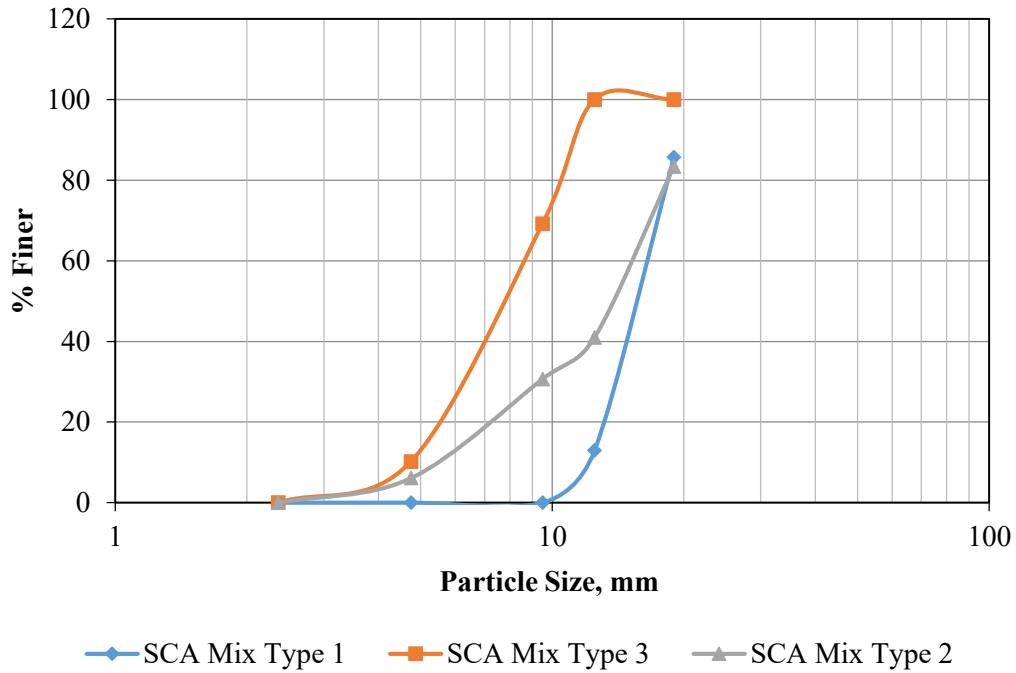
Figure 3.2: Gradation Curve for Stone Aggregate Sample

3.3.1.2 Specific Gravity and Absorption Capacity

Presence of permeable and impermeable pores within aggregate bulk necessitates the computation of specific gravity. The value of specific gravity aids in converting the weight into solid volume and therefore, in computing theoretical yield of concrete per unit volume. Specific gravity is the ratio of the density of a substance to the density of a reference substance; equivalently, it is the ratio of the mass of a substance to the mass of a reference substance for the same given volume. The reference substance is nearly always water at its densest (4°C) for liquids; for gases it is air at room temperature (21°C). Among different types of specific gravity values, engineers are mostly concerned with the values of bulk specific gravity. Bulk specific gravity refers to the ratio of oven-dry weight of aggregate to their bulk volume (volume of water displaced by the aggregate in a saturated, surface dry condition).

Absorption capacity can be defined to be aggregates capacity to absorb moisture. The value is typically represented as the percentage of the dry weight of aggregates. This values can be used to compute the change in weight of aggregate owing to the water absorbed in the pore spaces within particles.

The test method followed in determining specific gravity and absorption capacity of the coarse aggregates, conforms to the specification and requirements of ASTM C127 (2007). The obtained values were as follows:

Bulk Specific Gravity (Oven-Dry basis) = 2.63

Bulk Specific Gravity (SSD basis) = 2.64

Apparent Specific Gravity = 2.66

Absorption Capacity = 0.5 %

3.3.1.3 Unit Weight

Unit weight, also known as Specific weight, is the weight per unit volume of a material. The symbol used to designate unit weight is gamma (γ). These values are vital to calculate percentage of voids within aggregate. Moreover, this represents a mass-volume relation and can easily be used for conversion. Apart from these, unit weight aids in calculating amount of materials during mix design and thereby, selecting proportions for concrete mix. If the total volume of concrete to be cast is known, the weight of concrete bulk can easily be determined. Then, weight of each material can be computed based on their proportion in total concrete mass.

The unit weight value of stone chips were determined as per the test specification of ASTM C29 (2009) and it was calculated to be 1470 kg/m^3.

3.3.2 Properties of Brick Aggregates

3.3.2.1 Sieve Analysis and Fineness Modulus

Like stone aggregates, the gradation of the brick chips sample were also done as per ASTM C136 (2006) and fineness modulus for this sample were calculated. Figure 3.3 shows the gradation curve for brick aggregates:
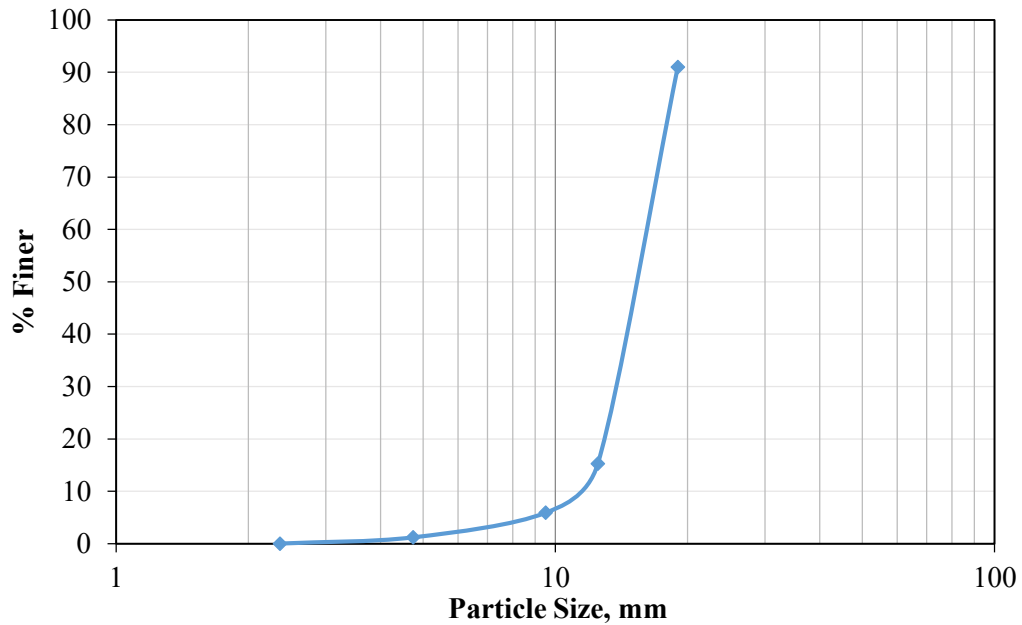
Figure 3.3: Gradation Curve for Brick Aggregate Sample

3.3.2.2 Specific Gravity and Absorption Capacity

The test method followed in determining specific gravity and absorption capacity of the brick chips sample, conforms to the specification and requirements of ASTM C127 (2007).

The obtained values of specific gravity and absorption capacity were as follows:

Bulk Specific Gravity (Oven-Dry basis) = 1.71

Bulk Specific Gravity (SSD basis) = 2.05

Apparent Specific Gravity = 2.58

Absorption Capacity = 19%

The high absorption capacity indicates brick to be a highly porous and permeable material than others.

3.3.2.3 Unit Weight

The unit weight value of brick chips were determined as per the test specification of ASTM C29 (2009) and it was calculated to be 1050 kg/m^3.

3.4 Fine Aggregates

Fine aggregate are basically sands won from the land or the marine environment or riverbed. In Bangladesh, fine aggregates (sand) are available in two forms – Local Sand or White sand and Sylhet Sand or Red sand. For this research, 100% of sylhet sand (Figure 3.4) mix was used.

Figure 3.4: Sylhet Sand

3.4.1   Properties of Sylhet Sand

3.4.1.1 Sieve Analysis and Fineness Modulus

As stated earlier the gradation or particle size distribution and fineness modulus calculation of both coarse and fine aggregates are performed in accordance with the specification ASTM C136 (2006). Figure 3.5 shows particle size distribution of the fine aggregates used for this study.
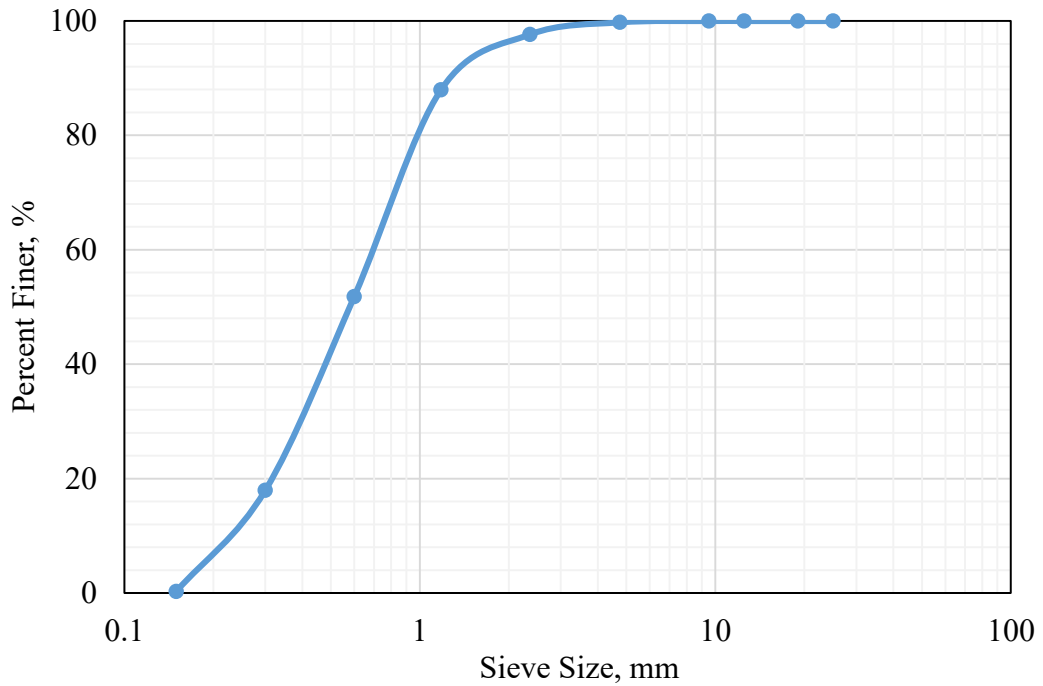
Figure 3.5: Gradation Curve for Sylhet Sand Sample

3.4.1.2 Specific Gravity and Absorption Capacity

The test method followed in determining specific gravity and absorption capacity of the fine aggregates, conforms to the specification and requirements of ASTM C128 (2009). The obtained values were as follows:

Bulk Specific Gravity (Oven-Dry basis) = 2.54

Bulk Specific Gravity (SSD basis) = 2.58

Apparent Specific Gravity = 2.61

Absorption Capacity = 1.1%

3.4.1.3 Unit Weight

The unit weight value of Sylhet sand were determined as per the test specification of ASTM C29 (2009) and it was calculated to be 1490 kg/m^3.

3.5 Chemical Admixture: Water Reducing Admixture

Water-reducing admixtures are added to concrete during mixing to increase workability, enhace durability, offer easier placement, control the setting time, and produce easier finishing with less segregation of the ingredients. This is accomplished while allowing a reduction of the total water content and providing the ability to control the time of setting to meet changing climatic conditions. The strength improvement resulting from water-reducing admixtures is primarily due to reducing the water cementitious materials ratio. The water reducing admixture, used in this study is Master Glenium ACE 30 II.

Master Glenium ACE 30 is an admixture based on second-generation polycarboxylic ether polymer with high early strength gains. Master Glenium ACE 30 is free of chloride & low alkali and is compatible with all types of cements. The specifiactions are given below:

a) Structure of Material: second-generation polycarboxylic ether polymer;

b) Aspect: Reddish Brown Liquid

c) Type: ASTM C494 (2008) Types F;

d) Relative Density: 1.07 ± 0.02 at 25°C;

e) pH: > 6

f) Chloride ion content : $< 0.2\%$

g) Dosage: Optimum dosage of MasterGlenium ACE 30 should be determined in trial mixes. As a guide, a dosage range of 500 ml to 1000ml per 100kg of cementitious material was normally recommended by the manufacturer. For this study, dosage of 0.8L, 1.0L and 1.2L per 100Kg of cement were chosen.

h) Applicability: As per the manufacturer, MasterGlenium ACE 30 is suitable for making precast concrete elements at all workability's including Rheoplastic or Super workable concrete having fluid consistence, no segregation, a low water binder ratio and, consequently high early and long term strengths.

MasterGlenium ACE 30 is a ready-to-use liquid which is dispensed into the concrete together with the mixing water. The plasticising effect and water reduction are higher if the admixture is added to the damp concrete after 50 to 70% of the mixing water has been added. Thorough mixing is essential and a minimum mixing cycle, after the addition of MasterGlenium ACE 30, of 60 seconds for forced action mixers is needed.

4.1 General

A comprehensive methodology helps to understand the fundamentals of the required experiments and their relevant procedures to be followed. This thorough understanding eventually aids in perceiving the rationale behind the selection of specific experimental schemes in order to meet the definite research objectives. The forthcoming sections of this chapter will discuss in details the approaches to be followed for the purpose of completing this particular research venture. Section 4.2 includes a general idea about separate testing segments of the whole experimental program. The following section 4.3, describes details of design of test specimen-number, variables considered, dimension and special features. Section 4.4 presents information regarding casting and curing process prior to the tests. Latter sections (4.5, 4.6, 4.7 and 4.8) describe the detail procedures of each testing to be carried out to determine necessary parameters for this task.

4.2 Experimental Program

For this individual research task, a number of testing such as slump test, compressive strength test and durability tests on concrete specimen of various mixes were performed. These tests, especially durability tests, were conducted with the intention of determining the resistance of different concrete mixes to chloride penetration which were later utilized to calculate service life of RC structures prepared using such concrete mixes. Therefore, this whole experimental program can be subdivided into two major segments:

Segment 1: Concrete Property Tests-

    a) Slump test on fresh concrete

    b) Compressive Strength of 28 days old hardened concrete

Segment 2: Durability Tests on Concrete Specimen-

    a) Rapid Migration Test

    b) Concrete Resistivity Measurement

4.3 Mix Design and Sample Preparation

A total no of 58 concrete mixes were considered in this study. The mixes were chosen to represent the commonly used concrete mixes of the country and were made following the typical volumetric ratio of 1:1.5:3 and 1:2:4 with a moderate amount of cement.

The variables considered were cement type, aggregate size and types, admixture content, water cement (w/c) ratio, and mix proportions so as to investigate the effects of their variation on the durability properties of a concrete mix. All the materials used in this experimental program are locally available and widely used. Moreover, the ranges of variables were selected as per the common construction practice.

A total of 6 cylinders for each variation were reserved for determining compressive strength whereas another set of cylinder (total 3) were for each durability test. The approximate quantities of ingredients per unit volume are given in Table 4.1.

Table 4.1: Summary of the Approximate Quantity of different Elements of Concrete Mix

Sl No	Mix Ratio	Cement & Admixture	CA	CA Size	W/C	Cement (kg/m^3)	CA (kg/m^3)	FA (kg/m^3)	Slump (mm)
1				¾ (100%)	0.33	419	1396	685	172
2				¾ (60%) + ½ (40%)	0.33	419	837.6+558.4	685	176
3				½ (100%)	0.33	419	1396	685	175
4				¾ (100%)	0.35	419	1396	685	174
5	1:1.5:3	OPC (1 L/100gm)	Stone	¾ (60%) + ½ (40%)	0.35	419	837.6+558.4	685	175
6				½ (100%)	0.35	419	1396	685	160
7				¾ (100%)	0.38	419	1396	685	161
8				¾ (60%) + ½ (40%)	0.38	419	837.6+558.4	685	170
9				½ (100%)	0.38	419	1396	685	176

Sl No	Mix Ratio	Cement & Admixture	CA	CA Size	W/C	Cement (kg/m³)	CA (kg/m³)	FA (kg/m³)	Slump (mm)
10				¾ (100%)	0.33	419	1396	685	144
11				¾ (60%) + ½ (40%)	0.33	419	837.6+558.4	685	150
12				½ (100%)	0.33	419	1396	685	140
13				¾ (100%)	0.35	419	1396	685	181
14		PCC (1 L/100gm)	Stone	¾ (60%) + ½ (40%)	0.35	419	837.6+558.4	685	192
15				½ (100%)	0.35	419	1396	685	185
16				¾ (100%)	0.38	419	1396	685	240
17				¾ (60%) + ½ (40%)	0.38	419	837.6+558.4	685	220
18				½ (100%)	0.38	419	1396	685	211
19				¾ (100%)	0.42	419	1396	685	54
20				¾ (100%)	0.45	419	1396	685	78
21		OPC (No Admix)	Stone	¾ (100%)	0.48	419	1396	685	103
22				¾ (100%)	0.5	419	1396	685	136
23	1:1.5:3			¾ (100%)	0.55	419	1396	685	134
24				¾ (100%)	0.42	419	1396	685	66
25				¾ (100%)	0.45	419	1396	685	144
26		PCC (No Admix)	Stone	¾ (100%)	0.48	419	1396	685	165
27				¾ (100%)	0.5	419	1396	685	173
28				¾ (100%)	0.55	419	1396	685	188
29				¾ (100%)	0.42	419	977	685	89
30		OPC (No Admix)	Brick	¾ (100%)	0.45	419	977	685	108
31				¾ (100%)	0.48	419	977	685	117
32				¾ (100%)	0.5	419	977	685	128
33				¾ (100%)	0.42	419	977	685	177
34		PCC (No Admix)	Brick	¾ (100%)	0.45	419	977	685	154
35				¾ (100%)	0.48	419	977	685	134
36				¾ (100%)	0.5	419	977	685	135

Sl No	Mix Ratio	Cement & Admixture	CA	CA Size	W/C	Cement (kg/m³)	CA (kg/m³)	FA (kg/m³)	Slump (mm)
37	1:2:4	OPC (No Admix)	Brick	¾ (100%)	0.42	329	1023.55	717.5	78
38				¾ (100%)	0.45	329	1023.55	717.5	106
39				¾ (100%)	0.48	329	1023.55	717.5	118
40				¾ (100%)	0.5	329	1023.55	717.5	125
41	1:1.5:3	OPC (0.8 L/100gm)	Stone	¾ (100%)	0.35	429	1120	672	178
42				¾ (60%) + ½ (40%)	0.35	429	672+448	672	100
43				½ (100%)	0.35	429	1120	672	160
44		OPC (1 L/100gm)	Stone	¾ (100%)	0.35	429	1120	672	210
45				¾ (60%) + ½ (40%)	0.35	429	672+448	672	200
46				½ (100%)	0.35	429	1120	672	170
47		OPC (1.2L/100gm)	Stone	¾ (100%)	0.35	429	1120	672	225
48				¾ (60%) + ½ (40%)	0.35	429	672+448	672	186
49				½ (100%)	0.35	429	1120	672	185
50	1:1.5:3	OPC (180 Kg Water)	Stone	¾ (100%)	0.35	514	1047	628	154
51				¾ (60%) + ½ (40%)	0.35	514	628.2+418.8	628	115
52				½ (100%)	0.35	514	1047	628	100
53		OPC (187 Kg Water)	Stone	¾ (100%)	0.35	534	1030	625	177
54				¾ (60%) + ½ (40%)	0.35	534	618+452	625	142
55				½ (100%)	0.35	534	1030	625	120
56		OPC (195.27 Kg Water)	Stone	¾ (100%)	0.35	558	1011	606	182
57				¾ (60%) + ½ (40%)	0.35	558	606.6+404.4	606	179
58				½ (100%)	0.35	558	1011	606	166

All of the concrete cylinders whether it was for compressive strength or for durability tests, were of diameter 100mm and height 200 mm. However, prior to the migration test the cylinders were sawed in such a way that each cylinder produced concrete slices of thickness 50±2 mm.

4.4 Curing

All test specimens were subjected to curing before testing in order to ensure proper hydration. All the cylinders were submerged in lime solution (Figure 4.1) prior to test and were removed from curing pond at 28th day of casting for compressive strength. As for the durability tests, the cylinders were also cured using lime water and were removed from curing spot just prior to start of test.

Figure 4.1: Curing of Concrete Cylinders

4.5 Slump Test on Fresh Concrete

Slump test was performed on fresh concrete with the intention of determining the workability of that concrete mix. All of the concrete mix variations were tested for slump as per the specifications of ASTM C 143 (2015) for this research. The equipment used to measure the slump were a metal mold which has the shape of a cone frustum and a measuring device such as ruler (Figure 4.2.c). The frustum of the metal mold has base diameter of 203 mm and top diameter of 102 mm with a height of 305 mm. It has open base and top perpendicular to the axis of the cone. It is also provided with foot pieces and handles (Figure 4.2.c). The associated

tamping rod has a circular cross-section with a diameter of 16 mm and approximately 600 mm in length.

Prior to the test the interior of the frustum metal mold was cleaned and oiled. Just after preparing the concrete mix, the mold was filled with fresh concrete paste in 4 approximately equal layers (Figure 4.2.a). Each layer was tamped with 25 evenly distributed strokes with the tamping rod. Then the mold was lifted upwards without disturbing the filled mix as shown in Figure 4.3 (b). The difference between the height of the mold and that of the collapsed mix denotes the slump value for that particular mix (Figure 4.2.c).

(a)   (b)

(c)

Figure 4.2: a) Filling the mold with fresh concrete; b) Lifting; c) Slump Measurement

4.6 Compressive Strength Measurement

The compressive strength was performed according to ASTM C39 (2005) (as shown in Figure 4.3). This test method determines the compressive strength of cylindrical concrete specimens such as molded cylinders and drilled cores. It is restricted to concrete having a density exceeding 800 kg/m^3 (50 lb/ft^3). The test is conducted by applying a compressive axial load to cylinders until the cylinder is crushed. The compressive strength of the specimen was calculated by dividing the maximum load attained during the test by the cross-sectional area of the specimen. The results of this test are usually used as a basis for quality control of concrete proportioning, mixing, curing, and placing operation (ASTM C39, 2005).Concrete cylinders of diameter 100 mm and height 200 mm were tested for compressive strength, after being removed from curing ponds. Compressive axial load was applied through a universal testing machine at a rate as prescribed in the standard.

Figure 4.3: Compressive Strength Measurement

4.7 Non Steady State Rapid Migration Test

Chloride migration coefficient for all the concrete specimens were evaluated in accordance with the nordtest method as described in the standard NT BUILD 492 (1999). This procedure

is usually applicable to the hardened concrete sample and aids in determining the non-steady state migration coefficient value of a particular mix.

The principle involves forcing the chloride ions to migrate from an outside source into the specimen with the help of an external electrical potential, applied axially across the sample for certain test duration. The specimen is later axially split upon completion of test duration and a silver nitrate solution is sprayed over one of the split sections. The chloride penetration depth can then be measured from the white silver chloride precipitation which can later be used to calculate the migration coefficient.

4.7.1   Sample Preparation and Preconditioning

After removing from the curing pond, the 100mm x 200mm concrete cylinder was cut into a 50 ± 2 mm thick slice as per the specifications of NT BUILD 492 (1999) (Figure 4.4.a). After sawing, the specimen was surface-dried and colored (Black/Green) (shown in Figure 4.4.b) along the side in order to prevent any kind of side permeation into the sample except through both end surfaces. The specimen was later placed inside the vacuum container, known as desiccator (Figure 4.4.c) for vacuum treatment upon drying of the applied color. During vacuum process, both end surfaces of the specimen were kept exposed.

Within few minutes of the vacuum process, the absolute pressure in the desiccator was set to a level in the range of 600-700 mm Hg. This pressure was maintained for three hours. After three hours, with the pump still kept running, the container was filled with saturated $Ca(OH)_2$ solution in such a way that all specimens become submerged. The solution was prepared by dissolving 10 gram of calcium hydroxide in 1L distilled water. Keeping the specimens immersed in calcium hydroxide solution, the pressure inside the desiccator was maintained for another hour before releasing the inside pressure and allowing air to reenter the container. Thereafter, the immersed specimens were kept in the solution as they were for 18 – 20 hrs until removing for migration test (Figure 4.4.d).

(a)   (b)

(c)   (d)

Figure 4.4: a) Sawing of concrete slices; b) Sample with color around the side; c) Desiccator and d) Preconditioning

4.7.2 Migration Test

With the vacuum process still running, the setup for chloride migration test was prepared as presented in Figure 4.5. After the 18-hour is elapsed, the cylindrical specimen was placed inside the rubber sleeve and secured with clamps was placed above the rubber support as shown in Figure 4.5.b. The rubber sleeve above the specimen was filled with 300 ml of 0.3 N NaOH (anolyte) solution. The glass catholytic reservoir was filled with about 12 liters of 10% NaCl (catholyte) solution. The steel mesh with steel rod (anode) was placed inside the rubber sleeve immersing it in the anolyte solution (Figure 4.5).

The anode and cathode of the setup were connected to the positive and negative poles of the power supply, respectively (Figure 4.5). Once power supply was on, a potential of 30V was set

and the initial current was measured to the nearest 0.001A. Depending on the initial current, potential was adjusted to a new value and a corresponding new initial current was recorded yet again as per the data presented in Table 4.2. The experiment was carried out for a duration specified in Table 4.2. At the expiration of test duration, the final current and voltage reading was recorded and power supply was turned off. For the time frame of test duration, both the initial and final temperature of the anolyte solution was recorded, using a thermometer.

Table 4.2: Voltage Adjustment and Test Duration Values as per NT BUILD 492 (1999)

Initial Current, I_0 for 30V (mA)	Voltage Adjustment (V)	Possible New Current, I (mA)	Test Duration (hour)
$I_0 < 5$	60	$I < 10$	96
$5 \leq I_0 < 10$	60	$10 \leq I < 20$	48
$10 \leq I_0 < 15$	60	$20 \leq I < 30$	24
$15 \leq I_0 < 20$	50	$25 \leq I < 35$	24
$20 \leq I_0 < 30$	40	$25 \leq I < 40$	24
$30 \leq I_0 < 40$	35	$35 \leq I < 50$	24
$40 \leq I_0 < 60$	30	$40 \leq I < 60$	24
$60 \leq I_0 < 90$	25	$50 \leq I < 75$	24
$90 \leq I_0 < 120$	20	$60 \leq I < 80$	24
$120 \leq I_0 < 180$	15	$60 \leq I < 90$	24
$180 \leq I_0 < 360$	10	$60 \leq I < 120$	24
$I_0 \geq 360$	10	$I \geq 120$	6

(a)
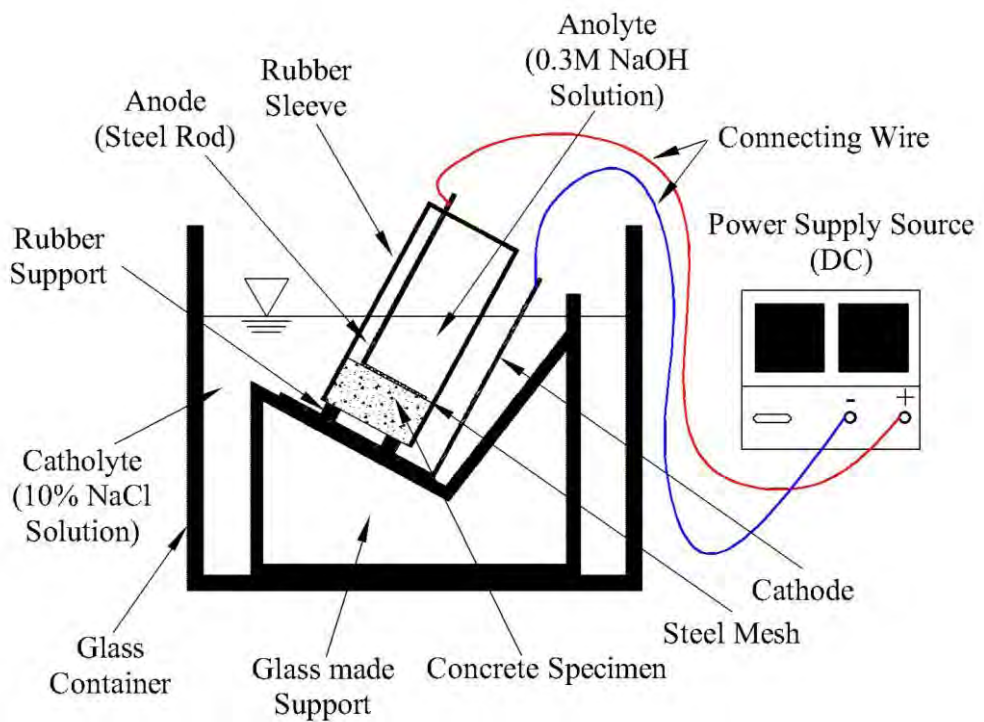
(b)

Figure 4.5: a) Real Time and b) Schematic Illustrations of RMT Setup

4.7.3 Measurement of Chloride Penetration Depth

The concrete specimen was removed from the rubber sleeve upon completion of migration test and rinsed with distill water. Blotting off excess water from the specimen surfaces, it was longitudinally split into two pieces just as depicted in Figure 4.6.a and 4.6.b. After splitting, 0.1M silver nitrate solution was sprayed adequately on one of the freshly split surfaces. The silver nitrate reacts with the Cl⁻ penetrated into the specimen and around after 15 minutes the white silver chloride precipitate (Figure 4.6.b and 4.6.c) became visible. It is referred to as the colorimetric method (technique) in which $AgNO_3$ was used as a colorimetric indicator. The penetration depths were measured using a ruler at intervals of 10 mm, starting at 10mm from the edge.

(a)   (b)

(c)
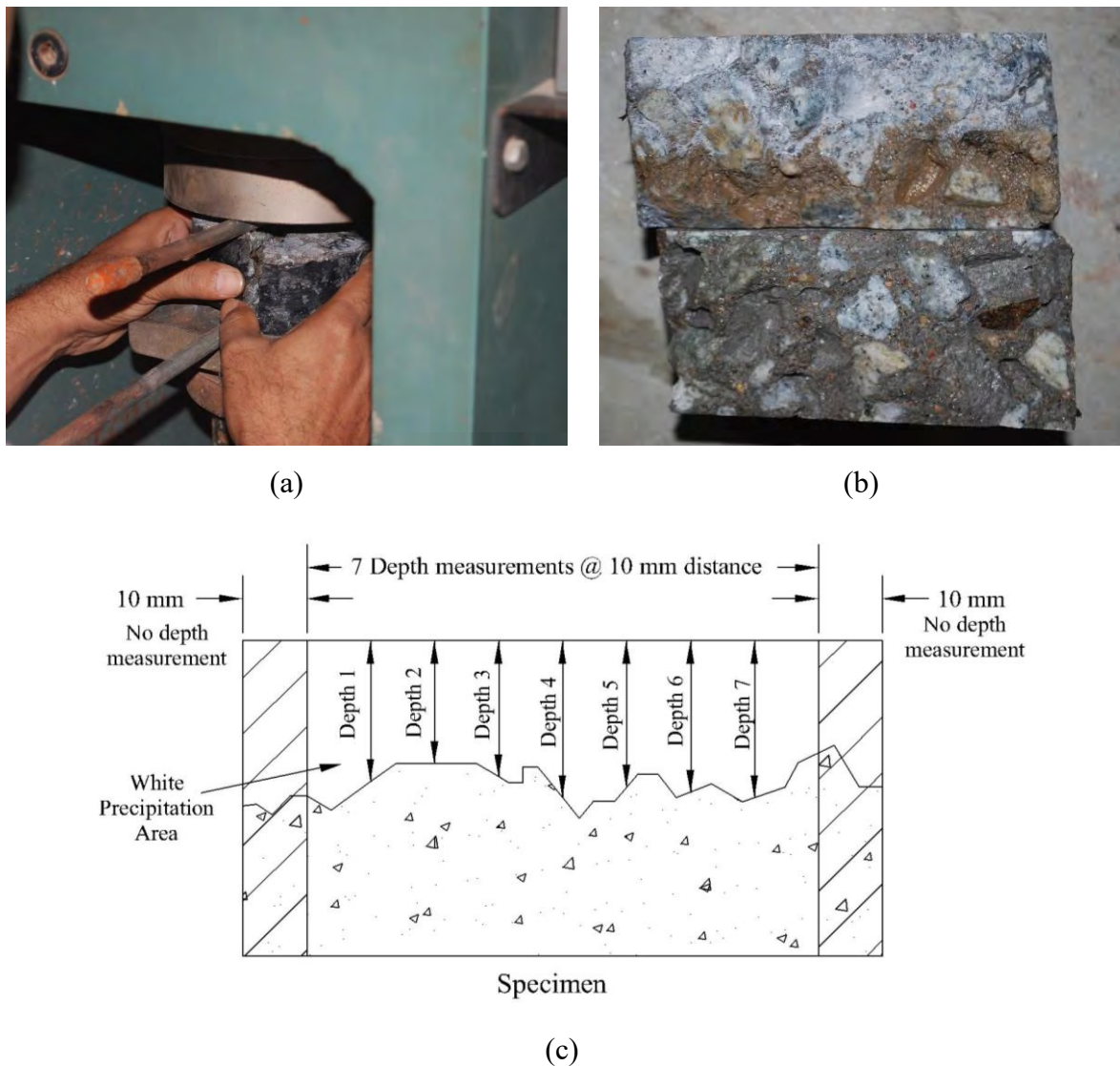
Figure 4.6: a) Splitting of Tested Sample; (b) Splitted Sample with one split with white precipitation from chloride penetration and (c) Penetration Depth Measurement

As per the NT BUILD 492 (1999) suggestions, no depth measurement was made in the zone within about 10 mm from each edge (Figure 4.6.c) to avoid effects of non-homogeneous degree of saturation and possible leakage. Seven depths were measured for each specimen in similar way as presented in Figure 4.6.c. Whenever, the penetration front was found to obstructed by aggregate, the depth measurement at that point was discarded and moved to the nearest front with no significant blocking. Finally, depth of penetration was determined from the mean of the remaining measurements. The non-steady-state migration coefficient was then calculated from the equation as stated in the code of NT BUILD 492 (1999). The coefficient depends on the voltage magnitude, temperature of anolyte measured at the beginning and the end of test and the depth of penetration of chloride ions for concrete casted.

This test method allows for a speedy evaluation of concrete resistance against the intrusion of chloride ions. Needless to state, this depth of intrusion in turn indicates the possibility of the chloride attack on steel reinforcement and its subsequent corrosion. NT BUILD 492 (1999) has suggested range of values of diffusion coefficient based on which concrete's resistance to chloride penetration can be estimated (Table 4.3).

Table 4.3: Estimation of Concrete Resistance to Cl⁻ Penetration (NT BUILD 492, 1999)

Diffusion Coefficient, D_{rcm}(X 10^{-12}) m^2/s	Resistance
≥2	Very Good
2<Drcm<8	Good
8< ρ<16	Acceptable
≤16	Unacceptable

4.8 Concrete Resistivity Measurement

Electrical resistivity of concrete poses significant importance in the determination process of the intensity of corrosion phenomena (Song and Saraswathy, 2007). After the depassivation of the protective layer, the corrosion rate of the embedded rebar in a RC element does not only depend on the availability of oxygen for corrosion to occur further but also depends on the concrete resistivity. Electrical resistance or Resistivity of concrete is in turn dependent of the hydration and microstructure of the concrete paste and actually measures the ease with which corrosion inducing ions such as Cl⁻ can migrate through the concrete.

4.8.1 Measuring Equipment and Related Principle

In this particular experimental program, "Proseq Resipod" meter, compliant to the industry standard CNS Farnell RM MKII resistivity meter, was used to quantify the electrical resistivity of all concrete mixes. This particular resistivity meter is based on the most common surface mounted probe known as the Wenner array (Song and Saraswathy, 2007; Carino, 1999) and follows the four electrode system principles suggested by Wenner (1915).

When through an alternating current source, a current is applied to the two outer probes (Figure 4.7), a potential drop can be observed between the two inner probes. Based on these values of current, voltage and probe spacing, the apparent resistivity of the mix can be found. The current is carried or transferred by the ions present in the pore solution of the concrete (Polder, 2001). The calculated resistivity depends on the spacing of the probes. A wider probe spacing is favored as it would eliminate the effect of concrete's in homogeneity and ensure more homogeneous current flow. However, this usually has to be offset against the need to avoid the influence of reinforcing steel. The most compromising and convenient probe spacing can be considered to be 30-50 mm (Polder, 2001; RILEM TC 154, 2000).
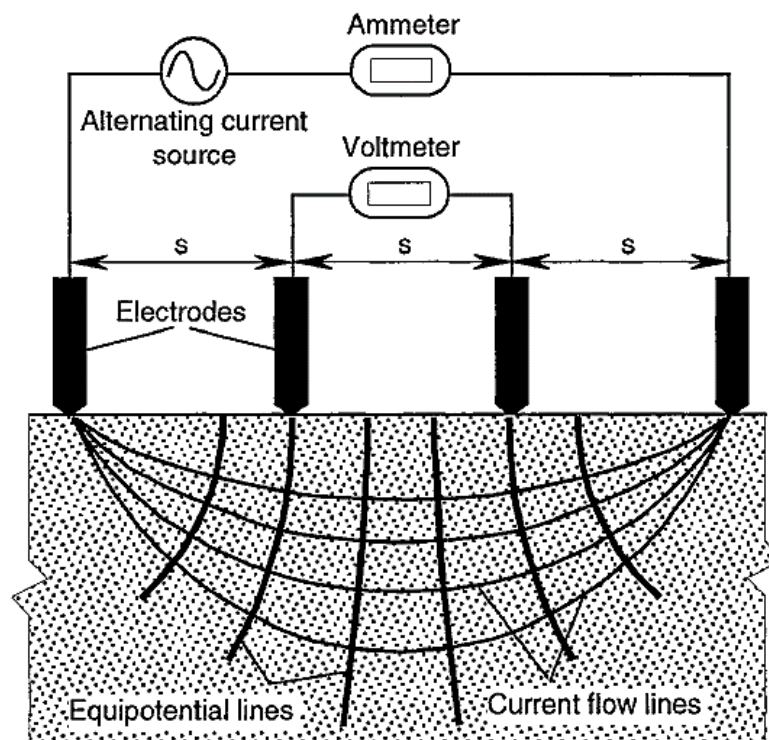
Figure 4.7: Four-Probe Resistivity Test (Carino, 1999; RILEM TC 154, 2000)

4.8.2 Resistivity Measurement

A good connection between the proseq resipod and the surface of a concrete cylinder is essential to obtain a reliable measurement and lessen the error. So as to ensure such purpose, the surface of the concrete cylinder was first cleaned of any kind of dirt or foreign material that would hinder from obtaining actual resistance value. Moreover, the surface was free of any kind of insulating coating as it would prevent ion transfer. After that, the cylinder was dipped in the water several times because a wet concrete surface would work as a good conduction medium for the current/ions to pass.

Placing the cylinders on a solid surface, the resipod was then pressed firmly over the cylinder's surface in such a way that the caps of the outer probes touched the concrete surface being tested. Once the reading on the display which shows a direct resistivity value of the tested mix reached a stable value, the data was recorded. Figure 4.8 represents the resistivity measurement process using proseq resipod.

Figure 4.8: Concrete Resistivity Measurement using Proseq Resipod

Resistivity measurements can be used to estimate the likelihood of corrosion which is higher with low resistivity (ρ) of the concrete whereas the likelihood of corrosion increases with high resistivity values. Empirical tests have arrived at the following typical values for the measured resistivity which can be used to determine the likelihood of corrosion (Table 4.4).

Table 4.4: Likelihood of Corrosion based on Concrete Restivity (Polder, 2001; RILEM TC 154, 2000):

Resistivity (ρ)	Corrosion Occurrence Risk
≥ 100	Negligible
$50 < \rho < 100$	Low
$10 < \rho < 50$	Moderate
≤ 10	High

Moreover, Langford and Broomfield (1987) has interpreted the following resistivity measurement values from the Wenner four-probe system that will aid in obtaining a general idea regarding the probable corrosion rate.

Table 4.5: Corrosion Rate based on Concrete Restivity:

Resistivity (ρ)	Corrosion Rate
≥ 20	Low
$10 < \rho < 20$	Low to moderate
$5 < \rho < 10$	High
≤ 5	Very High

5.1 General:

This chapter involves a thorough representation of all the obtained results in different experiments performed in the research and also provides a detailed analysis of any prevalent patterns in the data collected. The numerical outcomes are validated by suitable graphs, trend lines and bar charts to effectively infer any existing patterns among them. The chapter is discretized into several sections and each section provides a clear idea of a certain findings of the research. The major aspect of this research involves determination of durability parameters of concrete, in this case, diffusion coefficient and resistivity. Initially, in this chapter the effects of various concrete mixes which are commonly practiced in Bangladesh, on the both durability parameters are discussed on the basis of the graphical representations of the collected data. Later, correlation between the diffusion coefficient and the concrete resistivity, developed based on the experiment results of different types of concrete mixes, are presented in graphical form.

5.2 Effect of Aggregate Variation on Chloride Diffusion Coefficient of Concrete Samples

Prevalent construction practice in Bangladesh involves use of mainly two types of aggregates – stone and brick. This section portrays the detailed study on the effect of variation in aggregate types of similar size (19mm downgraded for this study) on the diffusion coefficient values. All other variants (aggregate size, water-cement ratio, mix ratio, cement type and admixture) are kept constant while comparing between samples of stone and brick aggregates.

5.2.1 CASE A: Concrete prepared using OPC and of Mix Proportion 1:1.5:3

Figure 5.2.1 shows the variation in diffusion coefficient values of concrete prepared using a mix proportion of 1:1.5:3 and ordinary portland cement (OPC) for both brick and stone aggregates.
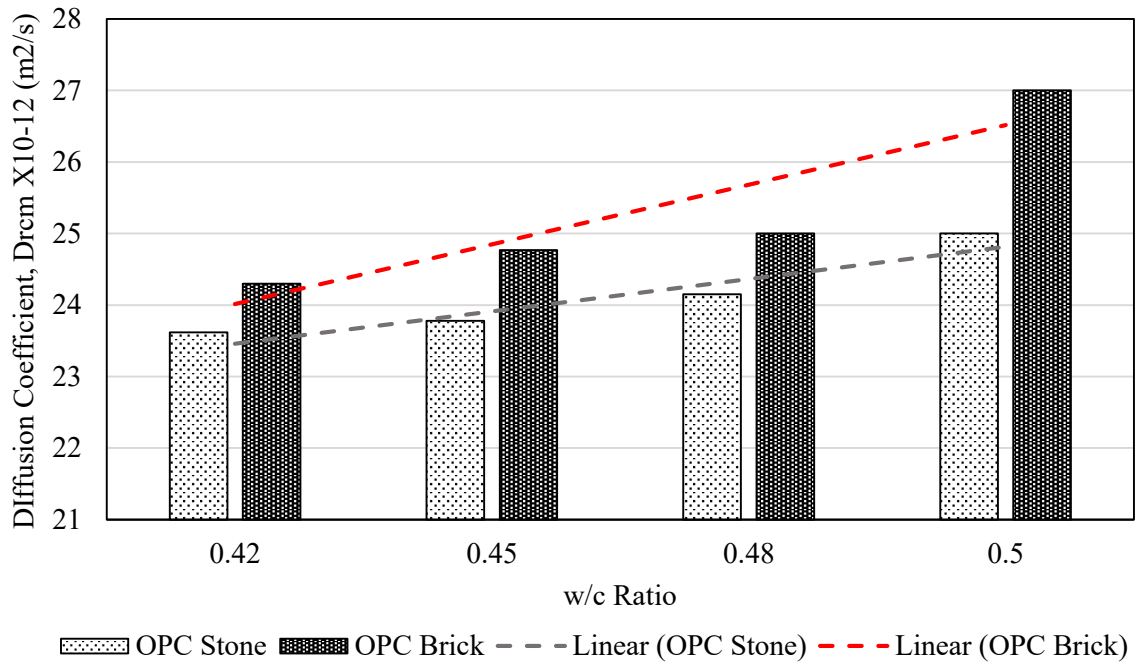
Figure 5.2.1: Effect of Aggregate Variation on Diffusion Coefficient for OPC (1:1.5:3) concrete

All the coefficient values were determined as following the standard NT Build 492 (1999). As per NT BUILD 492 (1999) and Elfmarkova et al. (2015), chloride diffusion coefficient is the measure of concrete's resistance to chloride penetration as diffusion controls the Cl$^-$ ingress at a certain depth of concrete. The higher the value of coefficients the lower the capability of a concrete to resist chloride penetration and thus chloride induced corrosion (Real et al., 2017; Elfmarkova et al., 2015).It can be inferred from the above figure that for a certain mix proportion (1:1.5:3) and cement type (OPC), concrete prepared using brick aggregates always demonstrates significantly higher value of diffusion coefficient than that of stone aggregate concrete irrespective of the water cement ratio (w/c) used. This can be numerically justified by 3%, 4.2%, 7.8% and a maximum 8% increase in diffusion coefficient values of concrete samples with brick aggregates as compared to those of stone aggregate for w/c ratio of 0.42, 0.45, 0.48 and 0.5 respectively. Both brick and stone aggregate concrete shows maximum diffusion coefficient values for w/c ratio 0.5. In case of stone aggregate the maximum diffusion coefficient (high permeability) can be observed to be 25 X 10^{-12} m^2/s whereas in case of brick aggregate concrete the maximum value is 27 X 10^{-12} m^2/s. Based on the above observations, concrete samples with brick aggregate can be considered to possess lower resistance to chloride ion penetration and thus can be said to have higher range of susceptibility to chloride induced

corrosion. This behavior of brick aggregate concrete can be attributed to its high absorption and permeability due to porous structure of bricks. Brick aggregates by nature contain fine capillaries which produce a highly porous microstructure of bricks. These pores facilitate continuous medium for a fluid flow inside the concrete and make it highly susceptible to chloride permeation. This high chloride ingress eventually accelerates the rusting of embedded rebar and reduces service life of the structure (Manzur et al., 2018).

Though stone aggregate shows better performance than bricks in respect of resistance to chloride ingress, diffusion coefficient values for both stone and brick aggregate concretes fall within the range of unacceptable category as per the specified values ($>16X10^{-12}m^2/s$) in NT BUILD 492 (1999) (shown in Table 4.2; Chapter 4).

If trend lines are drawn through the points of the bar chart for both stone and brick aggregate, both shows increase in diffusion coefficient values with increasing w/c ratio. When the w/c ratio is increased keeping cement content constant, more water occupy pore spaces in the concrete microstructure. As the hydration progresses, this water particles are evaporated keeping voids in their places which ultimately serve as continuous medium for chloride ion ingress.

5.2.2 CASE B: Concrete prepared using PCC and of Mix Proportion 1:1.5:3

In this section, effect of aggregate variation on the diffusion coefficient values of concrete prepared using Portland Composite Cement (PCC) has been evaluated and presented in Figure 5.2.2. This graphical presentation shows near about similar trend of higher values of diffusion coefficient for brick aggregate concrete as discussed in previous section for OPC concrete. Moreover, the trend lines show increase in the coefficient values for increasing w/c ratio for both stone and brick aggregate concrete. The increase can be observed to be from $11.95X10^{-12}$ m^2/s to $19X10^{-12}$ m^2/s for increase in w/c ratio from 0.42 to 0.5, in case of stone aggregate. In contrast, brick aggregate concrete shows the increase to be from $20X10^{-1}$ $^2m^2/s$ to $25X10^{-12}$ m^2/s for similar range of w/c ratio.
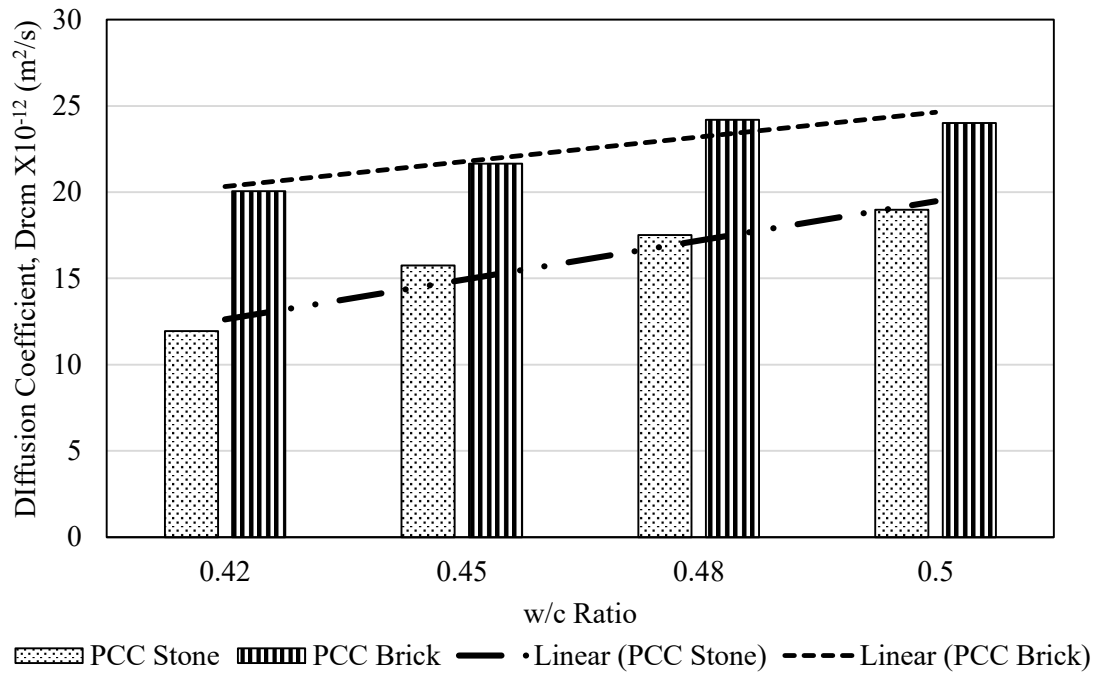
Figure 5.2.2: Effect of Aggregate Variation on Diffusion Coefficient for PCC (1:1.5:3) concrete

The maximum value of diffusion coefficient for concrete with PCC and brick aggregate has been found to be about 24 X 10^{-12}m^2/s for both w/c ratio of 0.48 and 0.5 while stone aggregate produces a relatively less upper bound value of 19 X 10^{-12}m^2/s for w/c ratio of 0.5 only. Use of PCC as an alternative to OPC improves the durability performance of both stone and brick aggregate to an extent but still, brick aggregate yields concrete with unacceptable or very poor resistance (diffusion coefficient values greater than 16 X 10^{-12}m^2/s) to chloride ingress regardless of the w/c ratio used. Comparatively, stone aggregate concretes with PCC and w/c ratio of 0.42 and 0.45 exhibit acceptable resistance to chloride penetration as their diffusion coefficient values, 11.95X10^{-12} m^2/s and 15.75X10^{-12} m^2/s, respectively, fall within the range of 8~16 X 10^{-12} m^2/s (NT BUILD 492, 1999). This can be due to the intrinsic properties (high absorption, presence of capillary pores etc.) of brick aggregates which counteract to minimize the positive effects imposed by the presence of pozzolanic substances of composite cement.

5.3 Effect of Aggregate Variation on Electrical Resistivity of Concrete Samples

Electrical resistivity of hardened concrete can be considered to be an important indicator of corrosion intensity (Song and Saraswathy, 2007) as it measures concrete's resistance against flow of ion (Sengul, 2014). In this section, the effect of aggregate types' variation on the

concrete resistivity values is compared keeping all other variants (aggregate size, water-cement ratio, mix ratio, cement type and admixture) constant.

5.3.1 CASE A: Concrete Prepared using OPC and of Mix Proportion 1:1.5:3
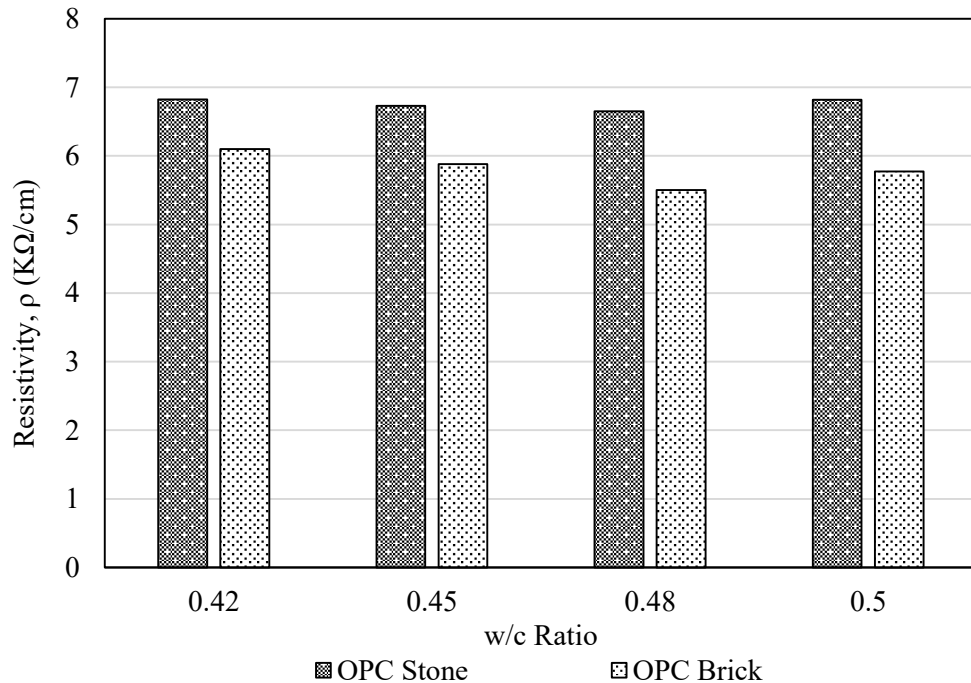
Figure 5.3.1: Effect of Aggregate Variation on Resistivity for OPC (1:1.5:3) Concrete

As per Hou et al. (2017), inclusion of coarse aggregate serves as a direct obstacle against ion flow and any alteration in its type affect the concrete resistivity. Figure 5.3.1 presents the effect of stone and brick aggregate (commonly used coarse aggregates in Bangladesh) use on the electrical resistivity of concrete samples containing OPC and of mix ratio 1:1.5:3.The bar chart shows a considerably higher degree of resistivity values for stone aggregate concretes than their brick counterparts. As it to put numerically the stone aggregate concrete exhibits about 27% increased resistance against current flow on average as compared to the brick aggregate concrete for w/c ratio ranging between 0.45 and 0.5. The maximum resistivity value for stone aggregate is 6.825 KΩ/cm for w/c ratio of 0.42. The value reduces to 6.1 KΩ/cm for brick aggregate concrete prepared using similar w/c ratio. This is the maximum resistivity data recorded for brick aggregate concrete. This discrepancy between stone and brick aggregate concrete is due to the difference in their microstructures. Brick with its porous microstructure displays high absorption capability which in conjunction with interconnected micro pores of concrete provide comparatively easier path for chloride ion flow.

Moreover, based on these resistivity measurements, the risk of corrosion occurrence and probable corrosion can also be determined. Both stone and brick aggregate concrete possess resistivity values ranging between 6.5-8 KΩ/cm and 5-6 KΩ/cm, respectively and all of which are less than 10 KΩ/cm. RILEM TC 154 (2000) and Polder (2001) have recommended high risk of corrosion probability for concretes with resistivity value less than 10 KΩ/cm. Langford and Broomfield (1987) suggested that concrete of resistivity within the range of 5-10 KΩ/cm can be assumed to be associated with high corrosion rate. Therefore, all the concrete mixes considered in this section whether it is of brick or stone aggregate, can be said to have high corrosion susceptibility.

5.3.2   CASE B: Concrete Prepared using PCC and of Mix Proportion 1:1.5:3

This section discusses the impact of two types of aggregates (stone and brick) on the concrete resistivity for mixes having mix proportion of 1:1.5:3 and PCC as cement. The overall trend of the variation is summarized in a graphical form as shown in Figure 5.3.2.
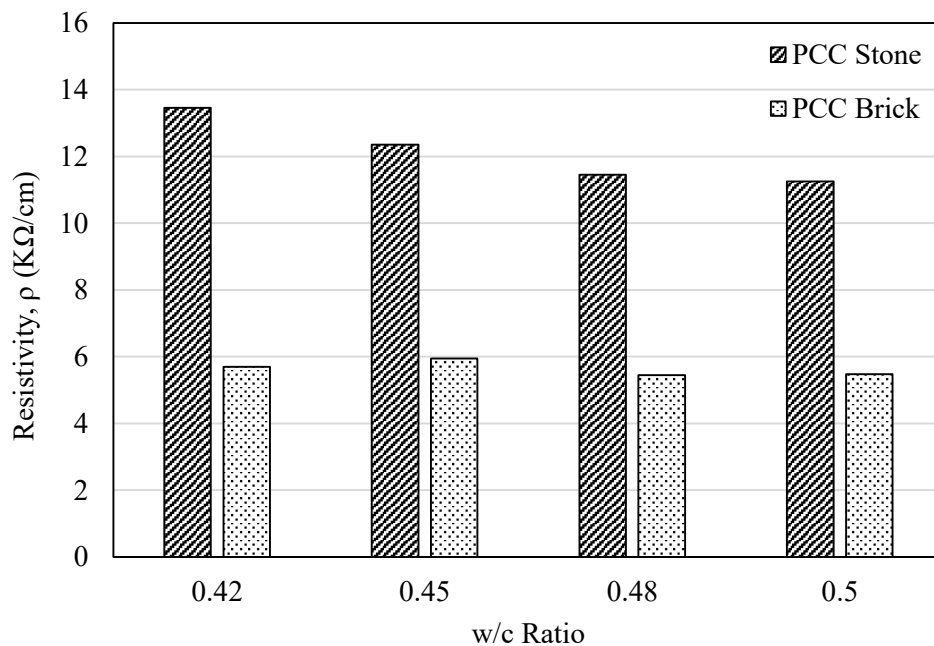
Figure 5.3.2: Effect of Aggregate Variation on Resistivity for PCC (1:1.5:3) concrete

Figure 5.3.2 presents noticeably much better performance of concrete with stone aggregate against chloride ion flow. Numerically, the resistance are observed to be 13.46, 12.35, 11.45, 11.25 KΩ/cm for w/c ratio of 0.42, 0.45, 0.48 and 0.5, respectively. However, brick aggregate concrete shows resistivity values in the range of 5.45 to 6 KΩ/cm for varying w/c ratio of

0.42~0.5. These observations, eventually, substantiate the discussion of section 5.2.2 on durability aspects of concrete with PCC and brick aggregate. Both these discussions (in section 5.2.2 and section 5.3.2) point toward the improved performance of PCC and brick aggregate concrete (as compared to the OPC one) but less resistance to ion flow in comparison with the stone equivalents.

As for the risk of corrosion occurrence, concretes with PCC and brick aggregate yield resistivity values less than 10 KΩ/cm making them susceptible to high corrosion risk (Polder, 2001; RILEM TC 154 2000). While, stone aggregate concretes incorporating composite cement exhibits moderate corrosion risk as their value fall within the range of 10-50 KΩ/cm (Polder, 2001; RILEM TC 154 2000).

In case of probable corrosion rate, the resistivity values of PCC and brick aggregate concrete are in the range of 5-10 KΩ/cm and of PCC and stone aggregate concrete are in the range of 10-20 KΩ/cm. Thus, as per Langford and Broomfield (1987), PCC and stone aggregate concrete will face low to moderate rate of corrosion whilst its brick aggregate counterpart will undergo high rate of corrosion.

5.4 Effect of Variation in Mix Proportion on Chloride Diffusion Coefficient of Concrete Samples

In Bangladesh, most construction practices involve preparation of concrete mixes following two basic types of volumetric ratio- 1:1.5:3 and 1:2:4. During this research program, the effect of these two variation of mix proportions on the durability aspects of concrete prepared using particular aggregate (brick) and cement (OPC) type was studied.

This section provides with the description on the changes in diffusion coefficient values of abovementioned concrete mixes for two variation of mix proportions. This variation trend is portrayed in the Figure 5.4.1 for different w/c ratio.
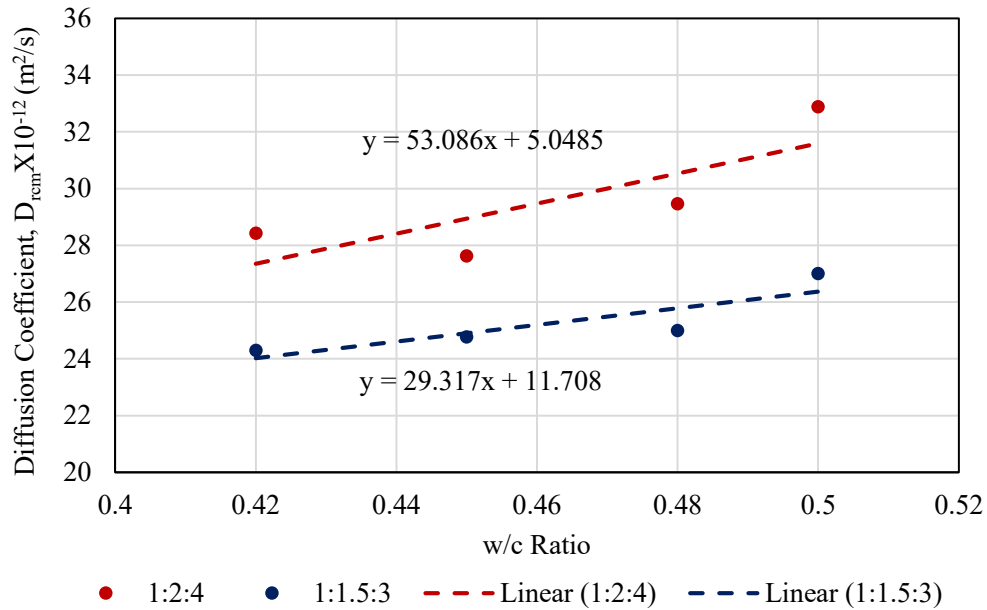
Figure 5.4.1: Effect of Variation in Mix Proportion on Diffusion Coefficient OPC Brick

It can be deduced from Figure 5.4.1 that concretes of mix proportion 1:2:4 usually demonstrate high values of chloride diffusion coefficient which in turn indicate lower resistance against chloride penetration of that mix. Usually, the values fluctuate within the range of $27 \times 10^{-12} \sim 32 \times 10^{-12}$ m²/s for w/c ratio varying between 0.42 and 0.5. On the other hand, concrete mixes with similar range w/c ratio and mix proportion of 1:1.5:3 can be detected to yield much less diffusion coefficient value ranging between $24 \times 10^{-12} \sim 27 \times 10^{-12}$ m²/s. In both these cases, the data trends follow straight line with positive slopes signifying increase in diffusion coefficient values for higher w/c ratio. Based on the observed values and Figure 5.4.1, it can quantified that concrete with mix proportion of 1:2:4 shows on average about 16~18% lower resistance as compared to that of 1:1.5:3. The fact that endorses such variation can be assumed to be the resulting lean and weak mix of concrete prepared following volumetric ratio of 1:2:4. Mix proportion 1:2:4 as compared to the ratio 1:1.5:3 involves usage of less amount of cement in concrete casting and thus provides inadequate surface area to bind the aggregates. This results in a weaker interfacial transition zone with high porosity.

The chloride resistance of concretes prepared using both types mix proportions can be classified as unacceptable as per NT BUILD 492 (1999) as all of their diffusion coefficient values have found to be less than the code specified value of 16×10^{-12} m²/s.

5.5 Effect of Variation in Mix Proportion on Resistivity of Concrete Samples
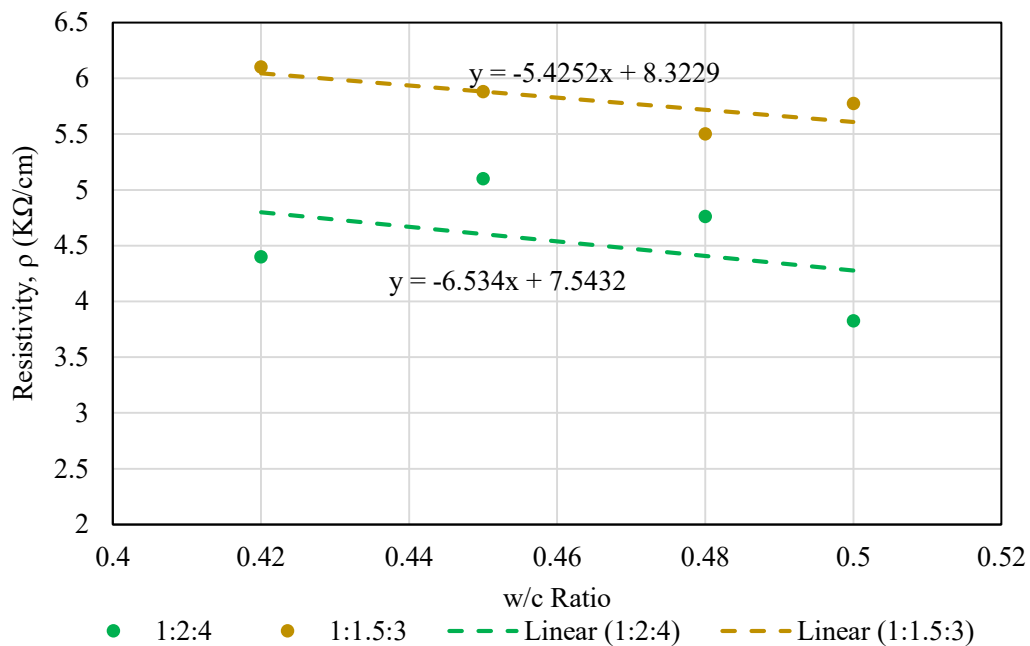
Figure 5.5.1: Effect of Variation in Mix Proportion on Resistivity OPC Brick

Figure 5.5.1 represents higher resistivity values in case of mix proportion 1:1.5:3 confirming the durability trends for 1:1.5:3 and 1:2:4 as discussed in section 5.4. It can be seen in the graph that the trend lines of the resistivity data, in case of both mix proportions follow straight line with negative slope for increasing w/c ratio. This signifies the decreasing trend of resistance to chloride permeability with increasing w/c ratio for both types of concrete mixes. However, the concretes of mix proportion 1:2:4 show 22% ~ 23% decrease, on average, in resistivity as compared to the resistivity data of concretes of proportion 1:1.5:3 for varying w/c ratio of 0.42-0.5. This eventually validates the previous statement (section 5.4) regarding formation of weaker concrete with high probability of chloride permeation for volumetric mix ratio of 1:2:4. Now, if the risk of corrosion occurrence are to be considered, both types of concrete will be rated to endure high corrosion risk (for resistivity values less than 10 KΩ/cm) (RILEM TC 154, 2000; Polder, 2001). This is because all the values for 1:1.5:3 and 1:2:4 range between 5.25~6 KΩ/cm and 4-4.7 KΩ/cm, respectively. However, in case of probable corrosion rate, concretes with 1:2:4 can be considered to face very high corrosion rate whereas concretes with proportions 1:1.5:3 may sustain high corrosion rate (Langford and Broomfield, 1987).

5.6 Effect of Variation in Coarse Aggregate Size and Gradation on Chloride Diffusion Coefficient of Concrete Samples for Varying W/C Ratio of 0.33-0.35

Aggregate, a major component of every concrete mix, has a significant effect on the properties of fresh and hardened concrete. Major of these properties depend on the type and particle size distribution of the coarse aggregate used. In this study, effect of variation in coarse aggregate size and gradation on the durability of hardened concrete in terms of chloride permeability and eventually in its service life is investigated. Chloride permeability is a function of the presence interconnecting voids which in turn relies on the aggregate size distribution within concrete to a great extent. For this study, three different combinations of stone (coarse) aggregates (SCA) were considered – SCA mix type 1[100% of ¾ inch (19mm) downgraded], SCA mix type 2 [60% of ¾ inch (19mm) downgraded + 40% of ½ inch (12.5mm) downgraded] and SCA mix type 3 [100% of ½ inch (12.5mm) downgraded]. The particle size distribution for all three cases are shown in Figure 5.6.1. The effect was studied for both OPC and PCC and w/c ratio within the range of 0.33 to 0.38. In order to improve the workability of concrete with such low w/c ratios, a constant amount (1L per 100 Kg of cement) of water reducing admixture Master Glenium ACE 30ii was used. The following sections provide discussion on the effect of three variation of aggregate size distribution on the chloride diffusion coefficient of different concrete mixes.
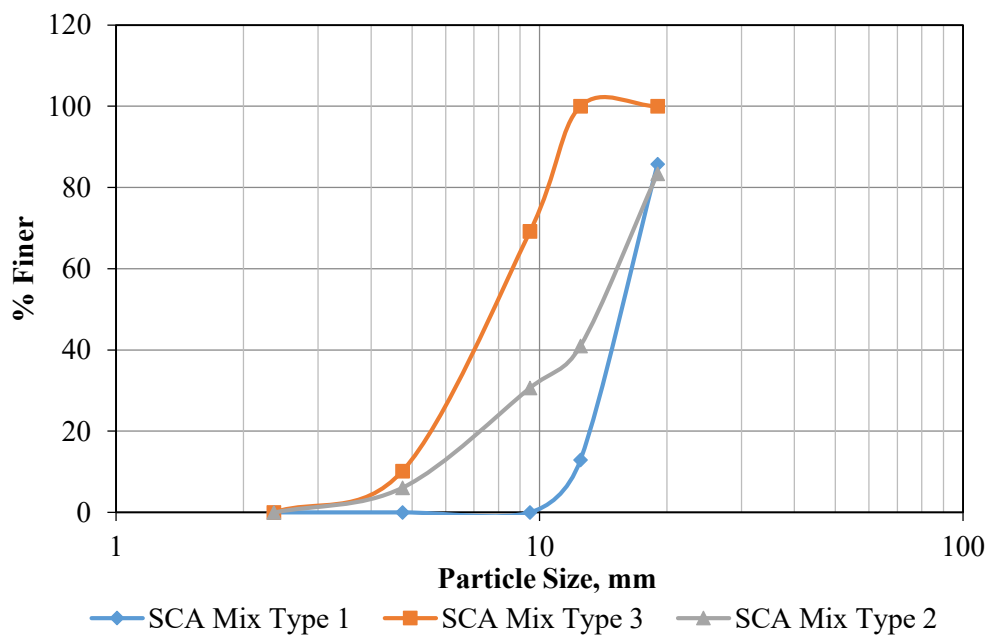
Figure 5.6.1: Particle Size Distribution for 3 Combinations of Stone Aggregate Size

5.6.1 CASE A: Concrete with OPC and W/C Ratio 0.33-0.38

Figure 5.6.2 presents a correlation between chloride diffusion coefficients and varying w/c ratio of 0.33-0.38 for 3 combination of stone aggregate size for concrete with OPC. All the correlations are seen to follow straight line with positive slopes. This confirms the previous assumptions for increase in diffusion coefficient due to increase in water content. From the graph it can be observed that concrete containing SCA mix type 1 shows high coefficient values as compared to the other two types of stone aggregate mix. The increase in diffusion coefficient values for SCA mix type 1 is found to be 5-19% as compared to that of type 2 for the w/c ratio ranged from 0.33-0.38 with low increment for higher w/c ratio. However, with respect to SCA mix type 3 the percentage of increase in diffusion coefficient values can be observed to be 5.25 on average for w/c ratio ranging between 0.33 and 0.38. The reason that might be assumed to contribute to such variation is the uniform gradation (shown Figure 5.6.1) and larger particle size in case of concrete with OPC and stone aggregate mix type 1 as compared to its other two counterparts. Presence of relatively uniform and larger particles in a mix increases the size and ratio of voids among particles and results in a concrete with relatively porous microstructure. Therefore, such concrete becomes highly permeable and susceptible to chloride intrusion.
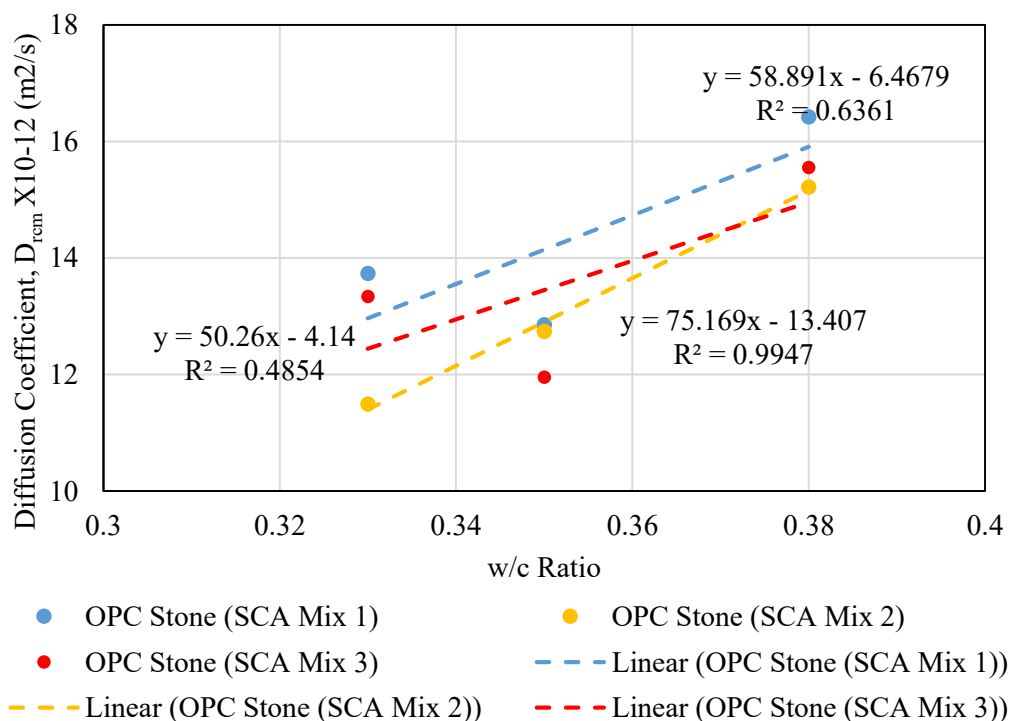
Figure 5.6.2: Effect of Variation in Stone Aggregate Size and Gradation on Chloride Diffusion Coefficient of Concrete Mixes with OPC

Between SCA mix type 2 and type 3, the chloride resistance of SCA mix type 2 can be presumed to be higher than that of SCA mix type 3 in almost all cases. This is because of the comparatively lower (about 2%-13.85% decrease) coefficient values of SCA mix type 2 than the diffusion coefficients of SCA mix type 3. The particle size distribution of SCA mix type 2 can be observed to be "well graded" as compared to the uniform gradation of SCA mix type 3 [100% of ½ (12.5 mm) inch downgraded]. Therefore, it produces a relatively packed concrete with less pores of small size. Therefore, the permeability of the concrete containing stone aggregate (SCA) mix type 2 is improved comparatively to that of SCA mix type 3.

The diffusion coefficient values in case of these three types of Stone aggregate mix are within the range $11X10^{-12}m^2/s$-$16X10^{-12}m^2/s$. Therefore, all the mixes can be considered as acceptable in resisting chloride ingress as per NT BUILD 492(1999).

5.6.2 CASE B: Concrete with PCC and W/C Ratio 0.33-0.38
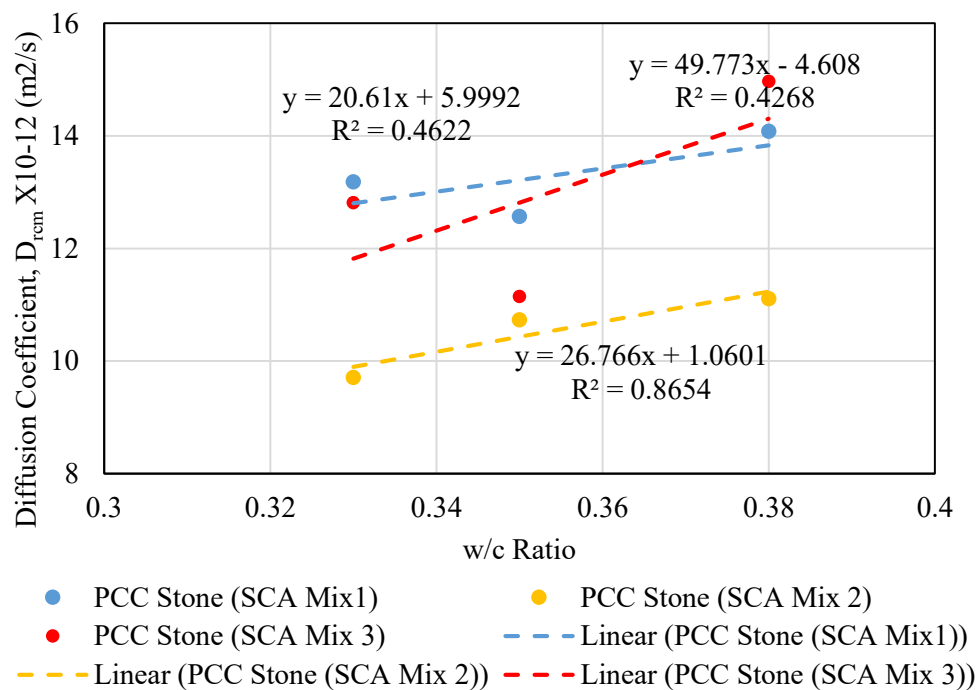
Figure 5.6.3: Effect of Variation in Stone Aggregate Size and Gradation on Chloride Diffusion Coefficient of Concrete Mixes with PCC

Figure 5.6.3 is the representation of the variation in chloride diffusion coefficients with varying w/c ratio of 0.33-0.38 for 3 combination of stone aggregate size for concrete containing PCC.

It can be inferred from the graph that concrete containing SCA mix type 2 shows on average 23%-24% and 21%-22% decrease in diffusion coefficient value with respect to those of SCA mix type 1 and Mix Type 3, respectively, for varying w/c ratio of 0.33 to 0.38. The reasons that can accredited to this phenomena is the presence of pore refining pozzolanic substances in PCC and the well distributed gradation of SCA mix type 2. Between SCA mix type 1 and SCA mix type 3, mix type 3 performs better in most cases. This is because of the comparatively better gradation and smaller particles for SCA mix type 3. However, in case of PCC, all three types of stone aggregate mixes produce concrete with acceptable resistance to chloride ingress.

5.7 Effect of Variation in Coarse Aggregate Size and Gradation on Resistivity of Concrete Samples for Varying W/C Ratio of 0.33-0.38

The following sections will discuss the effect of stone aggregate gradation on resistivity of concrete. The mix variations considered for resistivity measurement are same as that considered to study the effect on diffusion coefficient measurement.

5.7.1 CASE A: Concrete with OPC and W/C Ratio 0.33-0.38
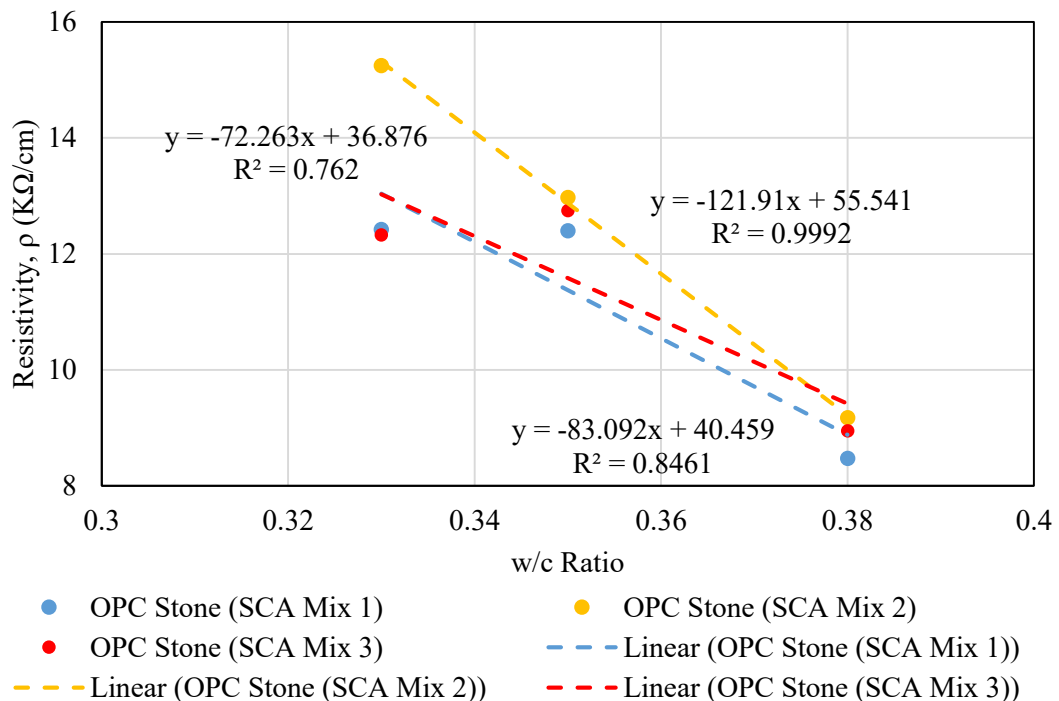
Figure 5.7.1: Effect of Variation in Stone Aggregate Size and Gradation on Resistivity of Concrete Mixes with OPC

Figure 5.7.1 represents the effect of aggregate gradation on the resistivity of concrete prepared with stone aggregate and OPC. Figure 5.7.1 also denotes the inverse relation between resistivity value and w/c ratio. It can be seen from the graph that concrete containing SCA mix type 2 shows 22.7% increase in resistivity with respect to SCA mix type 1 for w/c ratio of 0.33. This eventually reduces to 8.25% when w/c ratio of 0.38 is attained. As compared to mix type 3, the increase in resistivity of concrete containing SCA mix type 2 is also about 22.5-22.7% for w/c ratio of 0.33 and reduces gradually to insignificant value for increase in w/c ratio. However, the comparison between SCA mix type 1 and 3 displays less significant difference in their resistivity values for varying w/c ratio of 0.33-0.38.

5.7.2 CASE B: Concrete with PC and W/C Ratio 0.33-0.38
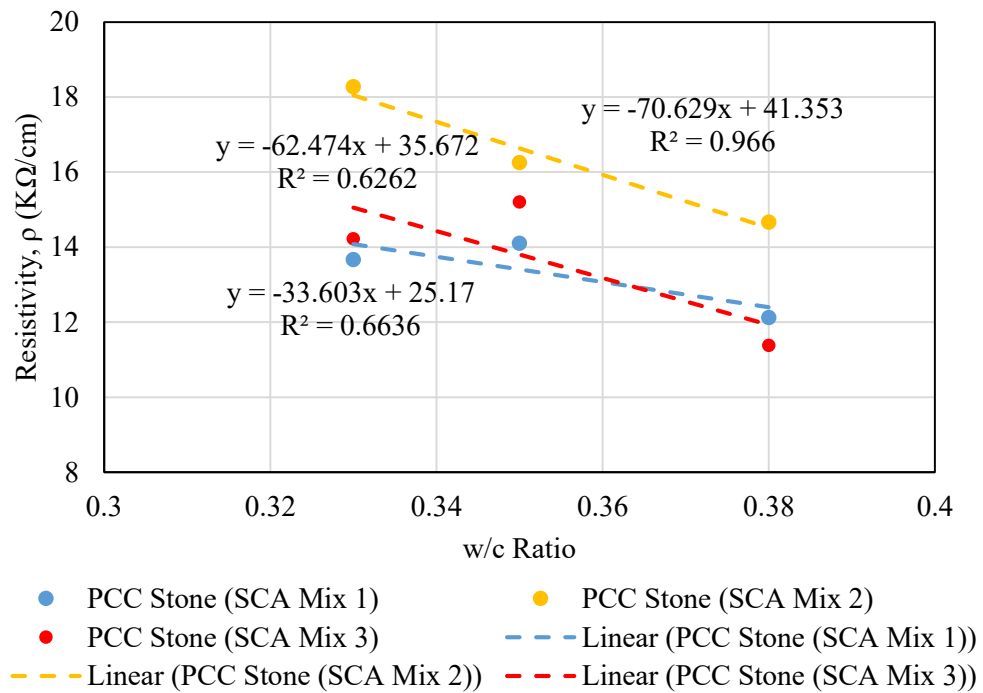
Figure 5.7.2: Effect of Variation in Stone Aggregate Size and Gradation on Resistivity of Concrete Mixes with PCC

Figure 5.7.2 represents the effect of aggregate gradation on the resistivity of concrete prepared with stone aggregate and PCC. The correlation with varying water content shows about on average 20.6-20.7% and 22.5-22.6% increase in resistivity of concrete containing SCA mix type 2 with respect to those of SCA mix type 1 and mix Type 3, respectively, for varying w/c ratio of 0.33 to 0.38. This observations, eventually, validates the statement regarding impact of pozzolanic substance and well graded aggregate mix on improvement of resistivity. Although

no such pronounced difference can be observed between resistivity of SCA mix type 2 and type 3, SCA mix type 3 performs slightly better than SCA mix type 1 because of the presence of smaller particle size.

5.8 Effect of Variation in Cement Type on Chloride Diffusion Coefficient of Concrete Samples

Current practices in construction industry of Bangladesh involve use of mainly two types of cement-CEM I or Ordinary Portland Cement (OPC) and CEM II or Portland Composite Cement (PCC), based on strength gaining purposes. Following segments focuses on the effect of these two types of cement on chloride diffusion coefficient of the mix.

5.8.1   CASE A: Stone Aggregate Concrete with High w/c Ratio (0.42-0.55)
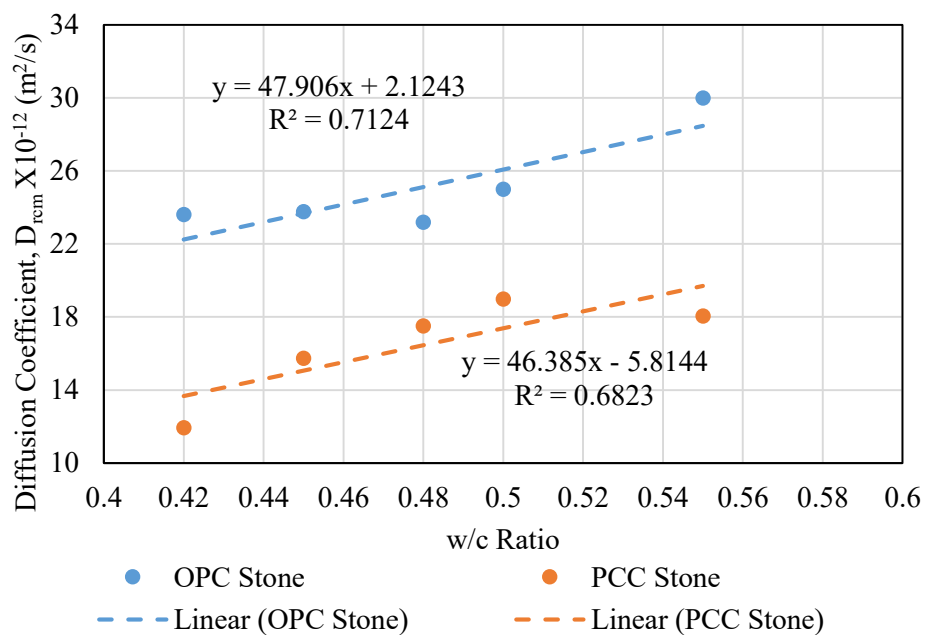
Figure 5.8.1: Effect of Variation in Cement Type on Chloride Diffusion Coefficient of Stone Aggregate

Due to presence of Pozzolanic substances that produces C-S-H gel essential for pore refinement, concrete with PCC can be presumed to perform better than that of OPC in strength gaining and resisting any kind of permeation. Figure 5.8.1 is the representation of the variation in chloride diffusion coefficients for stone aggregate concrete with OPC and PCC. This graphical illustration shows a considerably lower values of diffusion coefficients in case of

PCC which fluctuate between 12×10^{-12} m^2/s and 19×10^{-12} m^2/s for varying w/c ratio of 0.42~0.55. The trend line of this fluctuation can be considered as a straight line with a positive slope. In contrast, concretes with OPC return diffusion coefficient values in a range of 22×10^{-12} m^2/s - 30×10^{-12} m^2/s for increasing w/c ratio of 0.42 -0.55. The increase is seen to be about 55% higher on average as compared to the diffusion coefficients of concrete with PCC. Thus, concrete with stone and PCC can be expected to provide better resistance to chloride penetration and ultimately to corrosion induced damage, than its OPC counterpart. As per NT BUILD 492 (1999), concretes containing PCC and stone aggregate can be esteemed to possess acceptable resistance to chloride penetration (diffusion coefficients within the range of 8×10^{-12} m^2/s - 16×10^{-12} m^2/s) in most cases, except for w/c ratio higher than 0.5. Alternatively, all concretes with OPC and stone aggregate fall within the unacceptable category in resisting chloride ion ingress because all of their diffusion coefficient data are observed to be greater than the value of 16×10^{-12} m^2/s.

The reason that works behind the better performance of PCC concrete can be assumed to be its better pore refinement capability. PCC contains pozzolanic substances such as fly ash. These finer particles hydrate at later age to form substances like C-S-H gel which in turn refine the micropores, reduce the porosity and pore connectivity and improve the packing capacity of concrete (Hassan et al., 2000; Chen et al., 2014).

5.8.2 CASE B: Brick Aggregate Concrete with High w/c Ratio (0.42-0.50)

Figure 5.8.2 is the graphical representation of the variation in diffusion coefficient with varying w/c ratio for both OPC and PCC concrete. It can be inferred from the graph that even in case of brick aggregate concrete, addition of PCC as an alternative to OPC lowers the diffusion coefficient signifying comparatively improved resistance against chloride ion penetration.

Numerically, the decrease in case of PCC can be observed to be in the range of 12% to 20% for w/c ratio ranging from 0.42 to 0.5 as compared to OPC concrete. Despite of the improvement in chloride resistance for addition of PCC, the chloride resistance of the PCC concretes can also be categorized as unacceptable just like its OPC counterparts (NT BUILD 492, 1999).
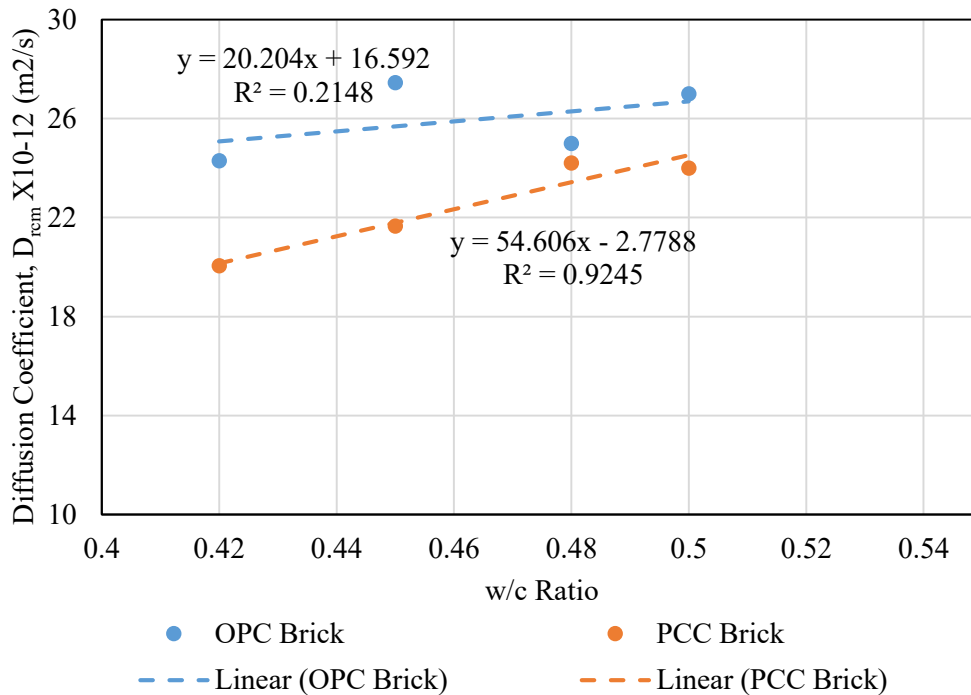
Figure 5.8.2: Effect of Variation in Cement Type on Chloride Diffusion Coefficient of Brick Aggregate

This can be because of the counteraction between high absorption capacity of brick aggregates and densification effect of the pozzolanic substances present in PCC. The porous microstructure of brick aggregate attribute to its high absorption capacity and provide a continuous medium for ion to flow. As a result brick aggregate concrete with OPC shows higher susceptibility to chloride penetration. PCC contains active silica that with $Ca(OH)_2$ produces C-S-H gel, essential for pore refinement. Therefore, use of PCC in brick aggregate concrete, rather than OPC, reduce chloride ion susceptibility but cannot fully diminish the negative effect of the porous microstructure of brick aggregate.

5.8.3   CASE C: Stone Aggregate Concrete with Low w/c Ratio (0.33-0.35)

Figure 5.8.3.1 to 5.8.3.3 presents effect of cement variation on the chloride diffusion coefficient values for concrete with stone aggregate (of varying size) and varying low w/c ratio of 0.33 ~ 0.38. In order to increase the workability of such concrete with low w/c ratio 1L of a water reducing admixture was used for per 100 kg of cement. In almost all cases considered here, PCC concrete shows better resistance to chloride induced corrosion than that of OPC.
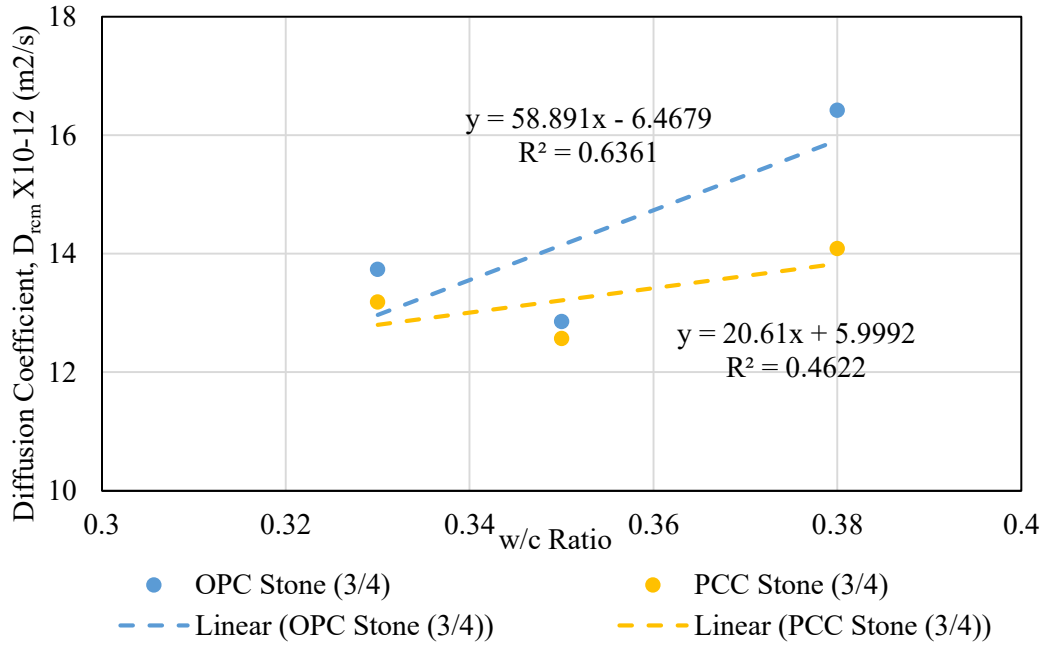
Figure 5.8.3.1: Effect of Variation in Cement Type on Chloride Diffusion Coefficient of SCA Mix Type 1 and Admixture
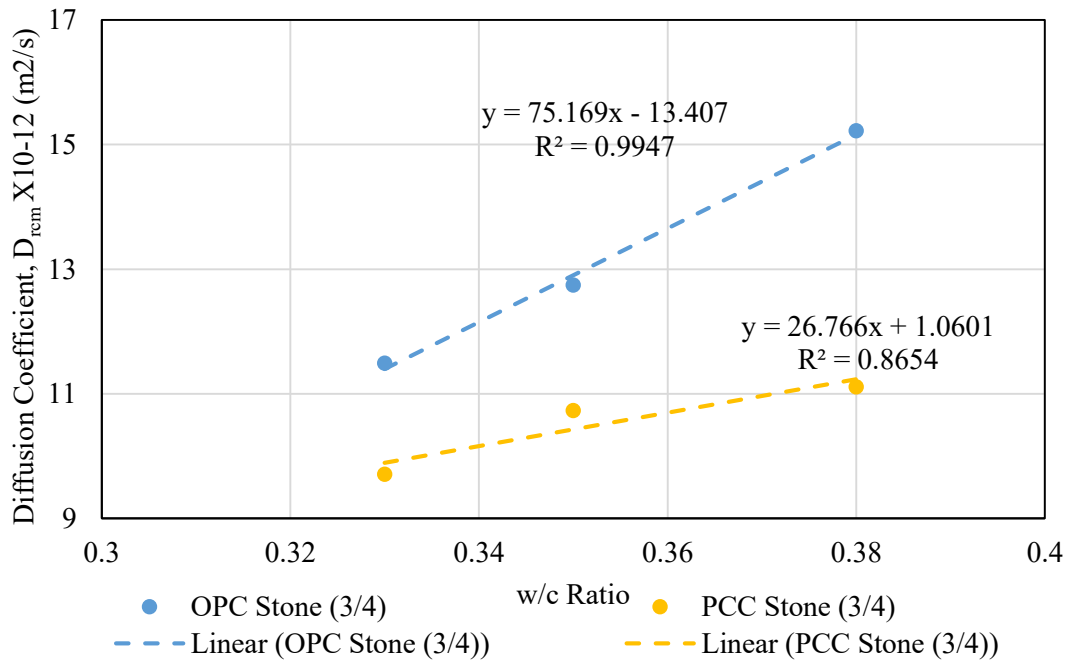
Figure 5.8.3.2: Effect of Variation in Cement Type on Chloride Diffusion Coefficient of SCA Mix Type 2 and Admixture

$$y = 50.26x - 4.14$$
$$R^2 = 0.4854$$

$$y = 49.773x - 4.608$$
$$R^2 = 0.4268$$
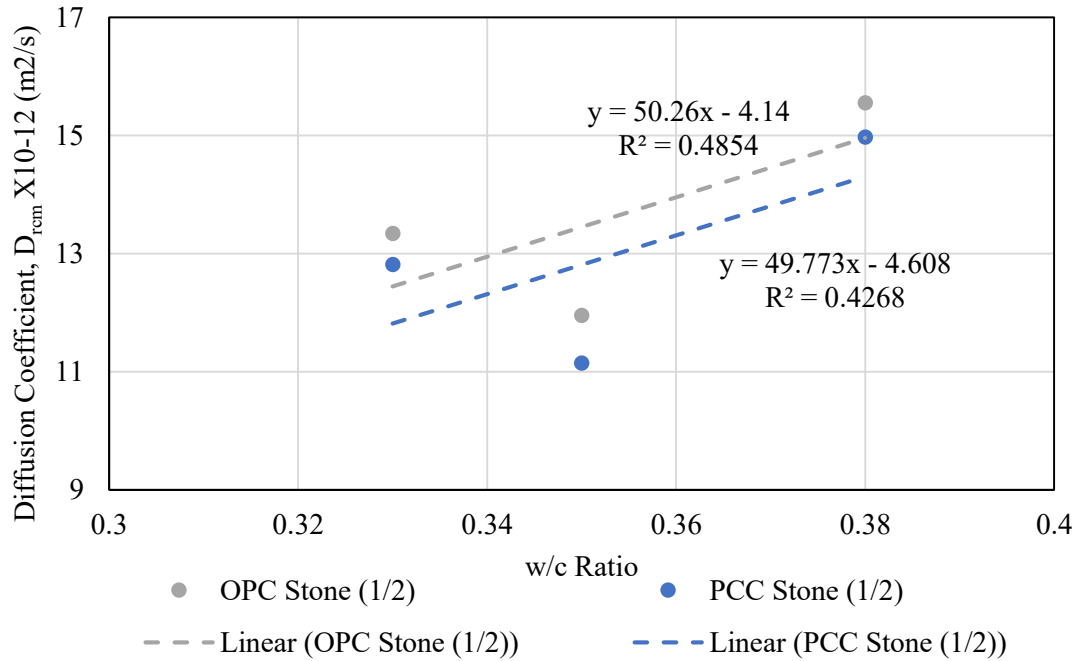
Figure 5.8.3.3: Effect of Variation in Cement Type on Chloride Diffusion Coefficient of SCA Mix Type 3 and Admixture

In case of concrete containing SCA mix type 1 [100% of ¾ inch (19mm) stone aggregate], as shown in Figure 5.8.3.1, PCC shows about 5-6% decrease on average in diffusion coefficient values with respect to the values obtained for OPC. The range of chloride diffusion coefficient values for PCC concrete is 12.5×10^{-12} m²/s $\sim 14 \times 10^{-12}$ m²/s for range of w/c ratio of 0.33-0.38. While the values of OPC concrete vary in the range of 13×10^{-12} m²/s $\sim 15.5 \times 10^{-12}$ m²/s for similar range of w/c ratio.

Figure 5.8.3.2 shows effect of variant cement types on diffusion coefficient values of concrete containing SCA mix type 2. The graph shows comparatively lower values of diffusion coefficient for PCC fluctuating within the range of 9×10^{-12} m²/s $\sim 11.1 \times 10^{-12}$ m²/s for w/c ratio range of 0.33-0.38. In contrast, concrete containing OPC demonstrates about 15% ~65% increase in their diffusion coefficient values for w/c ratio of 0.33-0.38.

As for concrete containing stone aggregate of mix type 3 [100% of ½ inch (12.5mm) downgraded], the difference between diffusion coefficients of OPC and PCC is observed to be $0.5 \sim 0.7$ $(\times 10^{-12})$ m²/s for w/c ratio varying between 0.33 and 0.38. Concrete with PCC shows comparatively lower values which usually fall within the limit of 11.8~15 $\times 10^{-12}$ m²/s. These observations can be supplemented by a graphical representation, as portrayed in Figure 5.8.3.3.

In all cases, concrete with PCC, stone aggregate and low w/c ratio can be concluded to possess acceptable resistance to chloride ingress based on their diffusion coefficient values. Similarly, in case of concrete with OPC, all mix variations result in acceptable resistance to chloride ingress. All of these above mentioned observations, eventually, validate the facts considered for better permeability performance of PCC as discussed in previous sections.

5.9 Effect of Variation in Cement Type on Resistivity of Concrete Samples

This section presents discussion on the effect of cement type variation on resistivity values of concrete samples for three different cases considered as shown below:

5.9.1   CASE A: Stone Aggregate Concrete with High w/c Ratio (0.42-0.55)

Concrete with higher electrical resistivity is considered to have lower chloride ion penetration and corrosion susceptibility. It can be deduced based on the graph shown in Figure 5.7.1 that concrete with PCC and stone aggregate shows much higher resistance to ion flow for w/c ratio less than 0.48 as compared to the concrete with OPC in it.
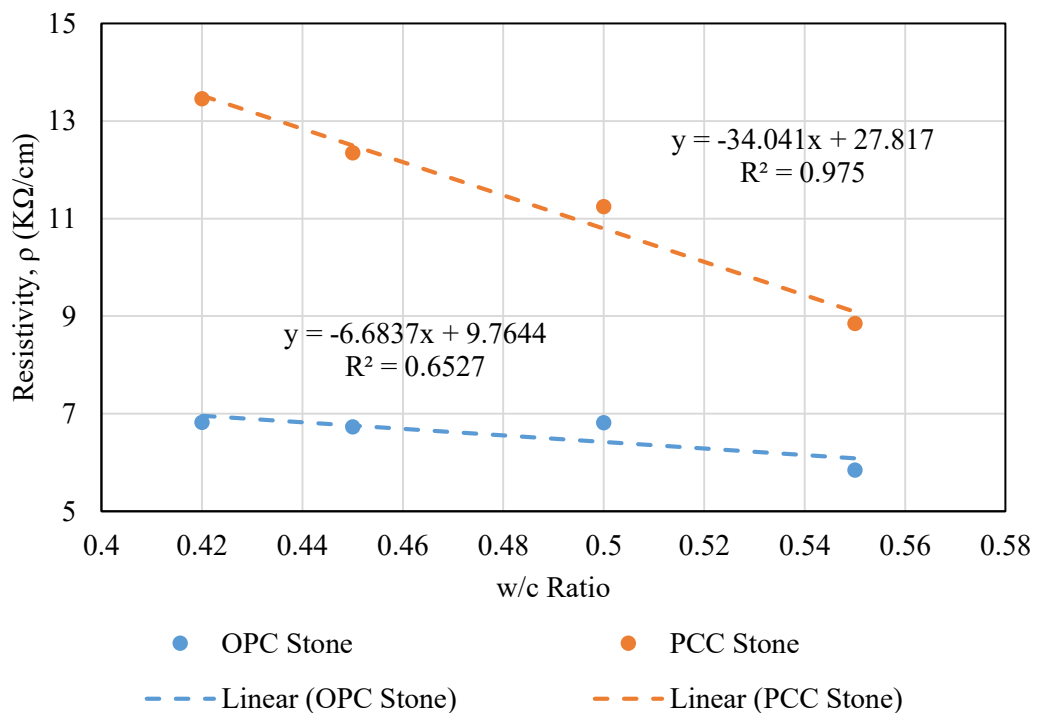
Figure 5.9.1: Effect of Variation in Cement Type on Resistivity of Stone Aggregate

From the graph (Figure 5.9.1) the increase in resistivity, in case of PCC, can be observed to be 91-93% on average as compared to the values for OPC. However, for higher range of w/c ratio (0.5-0.55) the increase is comparatively less (50-51% on average as compared to OPC).

Based on the resistivity data collected, concrete prepared with OPC and stone aggregate can be rated as to possess high corrosion risk for w/c ratio higher than 0.42 (RILEM TC 154, 2000; Polder, 2001). As for probable corrosion rate, concrete with OPC and stone aggregate likely to endure high corrosion rate (as per the recommended value in Table 4.5 by Langford and Broomfield, 1987). However, in case of PCC, the concrete mixes with w/c ratio in between 0.42 -0.5 likely to face moderate corrosion risk and low to moderate corrosion rate. While, the mixes with w/c ratio higher than 0.5 can be assumed to undergo high risk of corrosion and high corrosion rate. These observations show harmony with the pattern observed in case of chloride diffusion coefficient and validate that PCC is more effective than OPC from durability considerations.

5.9.2 CASE B: Brick Aggregate Concrete with High w/c Ratio (0.42-0.5)
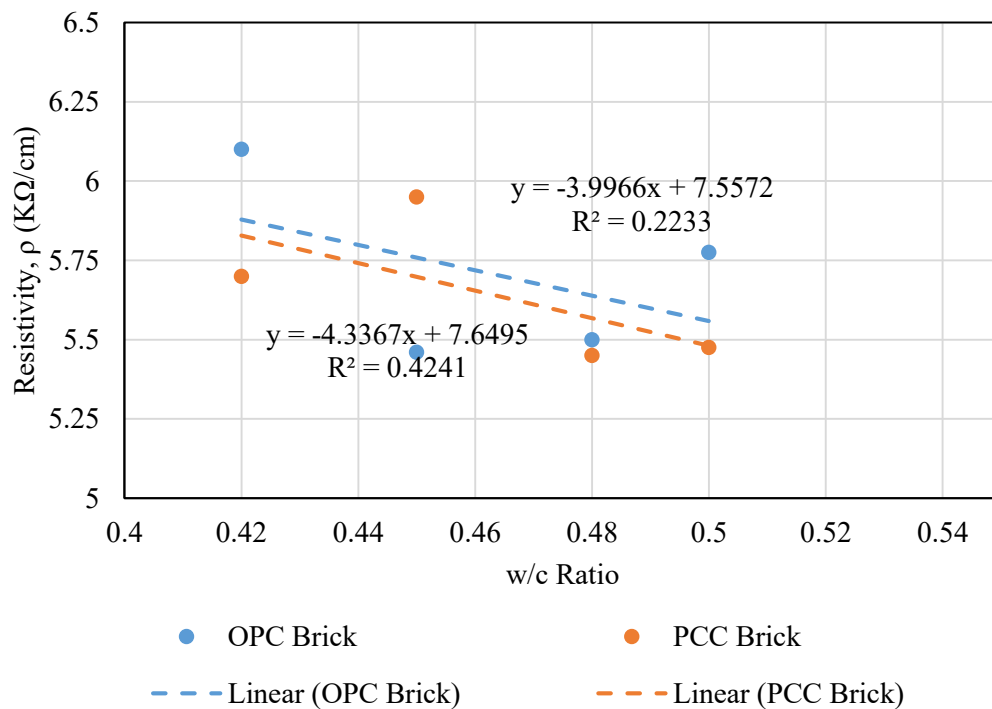
Figure 5.9.2: Effect of Variation in Cement Type on Resistivity of Brick Aggregate

It can be inferred from Figure 5.9.2 that PCC yields concrete is relatively better resistance to ion flow. However, the difference between resistivity values of OPC and PCC concrete for certain w/c ratio (0.42-0.5) is considerably low. This can be attributed to the high absorption capacity of brick aggregates that in turn minimize the pore refining effect induced by PCC. Nevertheless, the resistivity measurement cannot solely be considered as defining factor to distinguish between PCC and OPC in case of brick aggregate concrete. Instead it must be complemented with the diffusion coefficient data as it shows significant variation between OPC and PCC.

5.9.3 CASE C: Stone Aggregate Concrete with Low w/c Ratio (0.33-0.35)

Figure 5.9.3.1 to Figure 5.9.3.3 showcase effect of different cement type on resistivity values for stone aggregate concrete with low w/c ratio (0.33-0.35) and water reducing admixture (to attain workability objective).
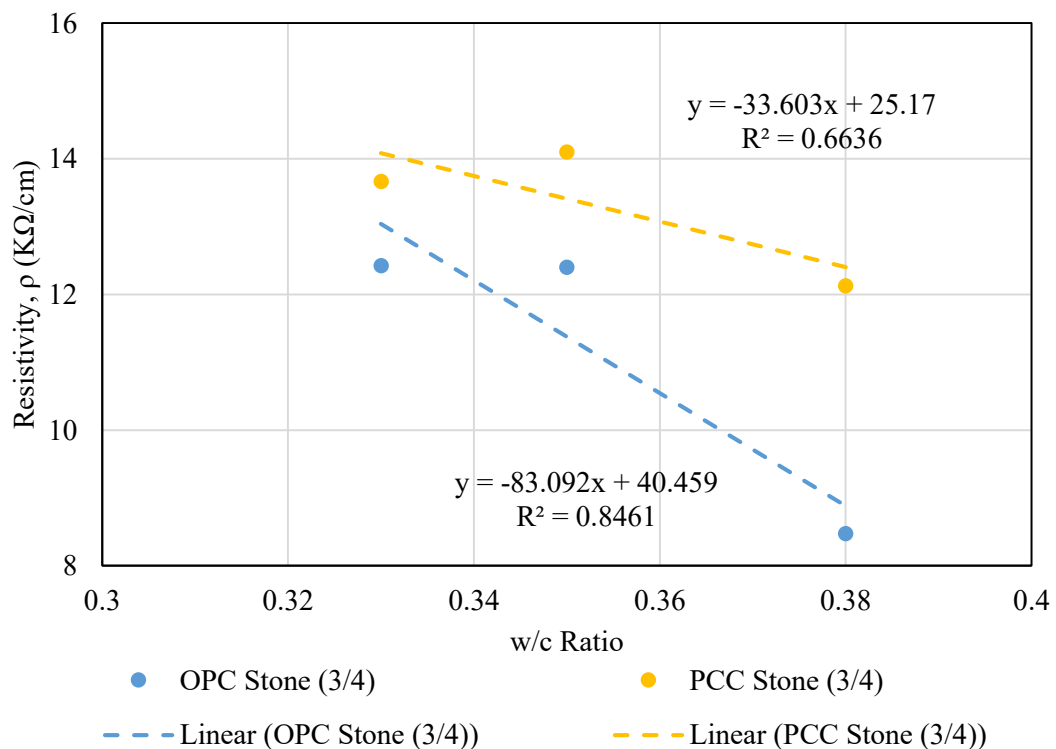
Figure 5.9.3.1: Effect of Variation in Cement Type on Resistivity of SCA Mix Type 1 and Admixture
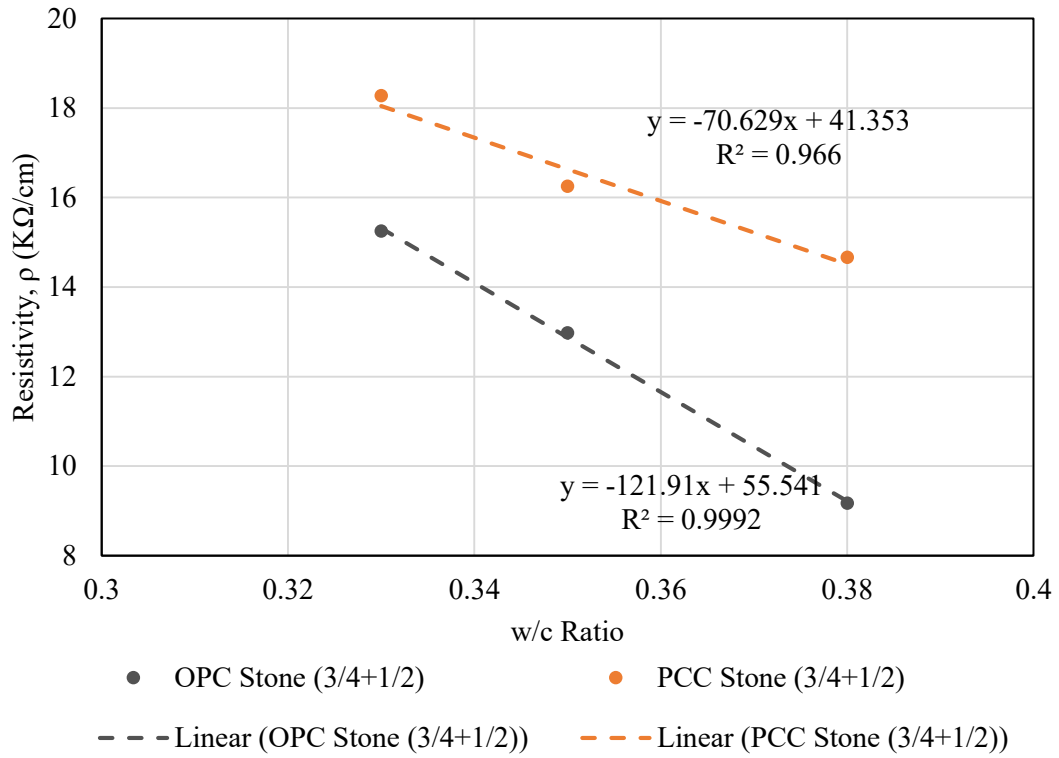
Figure 5.9.3.2: Effect of Variation in Cement Type on Resistivity of SCA Mix Type 2 and Admixture
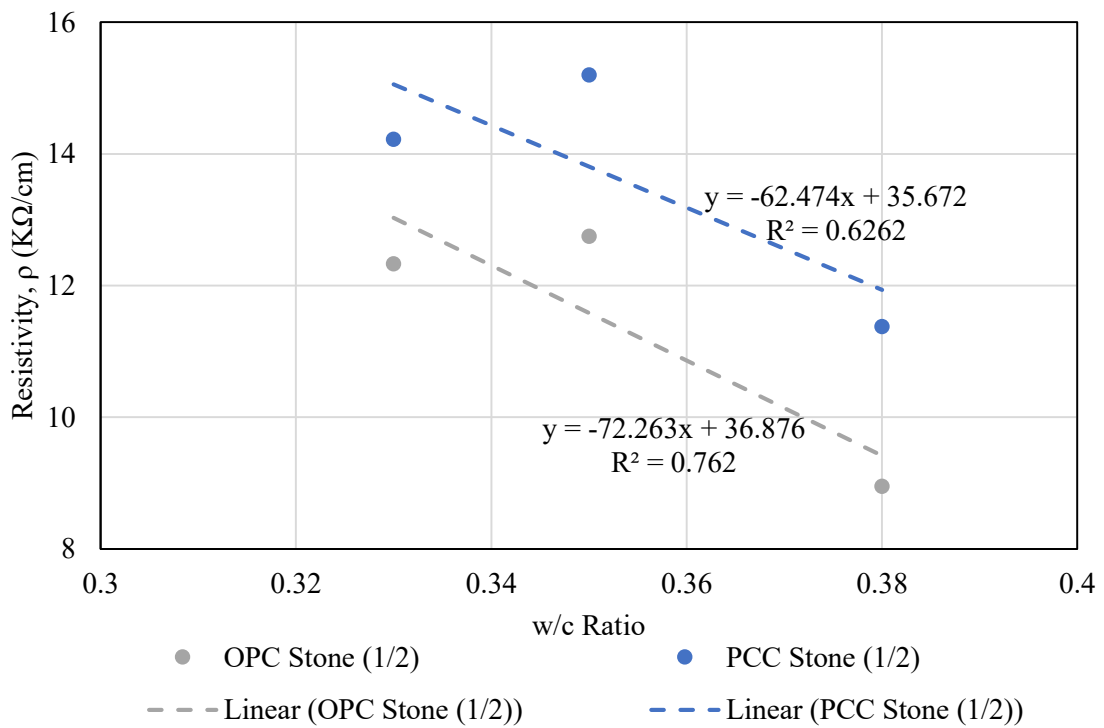
Figure 5.9.3.3: Effect of Variation in Cement Type on Resistivity of SCA Mix Type 3 and Admixture

Concrete containing PCC and stone aggregate mix of type 1 shows about 8-40% increase in resistivity values for varying w/c ratio of 0.33-0.38 as compared to its OPC counterpart. This observation is made based on the trend line shown in Figure 5.9.3.1. Figure 5.9.3.2 shows the trend line of the resistivity data of OPC and PCC concrete collected for mix prepared using SCA mix type 2. This figure also shows higher resistivity values in case of PCC. However, the increment, in this case, can be found to be in the range of 18%-57% for increase in w/c ratio from 0.33 to 0.38. As for concrete containing stone aggregates mix type 3 (shown in Figure 5.9.3.3), PCC portrays 20-21% increase, on average in resistivity value as compared to that of OPC for w/c ratio 0.33-0.38.

Based on the resistivity value, concrete with OPC and w/c ratio 0.37-0.38 can be concluded to face high risk of corrosion, as per RILEM TC 154 (2000) and Polder (2001), irrespective of the aggregate gradation. This is because the resistivity values for such mixes are less than code specified limiting value of 10 KΩ/cm. On the contrary, OPC with w/c ratio 0.33-0.36 and all PCC mixes show moderate corrosion occurrence risk. As for probable corrosion rate, all PCC mixes and OPC mixes with w/c ratio 0.33-0.36 can be considered to face low to moderate corrosion rate while OPC mixes with w/c ratio 0.37-0.38 will face high corrosion rate (as per the value shown in Table 4.3, Chapter 4).

5.10 Effect of Variation in Admixture Content and Cement Content on Chloride Diffusion Coefficient

For this study, three different admixture contents – 0.8L, 1L and 1.2L per 100Kg of cement were chosen to study their effect on the durability aspect of concrete structures. Usage of higher dosage of admixture provides higher slump. Therefore, varying admixture content was used to produce concrete with varying level of workability and observe effect of such variation on their chloride ingress resisting capability. Concrete mixes were prepared using 3 types stone aggregate mix as mentioned earlier (SAC mix type 1, SAC mix type 2 and SAC mix type 3) and a common w/c ratio of 0.35. Now, with the intention of reciprocating the situation without the usage of admixture, 180 Kg/m^3, 187.73 Kg/m^3 and 195.27 Kg/m^3 water content were used to prepare concrete mixes to maintain the equivalent slump. In order to maintain the w/c ratio of 0.35 the cement content was increased to 514 Kg/m^3, 534 Kg/m^3 and 558 Kg/m^3. These six types of mixes can be categorized as follows:

Table 5.1: Mix Variations with and without Admixture for Similar Slump

Mix Type	Mix Detail	Slump, mm
A	w/c = 0.35; 0.8L Admixture /100 Kg of Cement	100-178
B	w/c = 0.35; 1.0L Admixture /100 Kg of Cement	170-210
C	w/c = 0.35; 1.2L Admixture /100 Kg of Cement	185-225
D	w/c = 0.35; water content = 180 Kg/m^3; Cement = 514	100-154
E	w/c = 0.35; water content = 187.73 Kg/m^3; Cement = 534	120-177
F	w/c = 0.35; water content = 195.27 Kg/m^3; Cement = 558	166-182

The effect of these variations on chloride diffusion coefficient values is presented in the Figure 5.10.1.From the figure it can be depicted that use of admixture has a profound impact on the concrete's permeability. On the other hand, concrete mixes with lower w/c ratio and higher cement content fails to show similar level of performance in resisting chloride ingress. In almost all case of SCA mix type, increase in admixture content has a very insignificant but inverse effect on chloride resistance. In case of SAC mix type 3 (100% of ½ inch), increase in admixture content by 0.2 L/100Kg of cement results in increase in diffusion coefficient by 0.5-0.6 $X10^{-12}m^2$/s. While, in case of SCA mix type 1, the increase is $0.02X10^{-12}m^2$/s for change in admixture content from 0.8L to 1.0L and incase of mix type 2, the increase is $0.1X10^{-12}m^2$/s for change in admixture content from 0.8L to 1.0L.

However, mix type A, B and C in place of mixes D, E and F results in 44-46%, 41-43% and 33-34% improvement, on average, respectively, in chloride resistance. Higher cement content is required since often mixes are designed for high slump but without any admixture. Therefore, mixes D, E and F were prepared without admixture. However, from the result it is found that such practice of increasing the water content along with cement content does not show good performance from durability aspects.
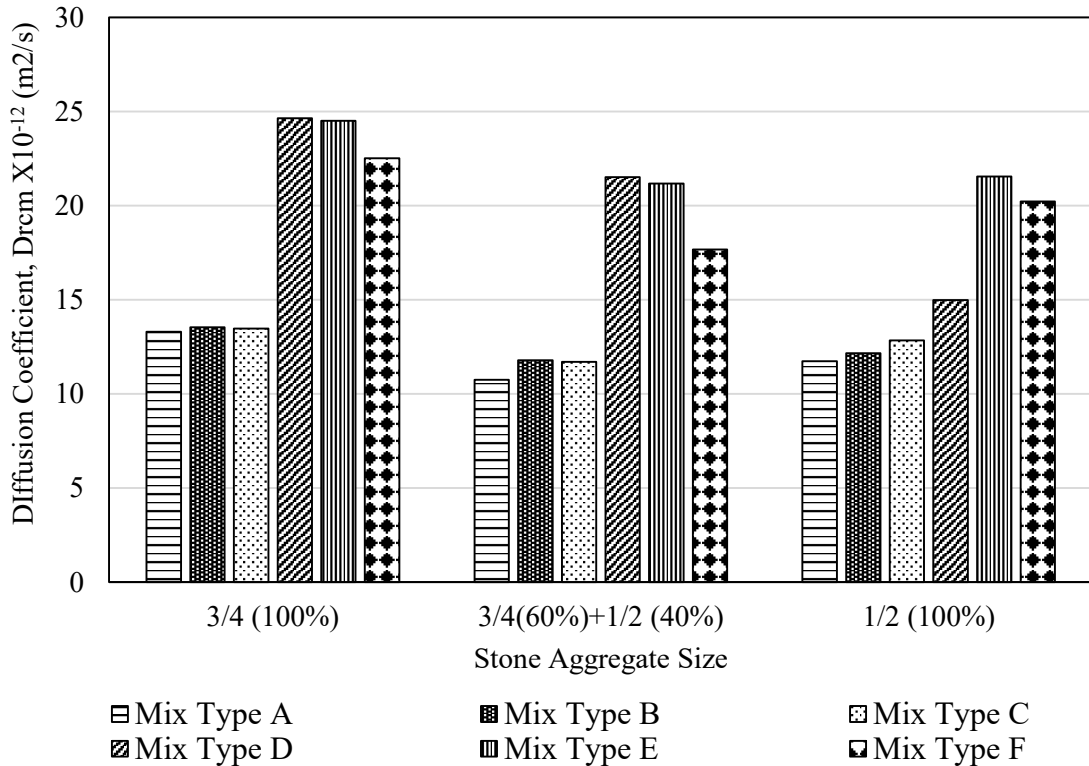
Figure 5.10.1: Effect of Admixture Content and Cement Content on Diffusion Coefficient

5.11 Effect of Variation in Admixture Content and Cement Content on Resistivity

The effect of mix type variations A, B, C, D, E and F (shown in table 5.1) on resistivity values is presented in the Figure 5.11.1. From the figure it can be depicted that use of admixture has a profound impact on the improvement of concrete's resistivity. On the other hand, concrete mixes with higher water and OPC cement content show lower resistivity indicating poor performance in resisting chloride ingress as compared to the mix with admixture. In case of SAC mix type 1, the resistivity value can be found to vary from 12.67 to 12 KΩ/cm for admixture content variation from 0.8L to 1.2L. In case of mix type 2, these values are 17.55 KΩ/cm to 13.7 KΩ/cm and in case of SAC mix type 3, 15.67 KΩ/cm to 13.3KΩ/cm. These observations validate the previous remarks on decrease in chloride resistance of concrete with increase in admixture content. However, addition of admixture to an optimum dosage can significantly improve the concrete's resistivity as compared to usage of higher cement content. As for mix type D, E and F, the resistivity can be seen to increase from 5.45 KΩ/cm to 6.55KΩ/cm and from 6.75KΩ/cm to 7.85KΩ/cm with increase in water content and cement content required to attain slump without admixture, in case of SCA mix type 1 and 2,

respectively. However, in case of SCA mix type 3, the value decreases from 8.35 KΩ/cm to 6.7KΩ/cm and then increases to 6.95KΩ/cm for cement content variation 514-558Kg/m^3.
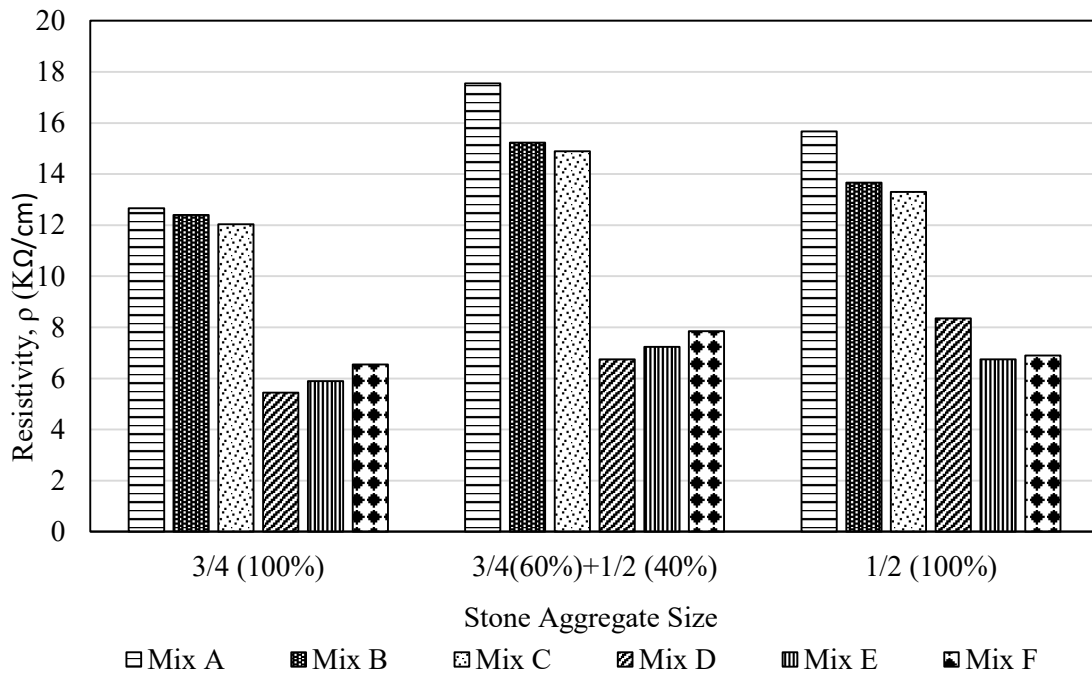
Figure 5.11.1: Effect of Admixture Content and Cement Content on Diffusion Coefficient

5.12 Correlation between Concrete Diffusion Coefficients and Electrical Resistivity of Concrete

Usage of diffusion coefficients, as a performance based parameter for assessing durability of RC structures, has been increased in recent years (Sengul, 2014). The diffusivity value signifies the concrete's resistance against chloride penetration. The higher the coefficient value, the lower the resistance. However, the concrete's resistance to ion flow can also be expressed in terms of electrical resistivity. The higher the resistivity value, the higher will be the concrete's resistance against chloride diffusion. In this study, an attempt has been made to correlate diffusion coefficients with resistivity values of the concrete mixes considered so that in future the relation can be used to evaluate one unknown value from another known one. The following sections contain details on the correlations established for the different types of concrete mixes.

5.12.1 CASE A: Stone Aggregate Concrete (w/c Ratio = 0.42~0.55)

Figure 5.12.1 represents the correlation between diffusivity and resistivity of stone aggregate concrete with w/c ratio of 0.42 to 0.55.

Figure 5.12.1: Correlation Between Diffusion Coefficients and Resistivity of Stone Aggregate Concrete (w/c ratio : 0.42~0.55)

It can be observed from the figure that in case stone aggregate concrete, diffusion coefficient varies inversely to the value of concrete resistivity and follows a trend line of equation y = $129.79x^{-0.865}$. The observed correlation produces an R value of 0.942 (R^2=0.888). This signifies 94% the observed data are close to the fitted regression and indicates a good correlation between chloride diffusion coefficients and resistivity value of concrete containing stone aggregate and w/c ratio>0.42. This correlation is mainly valid for resistivity data range of 5 kΩ/cm to 14 kΩ/cm.

5.12.2 CASE B: Brick Aggregate Concrete (w/c Ratio = 0.42~0.5)

Figure 5.12.2 shows the correlation between diffusion coefficients and electrical resistivity of brick aggregate concrete. This correlation is mainly valid for resistivity data range of 3.9 kΩ/cm to 6.1 kΩ/cm. In case of brick aggregate concrete, diffusion coefficient decreases with increasing resistivity values following a data trend of y = $95.959x^{-0.793}$. The coefficient of

correlation for this trend is found to be 0.789 (for R^2=0.6226) indicating existence of relatively moderate correlation. In order to obtain a more pronounced correlation more extensive data collection is required.
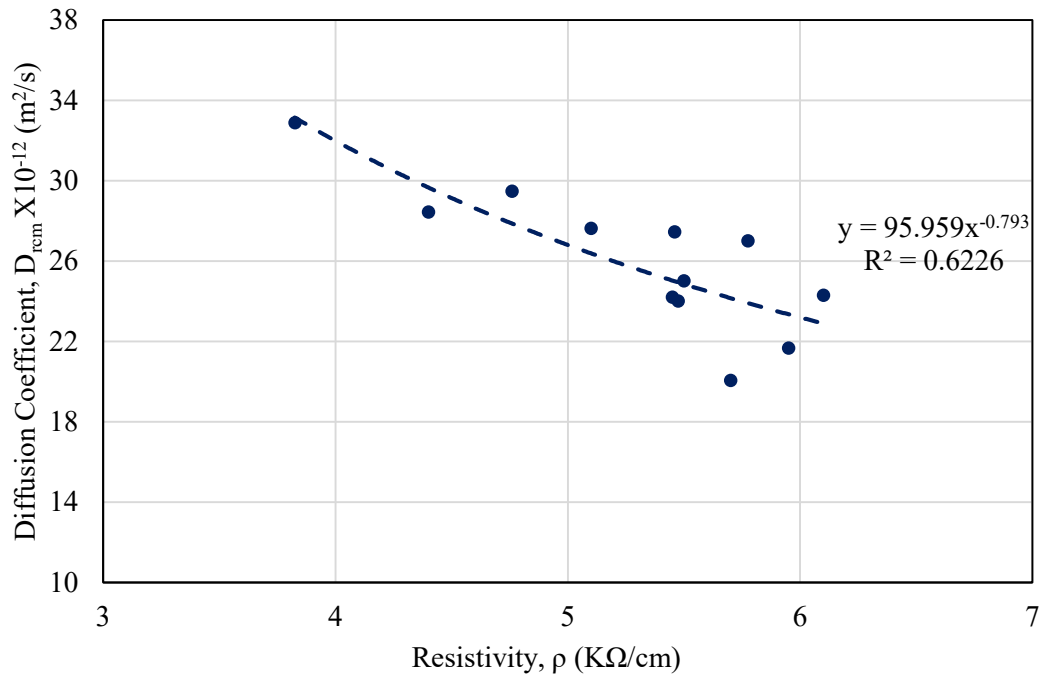
Figure 5.12.2: Correlation Between Diffusion Coefficients and Resistivity of Brick Aggregate Concrete (w/c ratio : 0.42~0.50)

5.12.3 CASE C: Stone Aggregate Concrete (w/c Ratio = 0.33~0.38)

Figure 5.12.3 displays the correlation between diffusion coefficients and electrical resistivity of stone aggregate concrete of low w/c ratio (0.33~0.38). In order to increase workability of such mixes a water reducing admixture was used.

This correlation follows data trend of equation $63.8x^{-0.626}$ and is mainly valid for resistivity data range of 8 kΩ/cm to 18 kΩ/cm. Moreover, the coefficient of correlation for this trend is found to be 0.943 (for R^2=0.8893) indicating fit of 93% of the dataset to the regression line. Therefore, the correlation can be considered as strong one and can be used for future data evaluation.
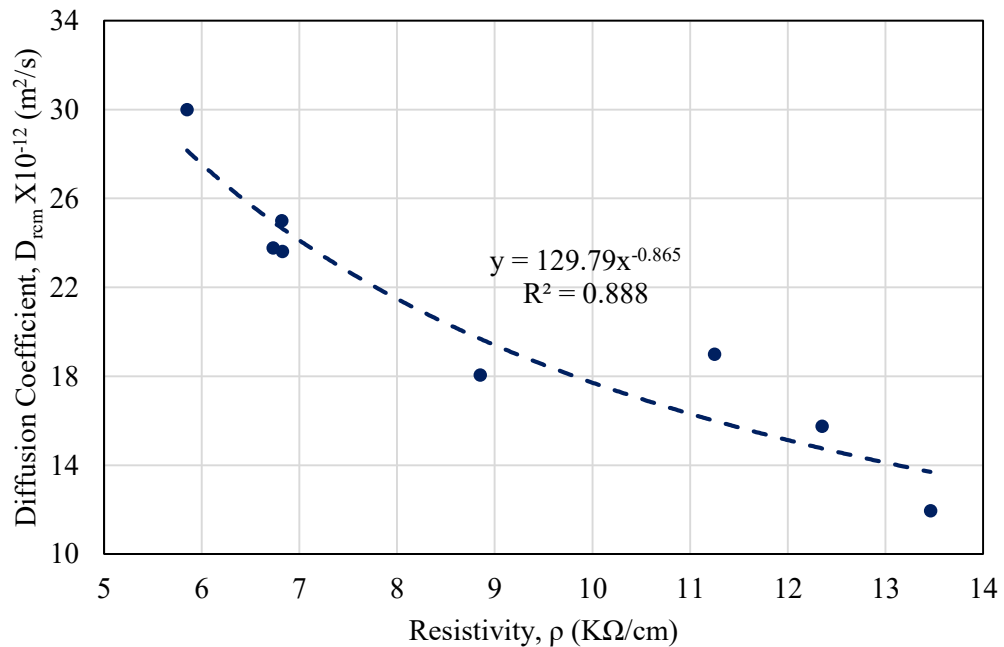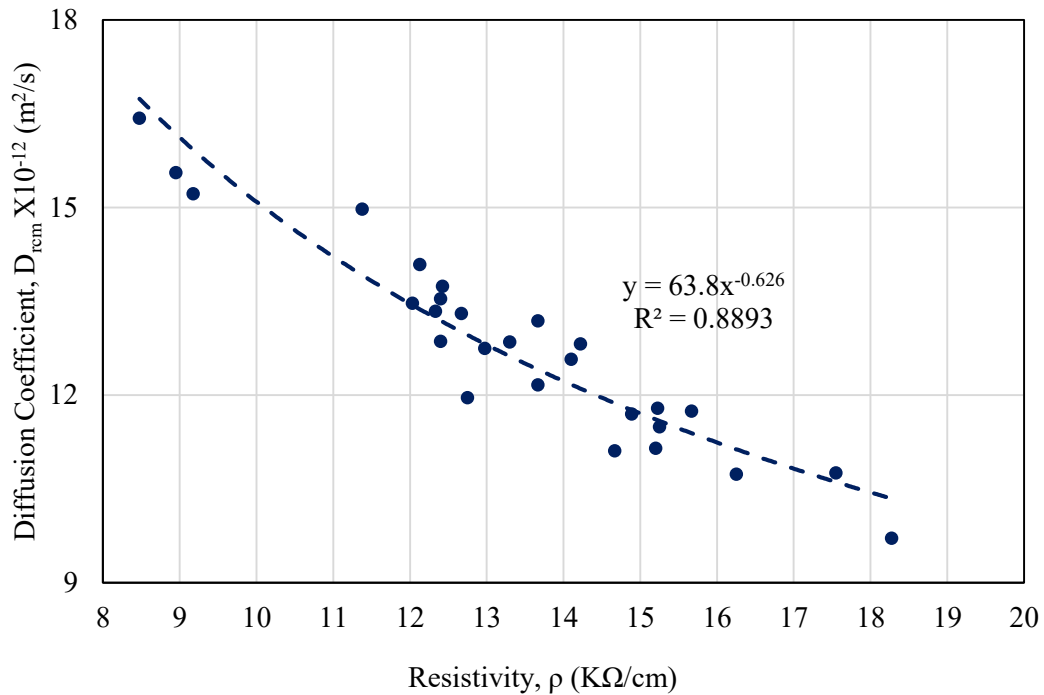
Figure 5.12.3: Correlation Between Diffusion Coefficients and Resistivity of Stone Aggregate Concrete (w/c ratio : 0.33~0.38)

5.13 Overview

The diffusion coefficient value for each concrete mix considered, determined from the test result of non-steady state migration test, was analyzed for variations. Higher value of diffusion coefficient signifies high permeability and thus low resistance to chloride intrusion. The obtained results show high chloride resistance of concrete with stone aggregate and PCC while lower resistance is observed in case of brick aggregate concrete. Usage of PCC in place of OPC imparts significant improvement to concrete's resistance to chloride ingress. Moreover, use of admixture also seems to improve concretes' permeability to a significant extent. All the observed pattern appear to comply with the established trends and provide quantitative basis to such trends for future use. Besides, these diffusivity data can further be used in calculating corrosion initiation time which is a significant portion of a RC element's total service life from durability perspective. Another durability parameter, resistivity of concrete was also measured. The resistivity values are in compliance with the established pattern, as well and show good correlation with the diffusion coefficient data. These correlation will aid in determining unknown value of any parameter from another known parameter value, in future.

6.1 General

Degradation of the serviceability of a reinforced concrete (RC) structure and the control over the deterioration over its service life are the key components to be considered in durability design of concrete infrastructures. The deterioration of the RC structures depends on the mix parameters, rebar and concrete properties and the environment that it is exposed to. As for the prevalent construction practice in Bangladesh, these durability concerns are often neglected. Thus, understanding the effects of commonly practiced concrete mix parameters such as mix proportions, w/c ratio, cement type etc. along with some of the design aspects like- cover, diameter of embedded rebar etc. on durability design considerations has become critical. This chapter attempts to shed light on their effects on the serviceability of RC structures and predict service life of such structures based on the results from the durability tests performed on some common concrete mixes of Bangladesh. The chapter is subdivided into several sections with each sections presenting different aspects. Initial sections present a general idea regarding service life modelling process followed by the sections outlining the effects of mix parameters on the corrosion initiation time. The latter sections discuss the time required for severe corrosion damage and its variation for changes in different variables. The chapter is concluded with the values of the predicted service life of different types of concrete mixes for a chosen set of exposure class and concrete cover parameter.

6.2 Service Life Modelling

Service life modelling involves determination of real time performance value such as service life of concrete structures by implementing the durability parameters like chloride migration coefficients. When a concrete structure is exposed to a marine environment like the southern belt of Bangladesh, it's service life primarily depends on the time required to initiate the corrosion of rebar and the time to occur severe damage due to the initiated corrosion process. Various service life models like Duracrete (1998; 2015), LNEC E465 (2005) etc. were developed to predict the time of corrosion initiation using large amounts of empirical data on the chloride ion penetration in concrete, migration coefficient of concrete, threshold chloride content to initiate corrosion of concrete, concrete cover and influence of blended cements on

corrosion of reinforcement. There are also some well-established methods for example-Mullard and Stewart (2009) to forecast the time for severe damage.

In order to attain the specified objectives of this research, the corrosion initiation time, crack initiation time and crack propagation time was evaluated as per the model suggested by Duracrete (1998), El Maaddawy and Soudki (2007) and Mullard and Stewart (2009), respectively. The following assumptions were made prior to the calculation:

a) Only chloride induced corrosion was considered.

b) Although carbonation accelerates free chloride formation, the interaction between carbonation and free chloride was omitted from present study due to lack of quantitative evidence (Wang et al., 2010).

c) Chloride ingress reducing effect of carbonation was not considered.

d) Chloride ingresses into concrete through diffusion only.

6.3 Equations, Parameters and Values Considered

In order to observe concrete performance for different environmental actions related to chloride induced corrosion, four types of exposure classes were considered. The exposure classifications, selected as per the specification of FIB Bulletin 34 (2006) are given below with corresponding chosen concrete cover value in parenthesis:

a) XD: Corrosion induced by chlorides other than from sea water-
   o XD1=Concrete surface with moderate humidity and exposed to airborne Cl- (25mm, 37.5mm and 50mm)
   o XD2=Structures like bridges exposed to spray containing Cl- (37.5mm, 50mm, 62.5mm and 75mm)

b) XS: Corrosion induced by chlorides from sea water-
   o XS1=Concrete structures near or on the coast and exposed to airborne Cl- (25mm, 37.5mm and 50mm)
   o XS2=Marine structures in tidal and splash zones and exposed to cyclic wet and dry (37.5mm, 50mm, 62.5mm and 75mm)

Considering these cover range and exposure categories, service life for different types of concrete were predicted in terms of corrosion initiation time, crack initiation time and crack propagation time. The relevant equations and affecting parameters with their corresponding values are given below:

a) Corrosion Initiation Time: Corrosion initiation time was calculated based on the model developed by Duracrete (1998) and slightly revised by DARTS (2004) research projects (FIB Bulletin 34, 2006):

$$Ccrit = Co + (Cs, \Delta x - Co)\left[1 - \text{erf}\left(\frac{x - \Delta x}{2.\sqrt{Ke.Kt.(\frac{to}{t})^a.Drcm(to).t}}\right)\right] \text{----------(6.1)}$$

Here,

Diffusion Coefficient at time t_o, D_{rcm} (m^2/s) from diffusion coefficient tests as per NT BUILD 492 (1999).

Time to initiate corrosion at cover x, t (years)

Environmental Variable, $K_e = \exp[be.\left(\frac{1}{Tref} - \frac{1}{Treal}\right)]$ ------------------------------(6.2)

	XD1	XD2	XS1	XS2	
Depth of Convection Zone, Δx (mm)	0	10	0	10	
Regression Variable, b_e (^oK)	4800				
Temperature of the Ambient, T_{real} (^oK)	303				
Standard Test Temperature, T_{ref} (^oK)	303				
Aging Exponent or Factor, α or a	0.65	0.3	0.65	0.3	OPC
	0.65	0.6	0.65	0.6	PCC
	-	0.45	-	0.45	PCC
Transfer Coefficient, K_t	1				
Chloride Concentration, C_{crit} or $C_{Dc,t}$ (% by weight of cement)	0.6				
Initial Chloride Concentration, C_o (% by weight of cement)	0.1				
Chloride Concentration at Δx, $C_{\Delta x,S}$ (% by weight of cment)	1	2	1.5	2	
Reference (RMT test) Time, t_o (years)	0.1233	0.1233	0.1233	0.1233	

All values considered here are chosen from FIB Bulletin 34 (2006). Values of aging exponent is mainly function of cement type and exposure classes. The composite cement used in this study contains both fly ash and slag. Therefore, corrosion initiation time were measured using

the values corresponding to fly ash added composite cement and slag added composite cement. Aging exponent value of the PCC used in this study can be expected to fall between these two values. Hence, it would be prudent to use the aging exponent determined through experimentation for such cement composition for future studies.

b) Crack Initiation Time: Crack initiation time was calculated based on the model developed by El Maaddawy and Soudki (2007):

$$t_{1st} = \left[\frac{7117.5(D+2\delta)(1+v+\Psi)}{365.icorr.Eef}\right]\left[\frac{2CFt}{D} + \frac{2\delta.Eef}{(D+2\delta)(1+v+\Psi)}\right] \text{-----------------------------------(6.3)}$$

Here,

Diameter of Reinforcing Bar, D (mm)

Concrete tensile strength, F_t (MPa) = 0.53 (compressive strength)$^{1/2}$

Effective Elastic Modulus, E_{ef}=(Elastic Modulus/1+Φ_{cr}) as per CSA Standard A23.3-94 (1994)

		XD1	XD2	XS1	XS2
Thickness of the Porous Zone around the Rebar, δ_0 (mm)	0.015				
Poisson's Ratio of Concrete, v	0.2				
Corrosion Current Density @ Temperature 20^0C, $i_{corr-20}$ (μA/cm^2)		0.175	2.586	2.586	6.035
Concrete Creep Coefficient, Φ_{cr}	2.35				

All values considered here are chosen from Duracrete (1998) and El Maaddawy and Soudki (2007). Compressive strength was measured in the laboratory for mixes considered.

c) Crack Propagation Time: Crack propagation time was calculated based on the model developed by Mullerd and Stewart (2009):

$$T_{sev} = Kr.\left[\frac{w-0.05}{Kc.ME.r(crack)}\right]\left[\frac{0.0114}{icorr.20}\right] \text{---(6.4)}$$

Here,

$$\text{Cover Cracking Parameter, } \Psi = \frac{C}{D.F_t} \text{---(6.5)}$$

$$\text{Cracking rate, r (crack) (mm/hr)} = 0.0008.\,e^{-1.7\Psi} \text{---(6.6)}$$

$$K_r = 0.95 \left[\exp\left(\frac{-0.3\,icorr.exp}{icorr,20}\right) - \frac{icorr,exp}{2500.icorr,20} + 0.3 \right] \text{----------------------------(6.7)}$$

Diameter of Reinforcing Bar, D (mm),

Cover, C (mm)

Concrete tensile strength, F_t (MPa) = 0.53 (compressive strength)$^{1/2}$[as per Mirza et al. (1979)]

Crack Width, w (mm)	1			
Confinement Factor, k_c	1.4			
Model Error for rate of Crack Propagation, $ME(r_{crack})$	1.04			
accelerated Corrosion Rate, $i_{corr\text{-}exp}$ ($\mu A/cm^2$)	100			
	XD1	XD2	XS1	XS2
Corrosion Current Density @ Temperature 20^0C, $i_{corr\text{-}20}$ ($\mu A/cm^2$)	0.175	2.586	2.586	6.035

All values and equations considered here are from Mullard and Stewart (2009).

6.4 Corrosion Initiation Time

In case of chloride induced corrosion, the corrosion of the rebar is initiated after the chloride content at rebar layer reaches a critical value required to depassivate the protective layer around the embedded rebar. The time required for the accumulation of the chloride ions inside the concrete to the critical level is defined as the corrosion initiation time (Wang et al., 2010; FIB Bulletin 34, 2006).

A full design approach for the modelling of chloride induced corrosion in uncracked concrete has been developed within the research project DuraCrete (1998) and slightly revised in the research project DARTS (2004). It is based on the limit-state equation 6.1, in which the critical chloride concentration C_{crit} is compared to the actual chloride concentration at the depth of the reinforcing steel at a time t C(x = a, t).

In Duracrete (1998; 2000a) model, it is assumed that critical chloride content is not affected by concrete quality. In some standards and directives, OVBB-Richtlinie (2003), the critical content for corrosion initiation is taken to be 0.5-0.6 (Fib Bulletin 76, 2015). In this research venture, the critical chloride content was taken to be 0.6 and time required to reach this value (corrosion initiation time) for the mixes tested for diffusion coefficient was calculated. The following sections present a detailed study on the effect of different mix proportion parameters on the corrosion initiation time. The calculations were made considering 4 exposure categories (XD1, XD2, XS1 and XS2) and five concrete cover parameters (25mm, 37.5mm, 50mm, 62.5mm and 75mm) for a constant bar diameter of 16mm.

6.5 Effect of Mix Proportion Parameters for Exposure class XS1

The XS1 exposure class includes the marine structures near or on the coast and are subjected to airborne salt. The corrosion severity of this category can be considered as a moderate one. For this exposure classes, corrosion initiation time was evaluated for 3 different concrete cover of 25mm, 37.5mm and 50mm.

6.5.1 Effect of Aggregate and Cement Type Variation

Figures 6.1.1 and 6.1.2 show variation in corrosion initiation time of stone and brick aggregate concrete with varying w/c ratio and cover for OPC and PCC, respectively.

Figure 6.1.1: Variation in Corrosion Initiation Time for Stone and Brick Aggregate (OPC)
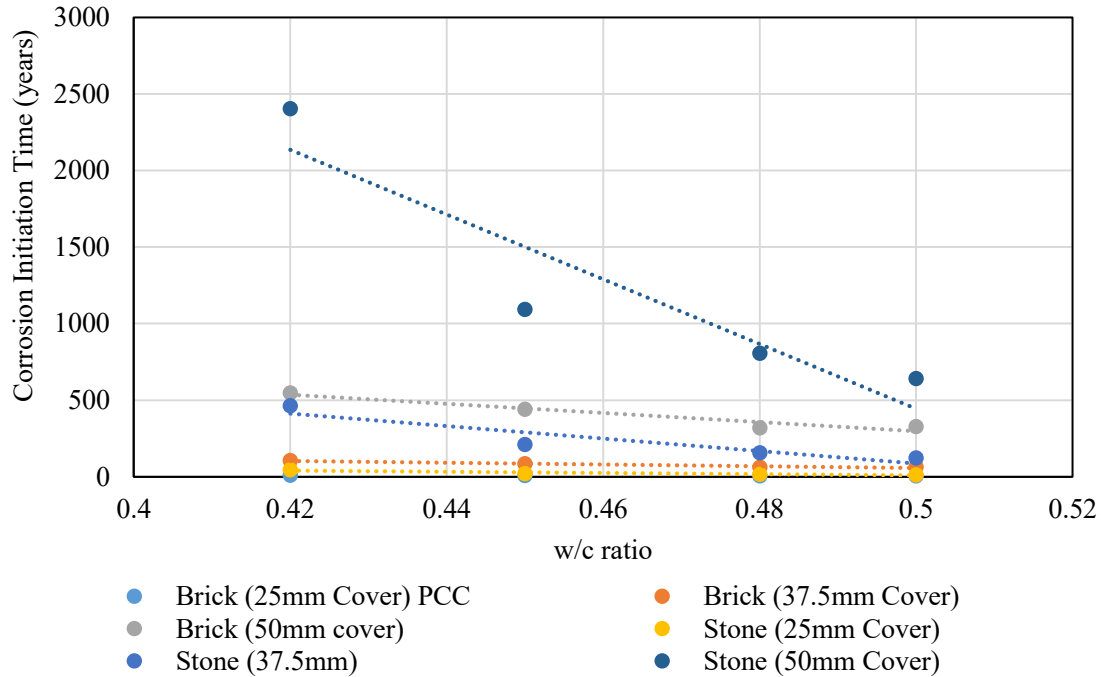
Figure 6.1.2: Variation in Corrosion Initiation Time for Stone and Brick Aggregate (PCC)

Both figure shows higher corrosion initiation time in case of stone aggregate irrespective of the cover. In general, the increase is 1 years, 7-8 years and 38 years on average as compared to the corrosion initiation time of concrete with brick aggregate and OPC for cover variation of 25mm, 37.5mm and 50mm, respectively. In case PCC these values are 16 years, 160 years and 480 years on average, respectively.

Moreover, based on the above observations it can also be deduced that addition of PCC in place of OPC increases the corrosion initiation time about 12-20 times for varying concrete cover of 25mm, 37.5mm and 50mm. For variation in cover from 25mm to 37.5mm, corrosion initiation time increases about 10 times and from 37.5 to 50mm, the increase is about 5 times.

6.5.2 Effect of Mix Proportion Variation

Figure 6.1.3 shows variation in corrosion initiation time with varying w/c ratio of 0.42-0.5 in case of brick aggregate concrete with mix proportions of 1:1.5:3 and 1:2:4. From the figure it can be observed that in almost all cases concrete with higher mix proportion results in early corrosion initiation. This can be attributed to the fact that mix proportion with high aggregate and low cement content (1:2:4) produces a more lean and porous concrete.
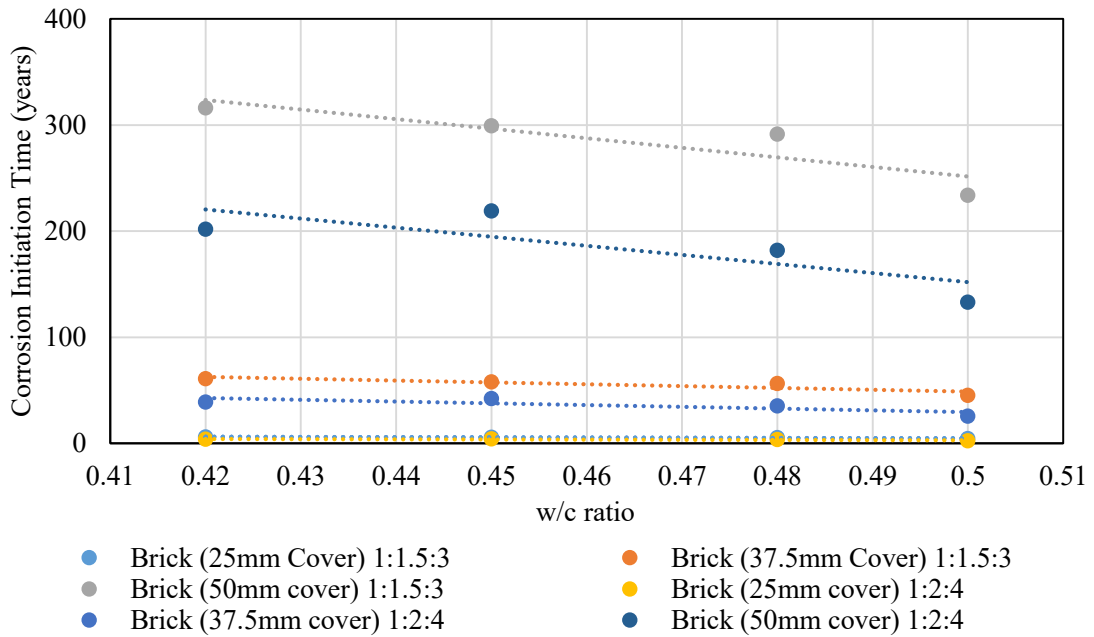
Figure 6.1.3: Variation in Corrosion Initiation Time Brick Aggregate with Variant Mix Proportion

Quantitatively, the increase in corrosion initiation time, in case of 1:1.5:3 proportion, can be observed to be about 2 years, about 19-20 years and 101 years, on average, with respect to that of mix proportion 1:2:4 for 25mm, 37.5mm and 50mm cover, respectively. Based on these observations it can also be presumed that increase in cover value results in about 10 times increase in corrosion initiation time for change in cover from 25mm to 37.5mm and about 5 times increase for change in cover from 37.5mm to 50mm.

6.5.3 Effect of Aggregate Gradation for OPC

Figures 6.1.4.1 to 6.1.4.3 show the effect of aggregate gradation of OPC concrete on the corrosion initiation time values. In all cases, SCA mix type 1 (100% of 19mm downgraded) results in least corrosion initiation time irrespective of the cover considered. From the trend lines it can be observed that all SCA mix type, for all cover variation considered, shows decreasing value of corrosion initiation with increase in w/c ratio. In almost all cases SCA mix type 2 shows higher corrosion initiation time. This because of the proper gradation of this coarse aggregate mix which results in a less permeable concrete. Whereas, between SCA mix type 1 and 3, type 3 shows higher corrosion initiation time.

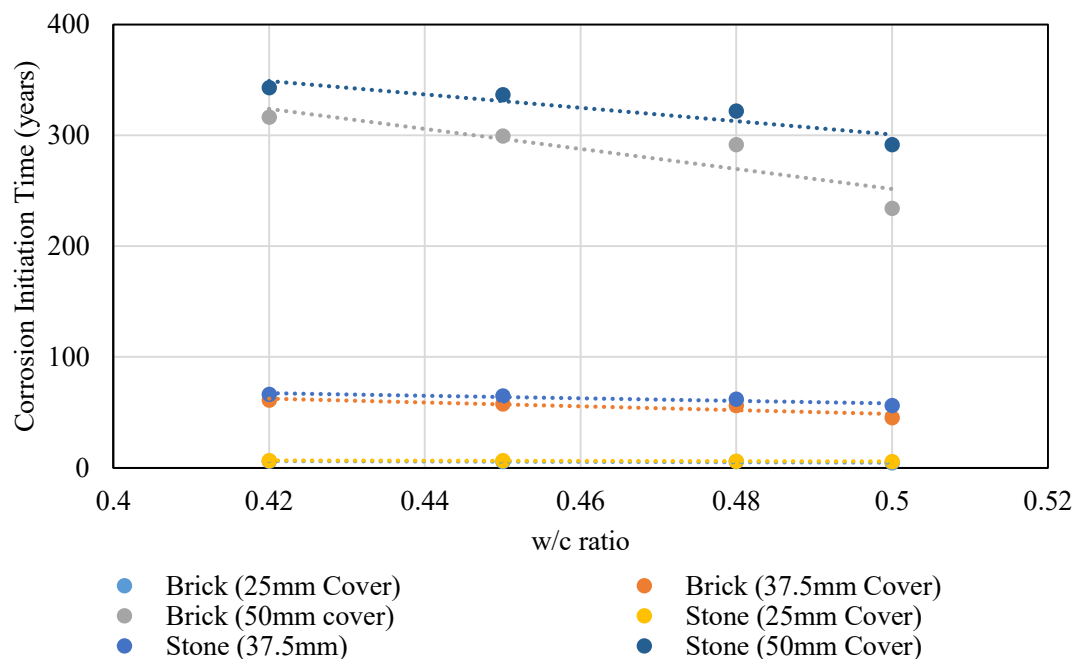Figure 6.1.4.1: Variation in Corrosion Initiation Time for Cover 25mm

Figure 6.1.4.2: Variation in Corrosion Initiation Time for Cover 37.5 mm

Figure 6.1.4.3: Variation in Corrosion Initiation Time for Cover 50 mm

From the graphs, it also can be deduced that increase in cover value from 25mm to 37.5mm results in about 10 times higher corrosion initiation times and from 37.5mm to 25mm shows about 5 times higher corrosion initiation time.

6.5.4 Effect of Aggregate Gradation for PCC

Figures 6.1.5.1 to 6.1.5.3 show the effect of aggregate gradation for concrete of PCC on the corrosion initiation time values. In all cases, SCA mix type 1 results in least corrosion initiation time irrespective of the cover considered. All SCA mix type 2 shows higher corrosion initiation time as compared to other mix types. This is due to the proper gradation of coarse aggregate mix that results in a less permeable concrete. It can be observed from the graph that all SCA mix type, for all cover variation considered, shows decreasing value of corrosion initiation with increase in w/c ratio.

From the graphs, it can also be deduced that increase in cover value from 25mm to 37.5mm results in about 10 times higher corrosion initiation times and from 37.5mm to 25mm shows about 5-5.5 times higher corrosion initiation time.
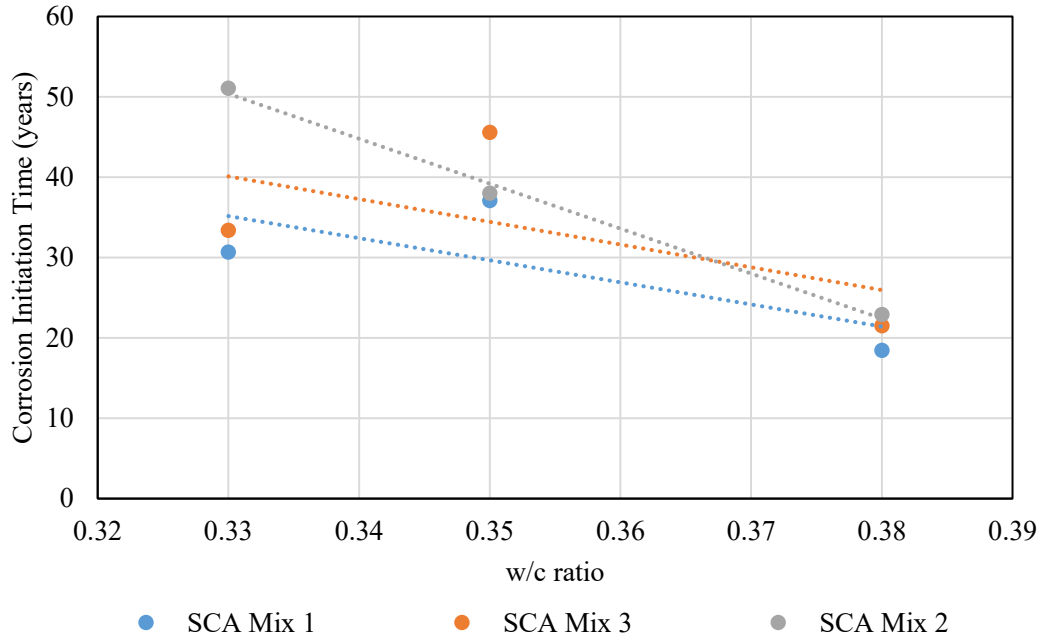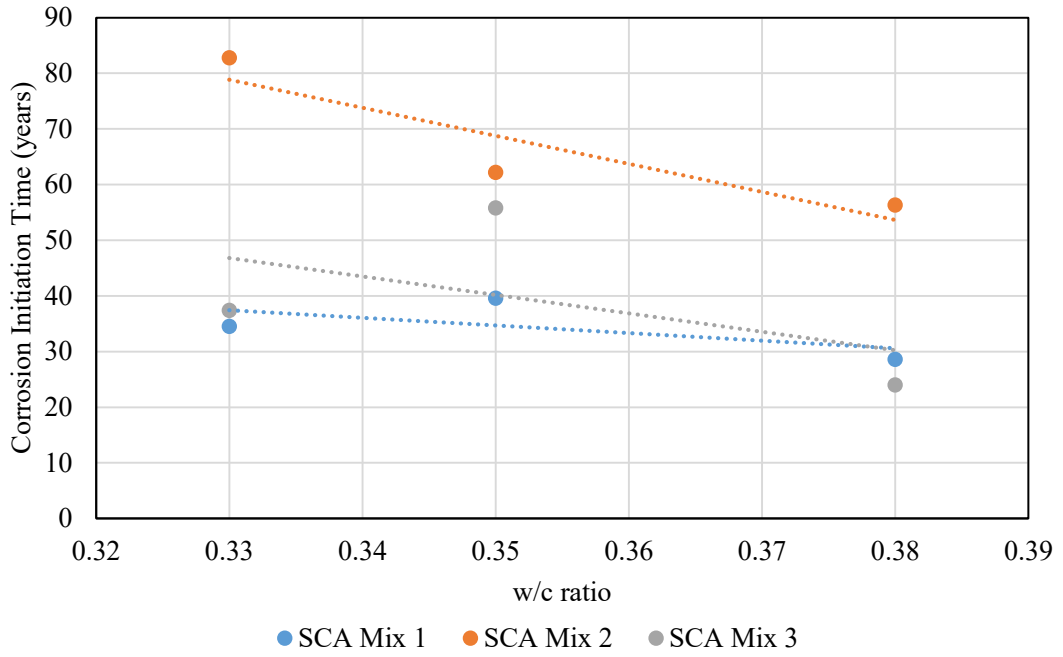
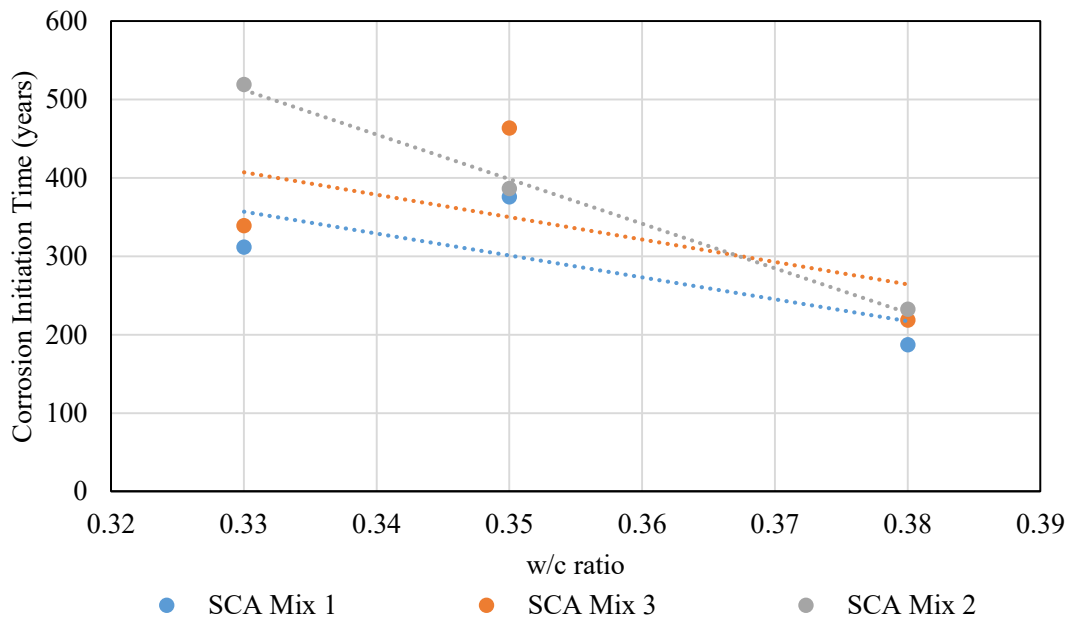Figure 6.1.5.1: Variation in Corrosion Initiation Time for Cover 25mm

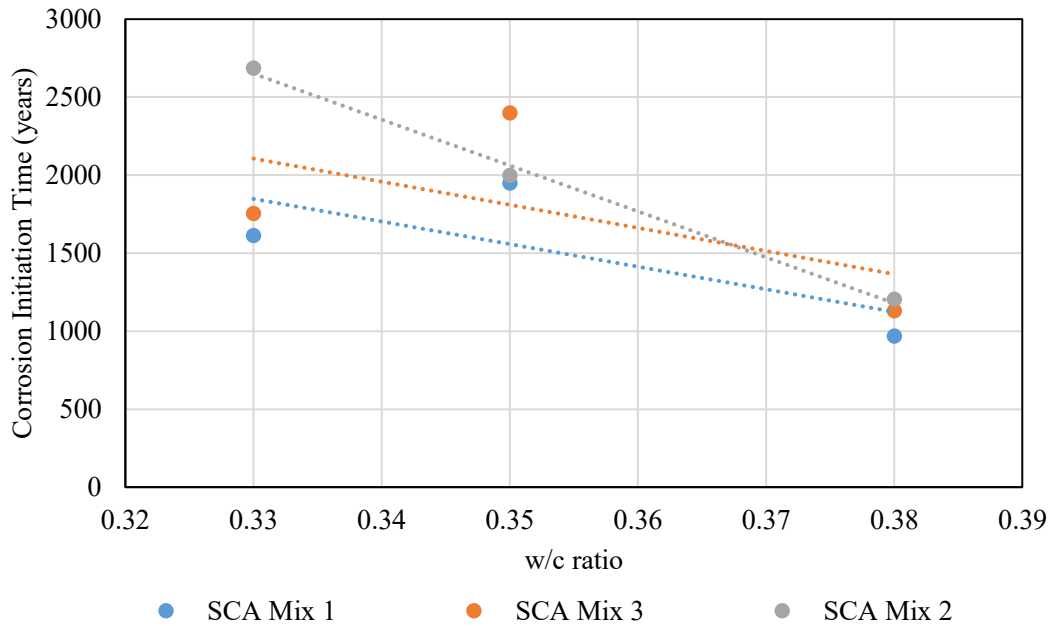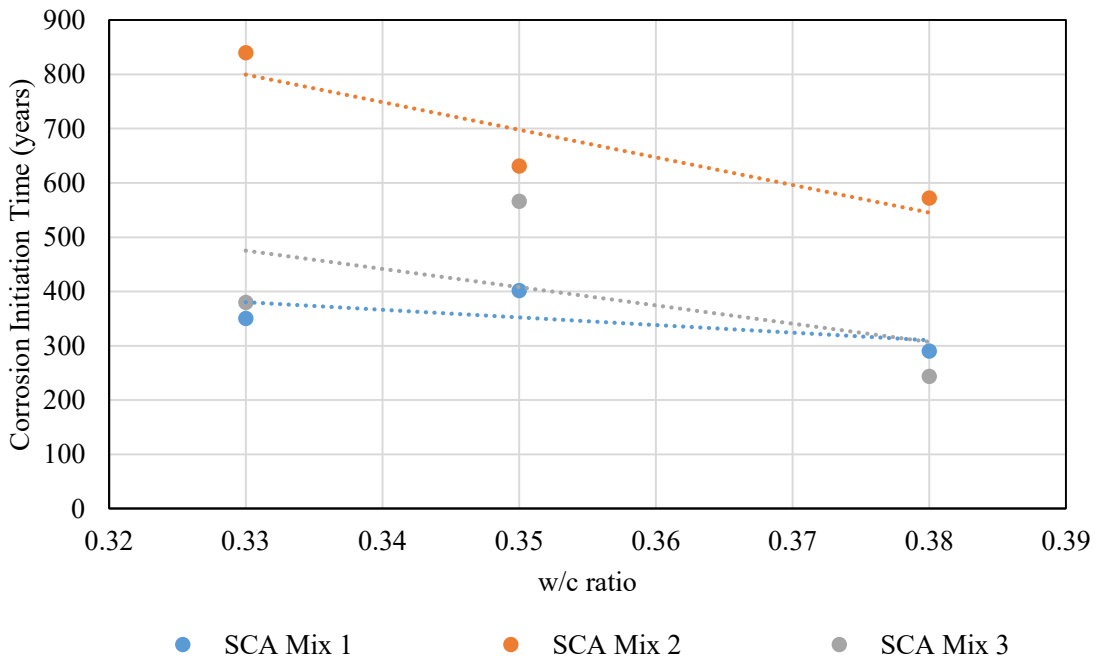Figure 6.1.5.2: Variation in Corrosion Initiation Time for Cover 37.5 mm
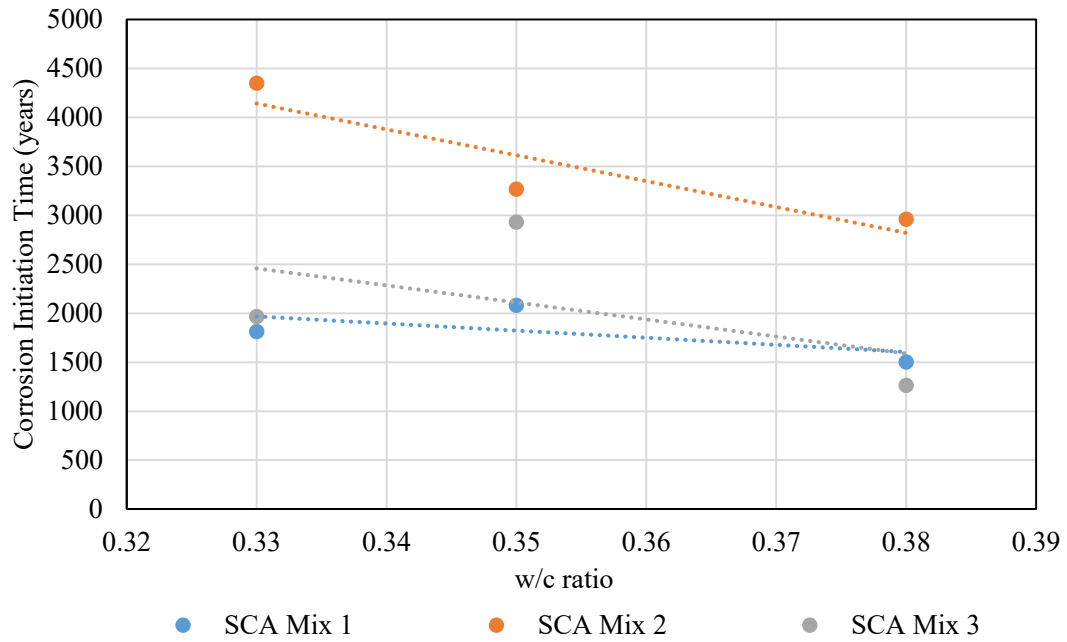
Figure 6.1.5.3: Variation in Corrosion Initiation Time for Cover 50 mm

6.5.5 Effect of Addition of Admixture

High strength concrete was prepared with low w/c ratio of 0.35. In order to achieve desired workability, three mixes were prepared with admixture. In addition, three mixes were prepared without admixture having higher water and cement content to maintain the low w/c ratio.

Figure 6.1.6 shows variation in corrosion initiation time for mixed with and without admixture. It can observed from the graph that higher admixture results in lower corrosion initiation time as admixture was observed to increase permeability. However, it still performs far well than the mixes with high cement and water content. In fact the corrosion initiation time for mixes with admixture remains within the range of 1680 years to 3245 years whereas the mixes with higher cement and water content reach 1260 years at maximum. However, the variation in cement content seems to have positive effect indicating improvement in permeability.
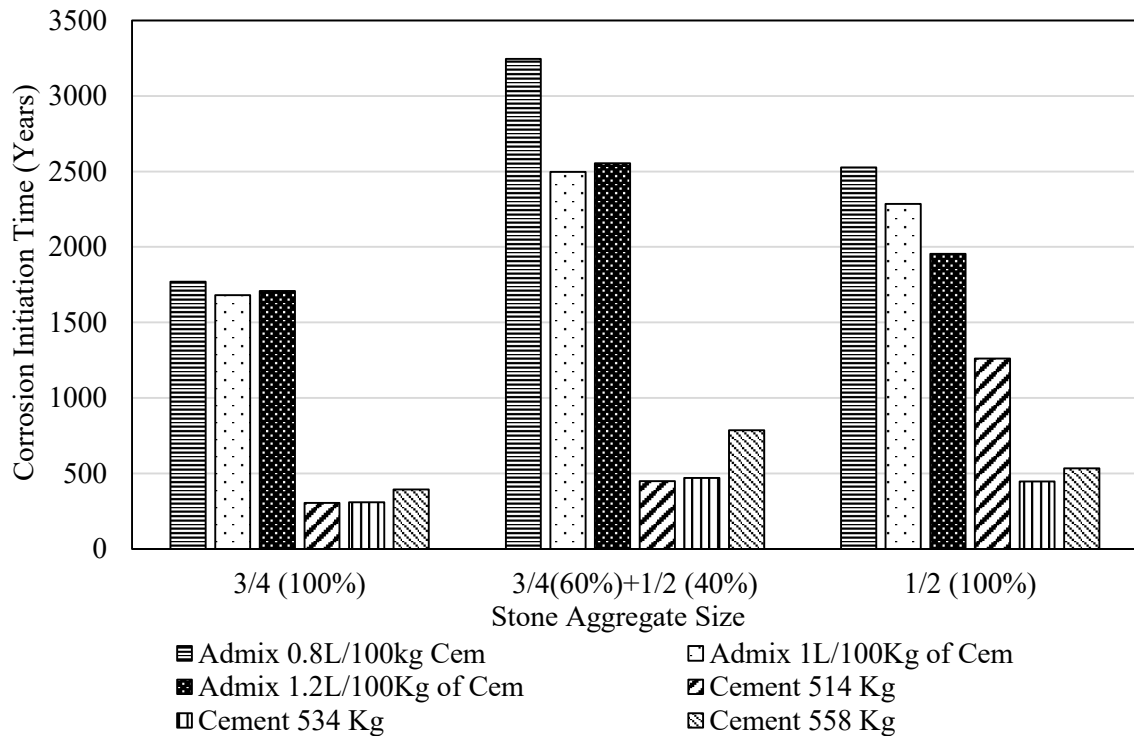
Figure 6.1.6: Variation in Corrosion Initiation Time for Cover 50 mm cover

6.6 Effect of Mix Proportion Parameters for Exposure Class XD2 and XS2

The corrosion severity of both these categories can be considered as high. For these exposure classes, corrosion initiation time was evaluated for 4 different concrete cover of 37.5mm, 50mm, 62.5mm and 75mm.

6.6.1 Effect of Aggregate and Cement Type Variation

Figures 6.2.1.1 and 6.2.1.4 show variation in corrosion initiation time of stone and brick aggregate concrete with varying w/c ratio and cover for OPC and PCC, respectively.

Based on the graphical presentation in Figures 6.2.1.1 to 6.2.1.4, it can be deduced that in all cases of stone aggregate concrete with PCC as a binder performs way better than the other counterparts. Even, brick with PCC shows higher corrosion initiation time and thus less corrosion susceptibility as compared to Stone with OPC and brick with OPC.
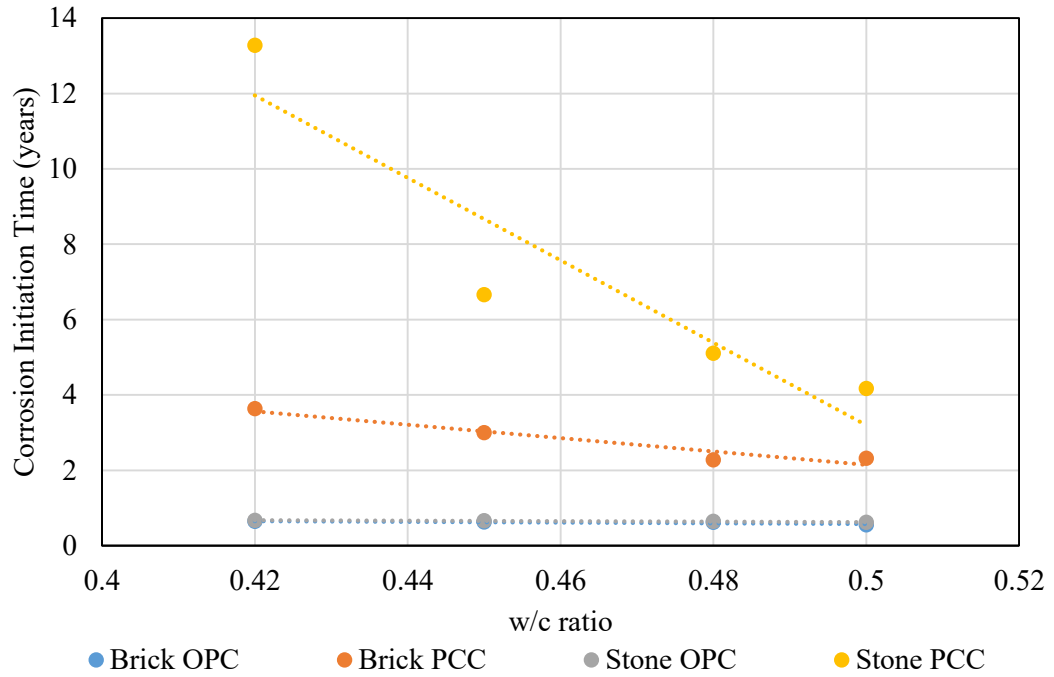
Figure 6.2.1.1: Variation in Corrosion Initiation Time for Variation in Aggregate and Cement Type (Cover 37.5 mm)
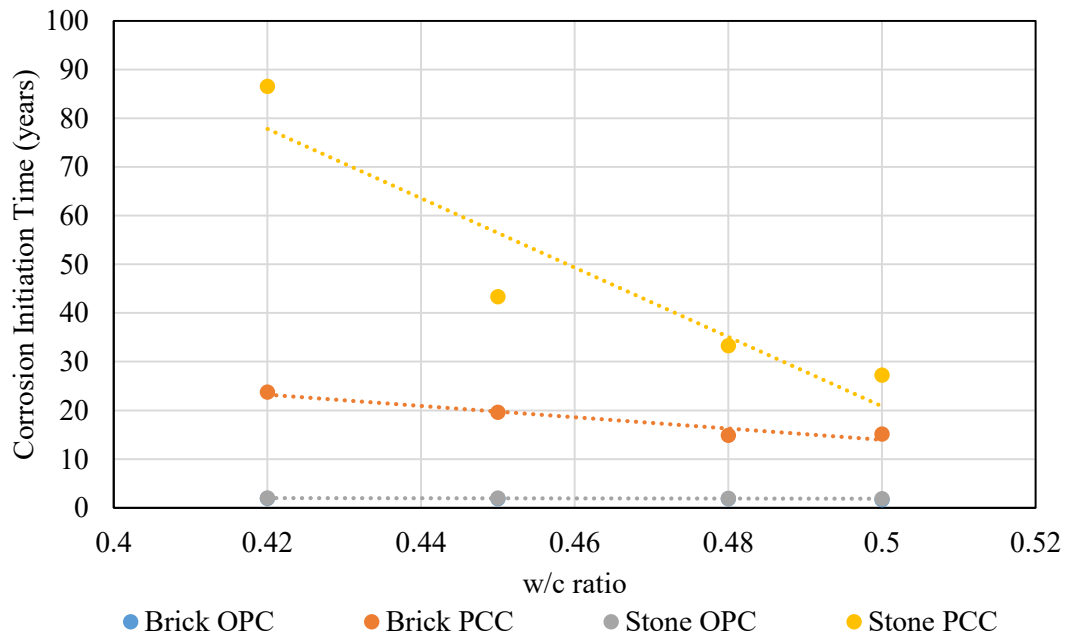
Figure 6.2.1.2: Variation in Corrosion Initiation Time for Variation in Aggregate and Cement Type(Cover 50 mm)
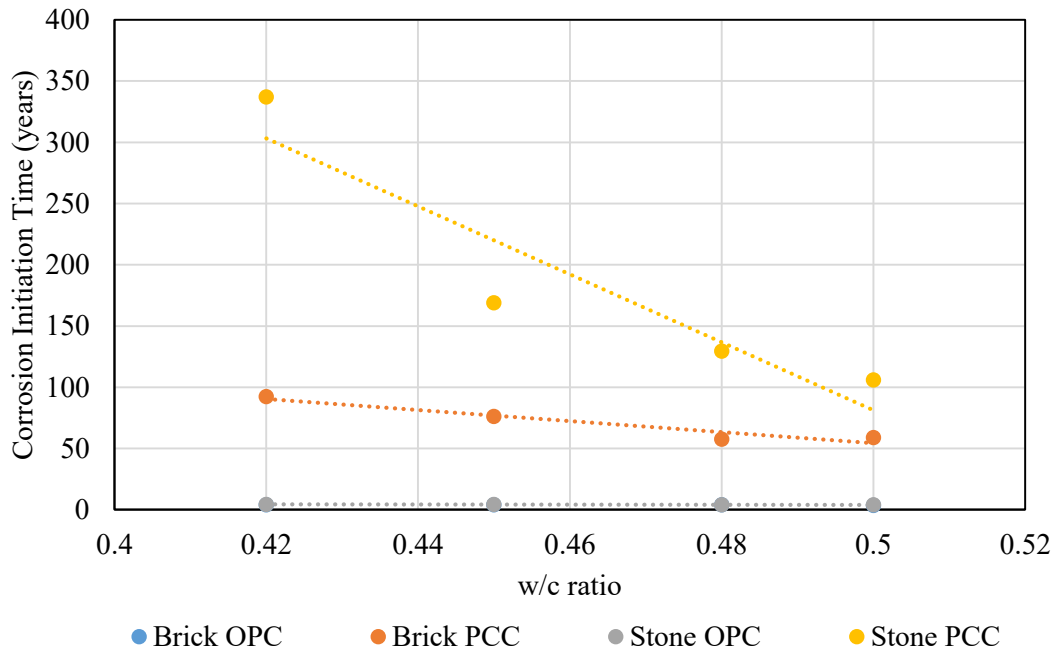
Figure 6.2.1.3: Variation in Corrosion Initiation Time for Variation in Aggregate and Cement Type (Cover 62.5 mm)
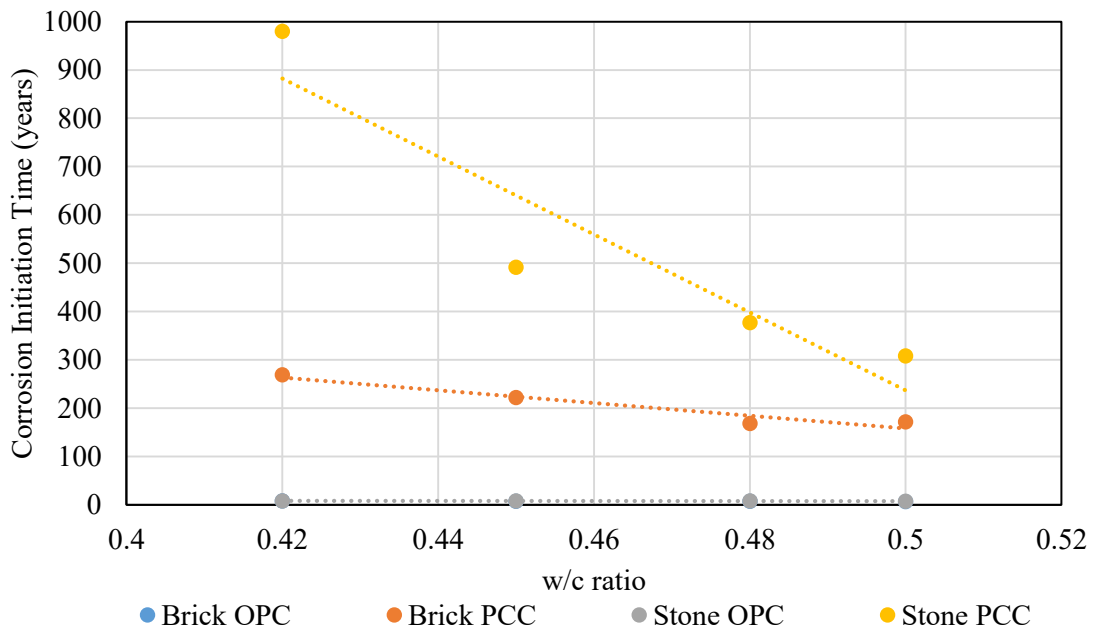
Figure 6.2.1.4: Variation in Corrosion Initiation Time for Variation in Aggregate and Cement Type (Cover 75 mm)

6.6.2 Effect of Mix Proportion Variation

Figures 6.2.2.1 to 6.2.2.4 show variation in corrosion initiation time with varying w/c ratio of 0.42-0.5 in case of brick aggregate concrete with mix proportions of 1:1.5:3 and 1:2:4 for

different cover parameters. From the figures it can be observed that in almost all cases concrete with higher mix proportion results in early corrosion initiation. This can be attributed to the fact that mix proportion with high aggregate and low cement content (1:2:4) produces a more lean and porous concrete.

Figure 6.2.2.1: Variation in Corrosion Initiation Time for Mix Variation sand Cover 37.5 mm

Figure 6.2.2.2: Variation in Corrosion Initiation Time for Mix Variations and Cover 50 mm

Figure 6.2.2.3: Variation in Corrosion Initiation Time for Mix Variations and Cover 62.5 mm
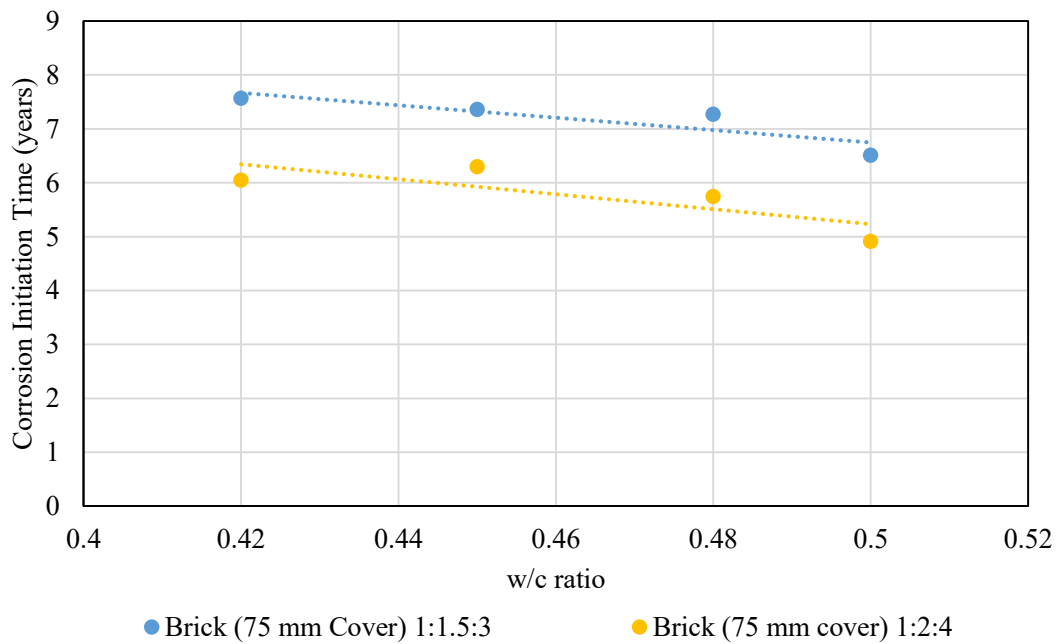
Figure 6.2.2.4: Variation in Corrosion Initiation Time for Mix Variations and Cover 75 mm

6.6.3 Effect of Aggregate Gradation for OPC

Figures 6.2.3.1 to 6.2.3.4 show the effect of aggregate gradation on the corrosion initiation time values for concrete with OPC. In all cases, SCA mix type 1 (100% of 19mm downgraded) results in least corrosion initiation time irrespective of the cover considered and SCA mix type

2 shows higher corrosion initiation time. This is due to the proper gradation of this coarse aggregate mix that results in less permeable concrete. All aggregate gradation type shows decreasing trend of corrosion initiation time with increasing w/c ratio. From the graphs, it can also be deduced that increase in cover value from 25mm to 37.5mm results in considerably higher corrosion initiation times.
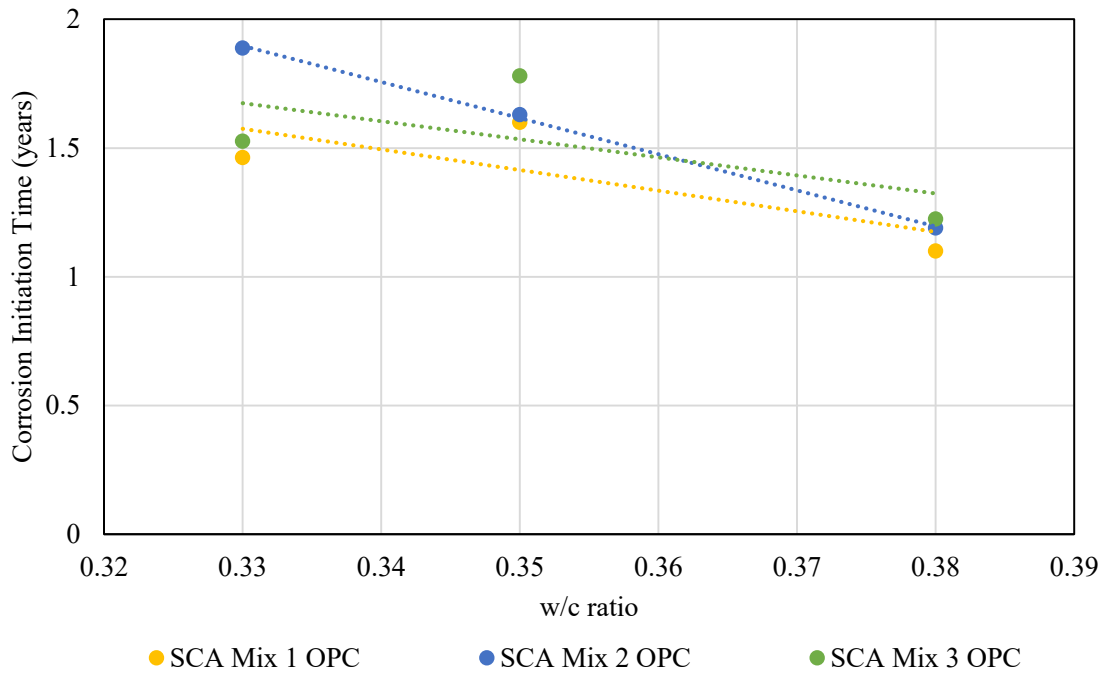
Figure 6.2.3.1: Variation in Corrosion Initiation Time for Cover 37.5 mm
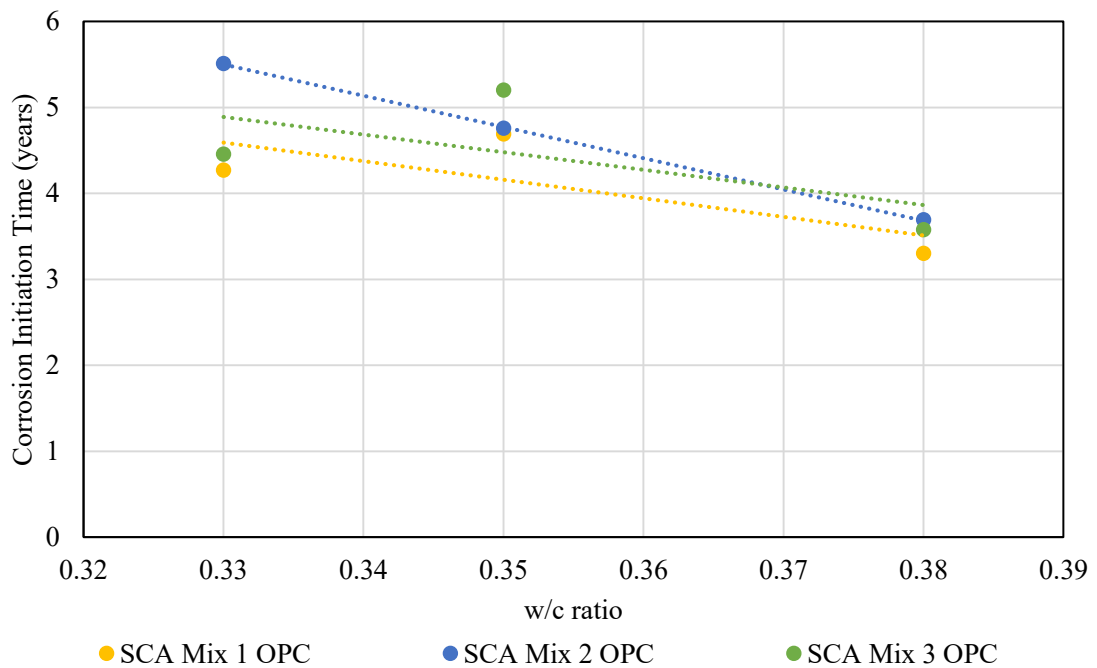
Figure 6.2.3.2: Variation in Corrosion Initiation Time for Cover 50 mm
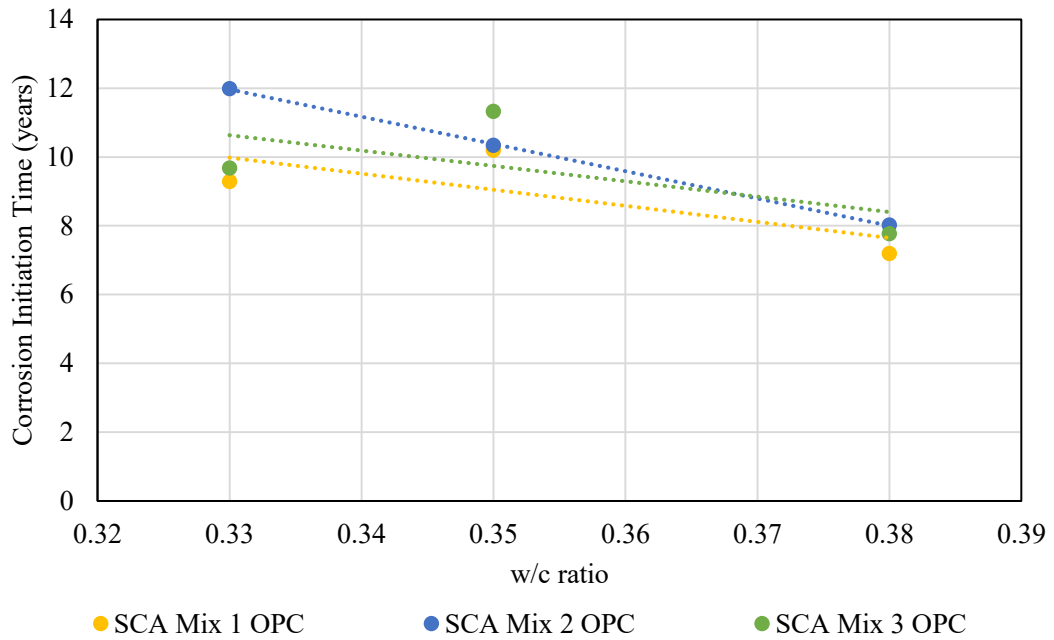
Figure 6.2.3.3: Variation in Corrosion Initiation Time for Cover 62.5 mm
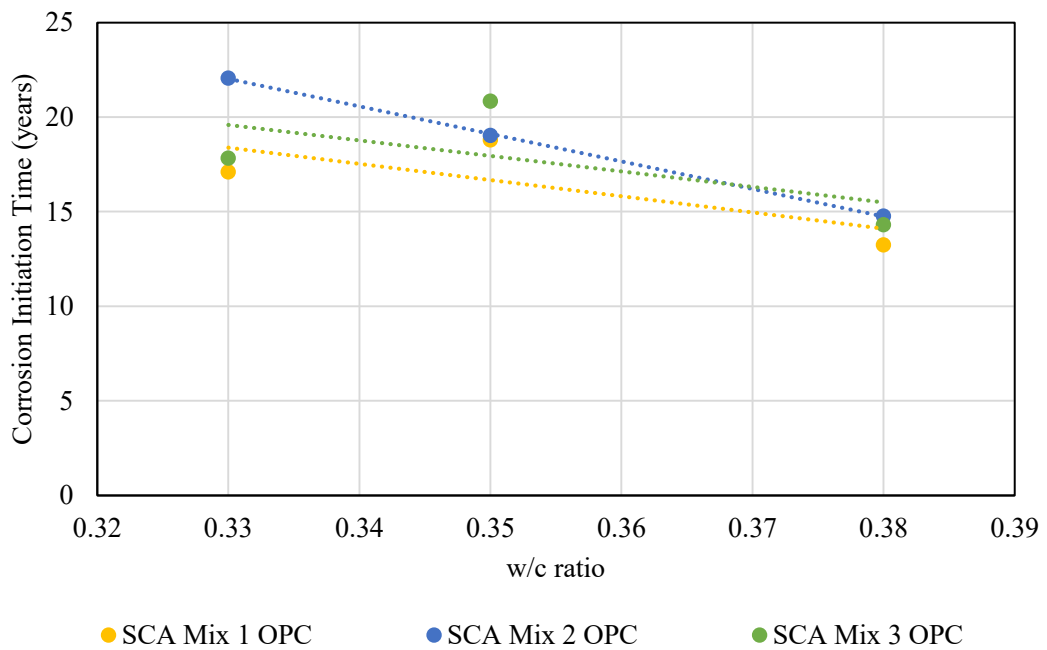
Figure 6.2.3.4: Variation in Corrosion Initiation Time for Cover 75 mm

6.6.4 Effect of Aggregate Gradation for PCC

Figures 6.2.4.1 to 6.2.4.4 show the effect of aggregate gradation on the corrosion initiation time values for concrete with PCC. Just like OPC, PCC concrete also shows similar trend of least corrosion initiation time value in case of SCA mix type 1 irrespective of the cover considered.

In almost all cases, SCA mix type 2 shows higher corrosion initiation time. This because of the proper gradation of this coarse aggregate mix which results in a less permeable concrete.
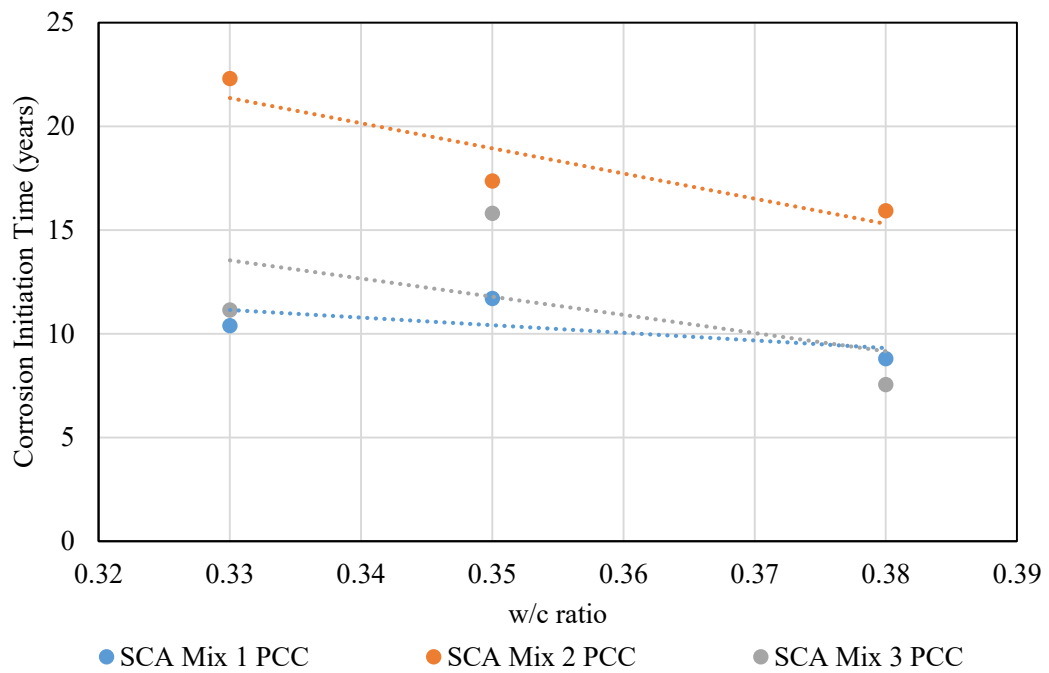
Figure 6.2.4.1: Variation in Corrosion Initiation Time for Cover 37.5 mm
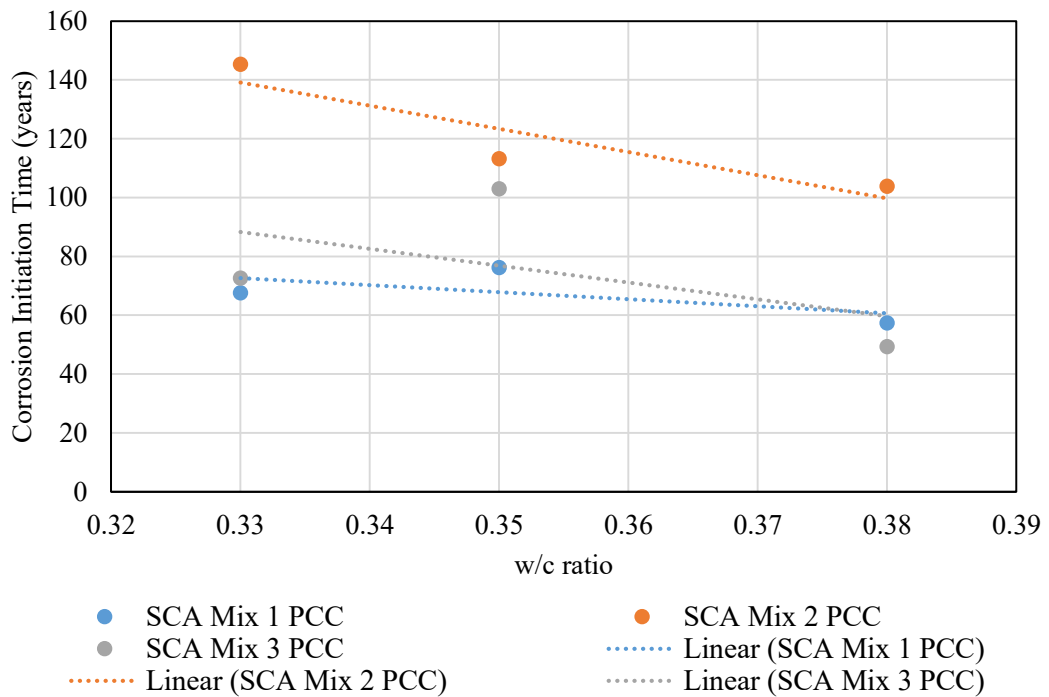
Figure 6.2.4.2: Variation in Corrosion Initiation Time for Cover 50 mm

Figure 6.2.4.3: Variation in Corrosion Initiation Time for Cover 62.5 mm

Figure 6.2.4.4: Variation in Corrosion Initiation Time for Cover 75 mm

From the graphs, it can also be deduced that increase in cover value from 25mm to 37.5mm results in significantly higher corrosion initiation times.

6.6.5 Effect of Addition of Admixture

High strength concrete was prepared with low w/c ratio of 0.35. In order to achieve desired workability, three mixes were prepared with admixture. In addition, three mixes were prepared without admixture having higher water and cement content to maintain the low w/c ratio. Figure 6.2.5 shows variation in corrosion initiation time for varying admixture and cement content. It can observed from the graph that higher admixture results in lower corrosion initiation time as admixture was observed to increase permeability. However, it still performs far well than the mixes with high cement and water content. However, the variation in cement content seems to have positive effect indicating improvement in permeability.
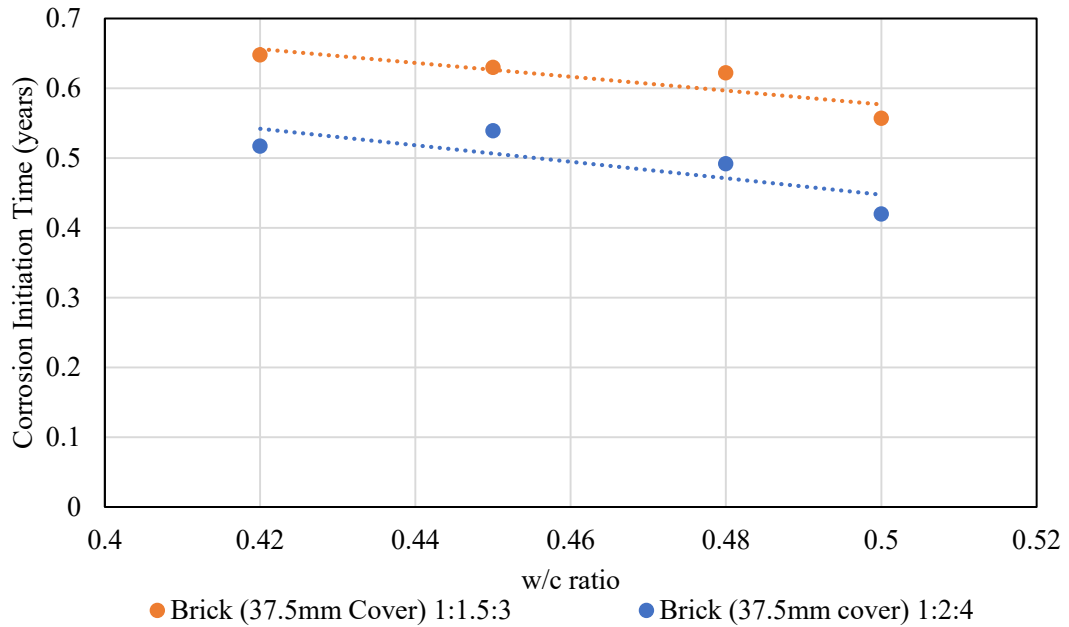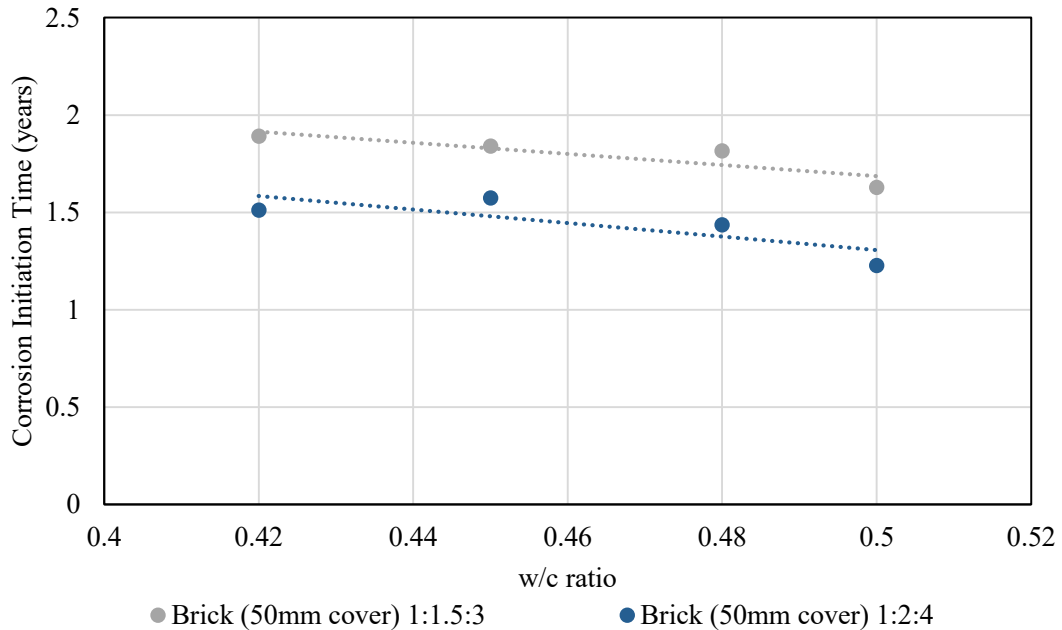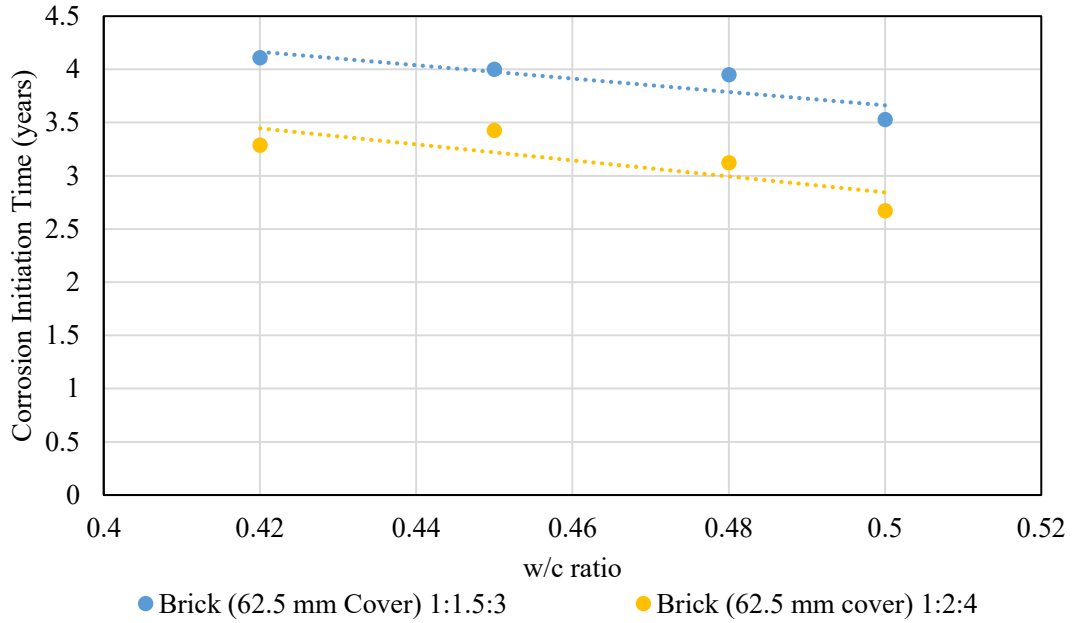

Figure 6.2.5: Variation in Corrosion Initiation Time for Cover 50 mm cover

6.7 Effect of Mix Proportion Parameters for Exposure Class XD1

The XD1 exposure class experiences low severity of corrosion as the structures are exposed to airborne Cl- from any other water source than sea water. For this exposure classes, corrosion initiation time was evaluated for 3 different concrete cover of 25mm, 37.5mm and 50mm.

6.7.1 Effect of Aggregate and Cement Type Variation

Figures 6.3.1 and 6.3.2 show variation in corrosion initiation time of stone and brick aggregate concrete with varying w/c ratio and cover for OPC and PCC, respectively. Both

figure shows higher corrosion initiation time in case of stone aggregate irrespective of the cover. Brick shows lower value of corrosion initiation because brick itself has a high absorption capacity and a porous microstructure.
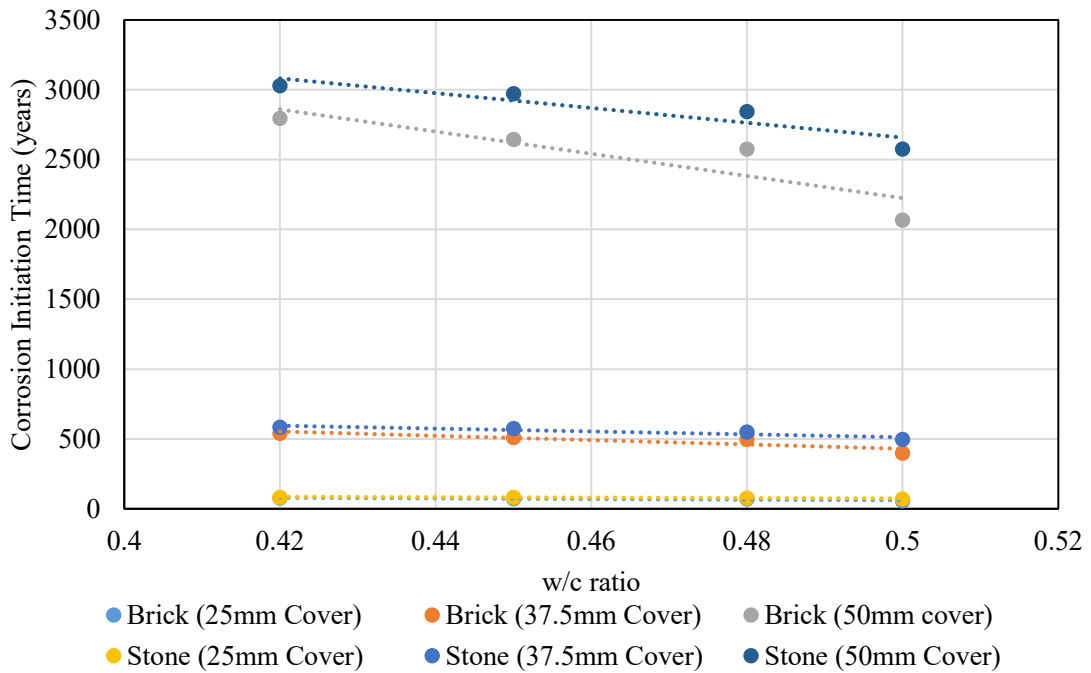
Figure 6.3.1: Variation in Corrosion Initiation Time for Stone and Brick Aggregate (OPC)
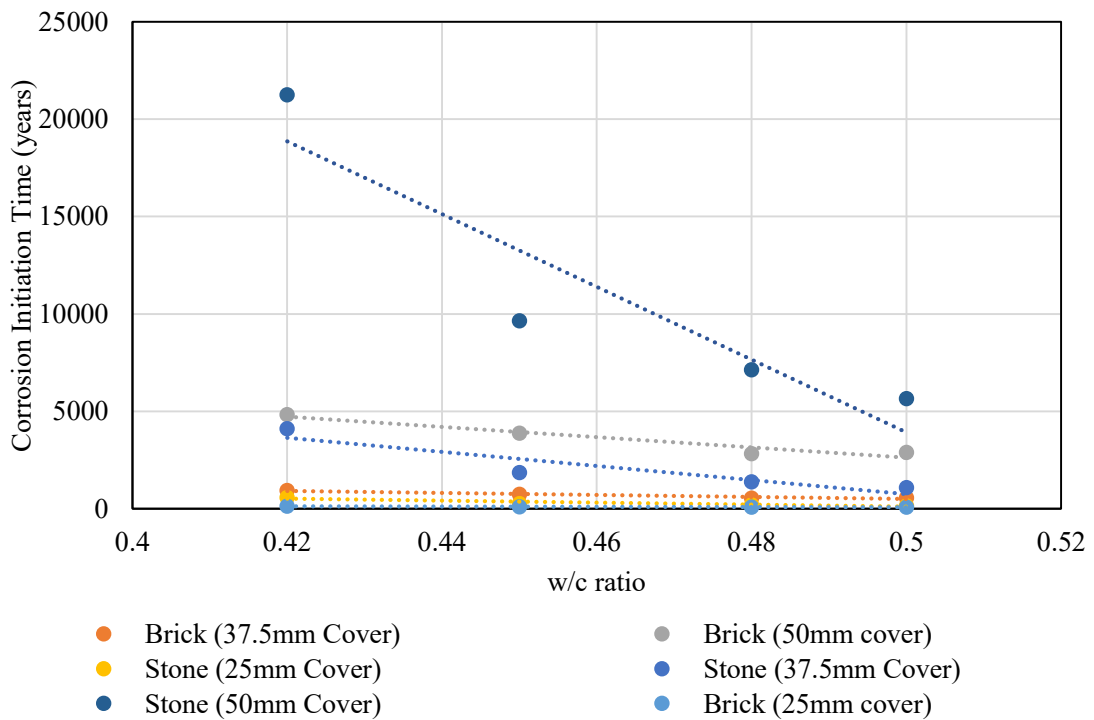
Figure 6.3.2: Variation in Corrosion Initiation Time for Stone and Brick Aggregate (PCC)

6.7.2 Effect of Mix Proportion Variation

Figure 6.3.3 displays variation in corrosion initiation time with varying w/c ratio of 0.42-0.5 in case of brick aggregate concrete with mix proportions of 1:1.5:3 and 1:2:4. From the figure it can be observed that in almost all cases concrete with higher mix proportion results in early corrosion initiation. The fact that influences such phenomena is that mix proportion with high aggregate and low cement content (1:2:4) produces a more lean and porous concrete.
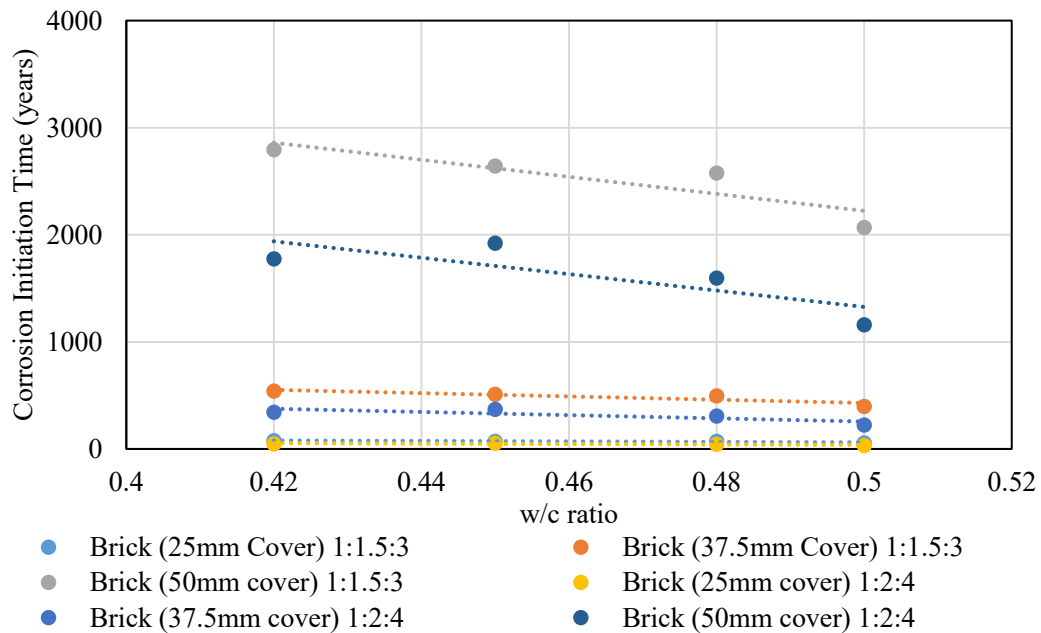
Figure 6.3.3: Variation in Corrosion Initiation Time Brick Aggregate with Variant Mix Proportion

6.7.3 Effect of Aggregate Gradation for OPC

Figures 6.3.4.1 to 6.3.4.3 show the effect of aggregate gradation on the corrosion initiation time values for concrete with OPC. In all cases, SCA mix type 1 results in least corrosion initiation time irrespective of the cover considered. All SCA mix type shows decreasing value of corrosion initiation with increase in w/c ratio. In almost all cases SCA mix type 2 shows higher corrosion initiation time. This is because of the proper gradation of this coarse aggregate mix which results in a less permeable concrete.
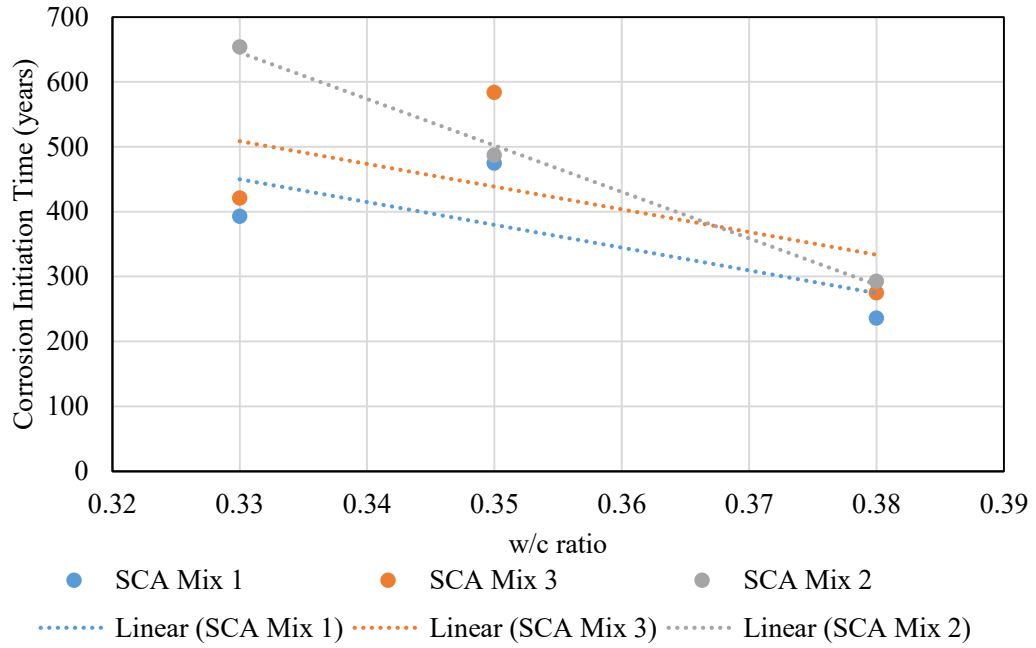
Figure 6.3.4.1: Variation in Corrosion Initiation Time for OPC and Cover 25mm
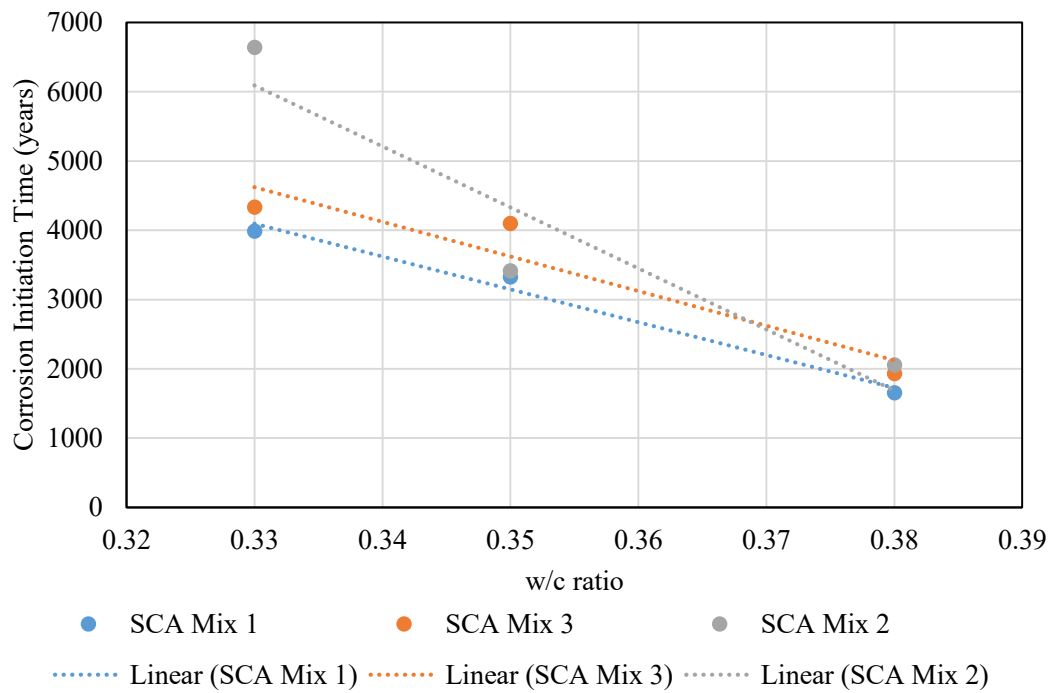
Figure 6.3.4.2: Variation in Corrosion Initiation Time for OPC and Cover 37.5 mm
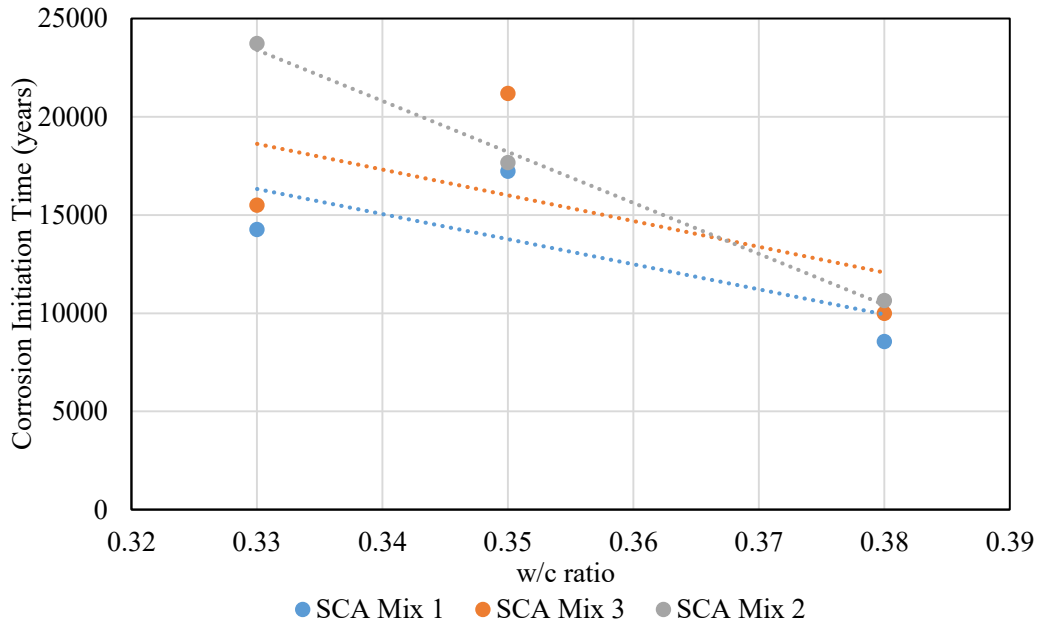
Figure 6.3.4.3: Variation in Corrosion Initiation Time for OPC and Cover 50 mm

From the graphs, it can also be deduced that increase in cover value from 25mm to 37.5mm results in about 10 times higher corrosion initiation times and from 37.5mm to 25mm shows about 3.5~4 times higher corrosion initiation time.

6.7.4 Effect of Aggregate Gradation for PCC

Figures 6.3.5.1 to 6.3.5.3 show the effect of aggregate gradation on the corrosion initiation time values for concrete containing PCC. In all cases, SCA mix type 1 results in least corrosion initiation time irrespective of the cover considered and SCA mix type 2 shows higher corrosion initiation time. This is because of the proper gradation of this coarse aggregate mix which results in a less permeable concrete. All SCA mix type, for all cover variation considered, shows decreasing value of corrosion initiation with increase in w/c ratio.
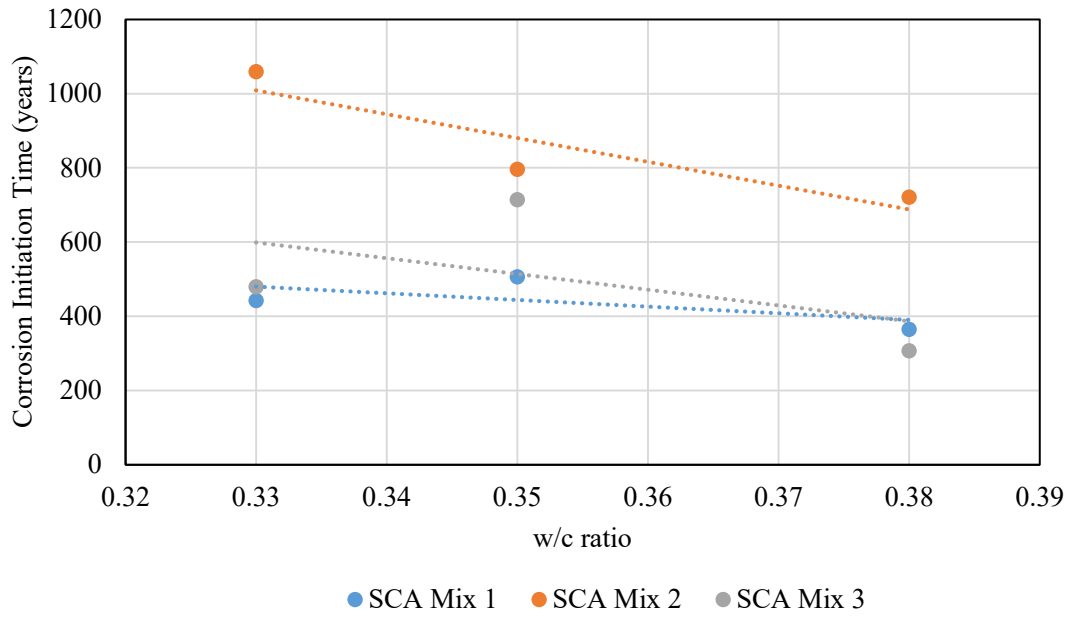
Figure 6.3.5.1: Variation in Corrosion Initiation Time for PCC and Cover 25mm
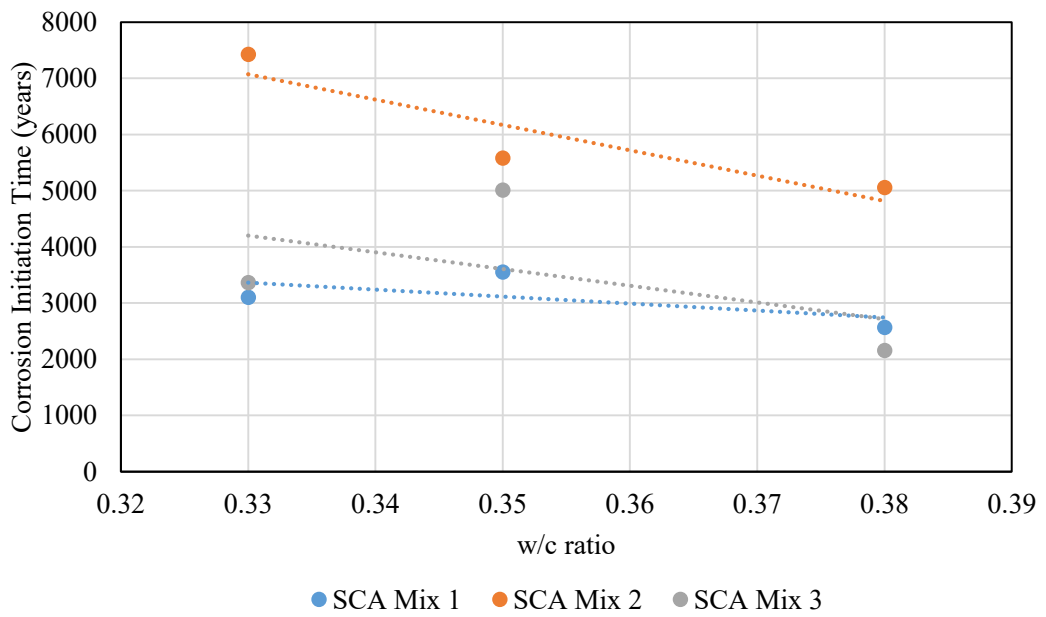
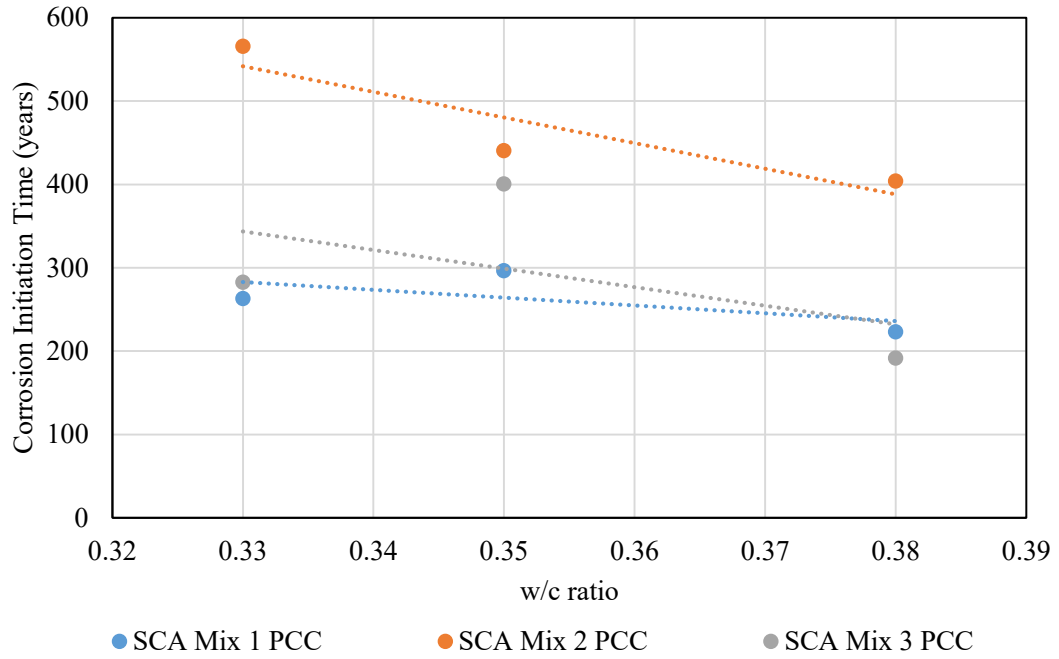Figure 6.3.5.2: Variation in Corrosion Initiation Time for PCC and Cover 37.5 mm
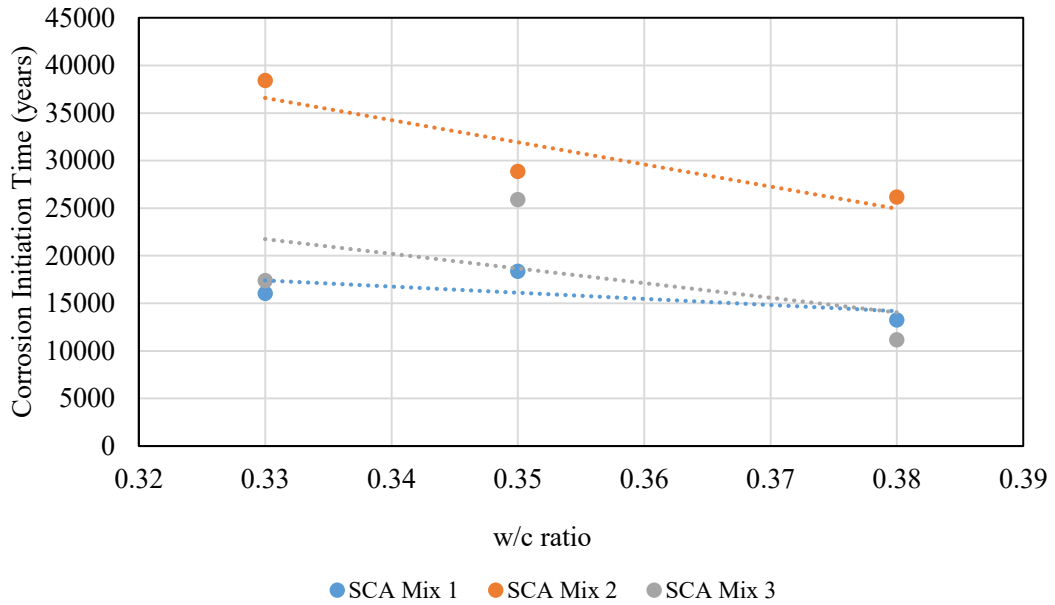
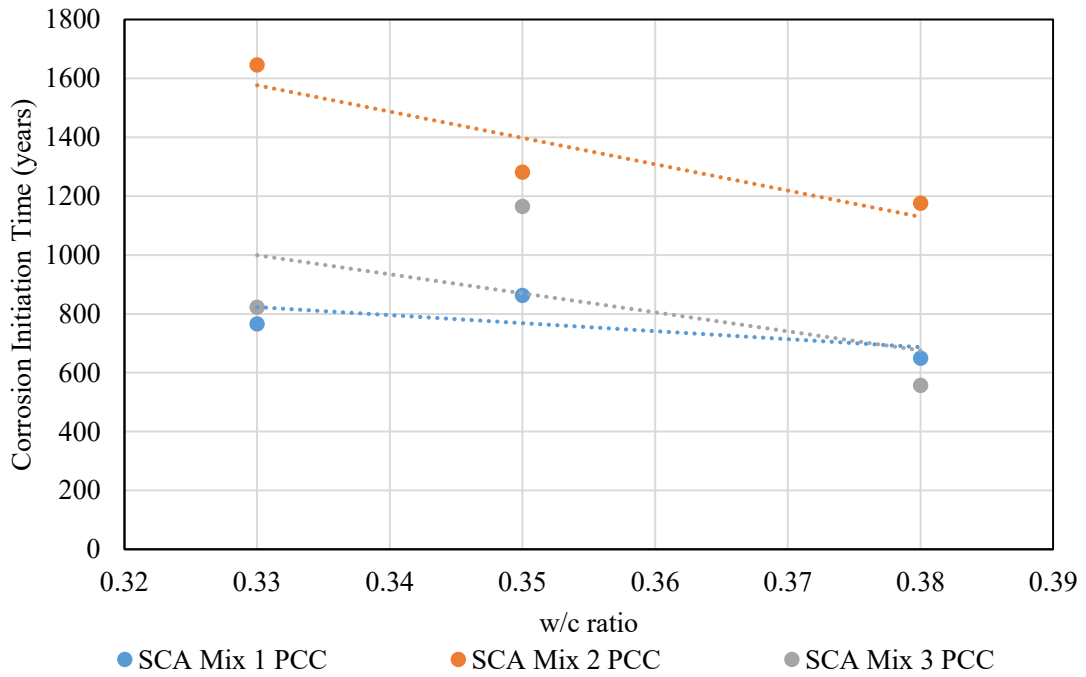Figure 6.3.5.3: Variation in Corrosion Initiation Time for PCC and Cover 50 mm

6.7.5 Effect of Addition of Admixture

High strength concrete was prepared with low w/c ratio of 0.35. In order to achieve desired workability, three mixes were prepared with admixture. In addition, three mixes were prepared without admixture having higher water and cement content to maintain the low w/c ratio. Figure 6.3.6 shows variation in corrosion initiation time for varying admixture and cement content. It can observed from the graph that higher admixture results in lower corrosion initiation time as admixture was observed to increase permeability. However, it still performs far well than the mixes with high cement content. Nevertheless, the variation in cement content seems to have positive effect indicating improvement in permeability.
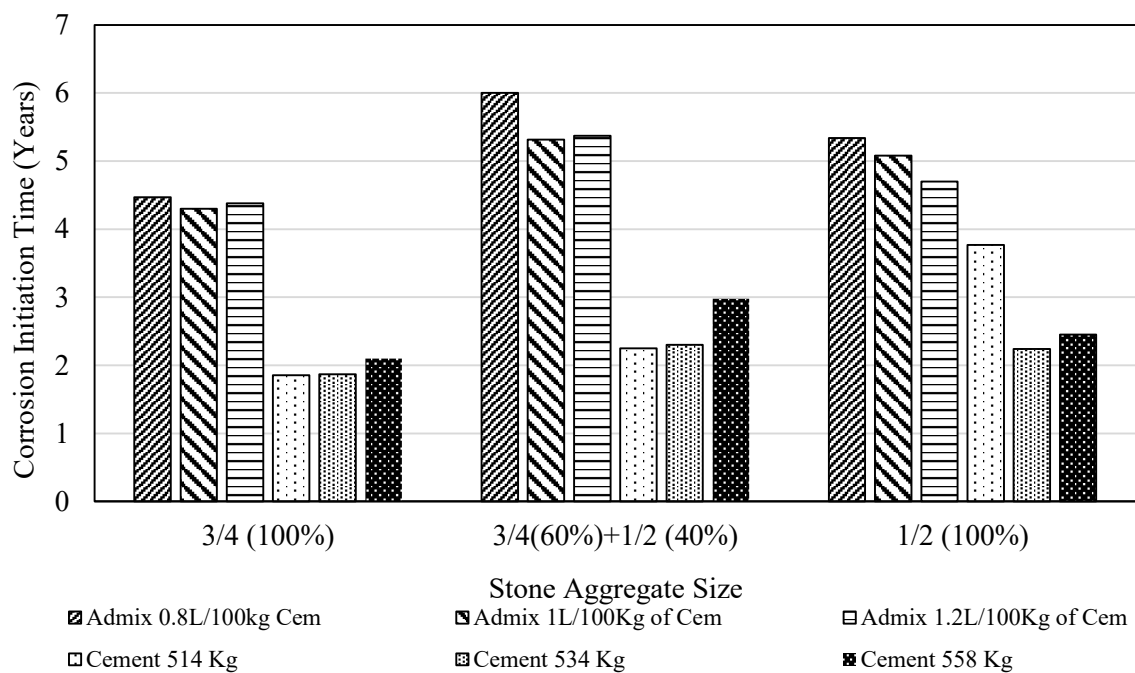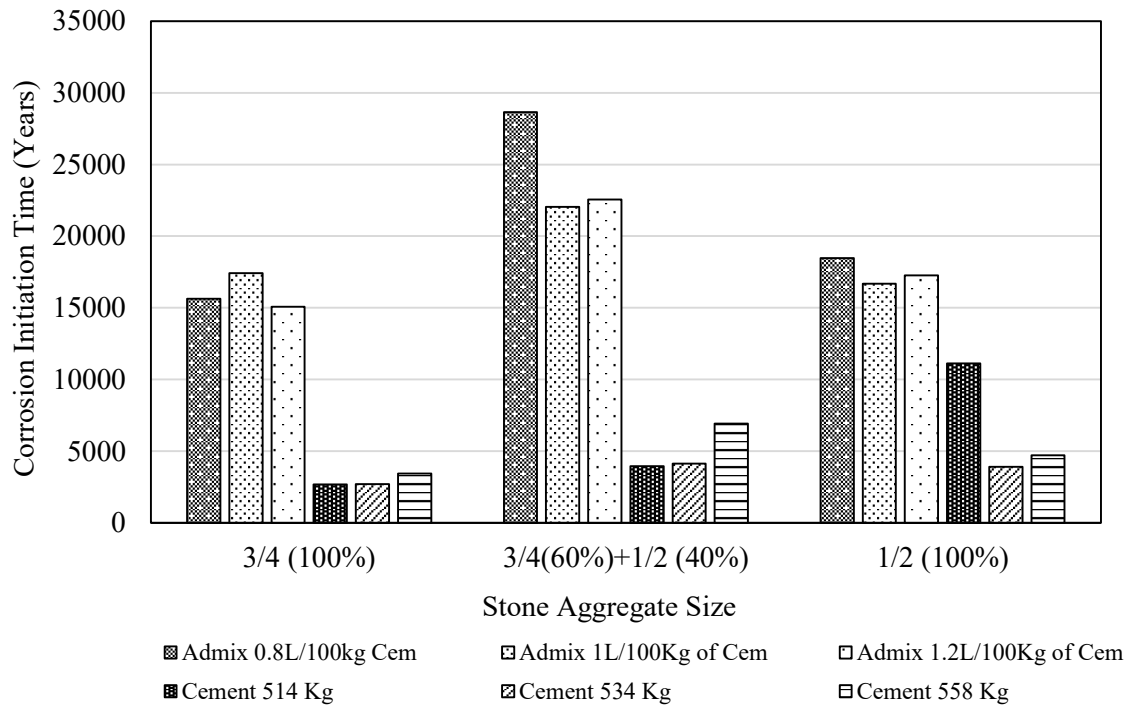
Figure 6.3.6: Variation in Corrosion Initiation Time for Variation in Admixture and Cement Content (Cover 50 mm)

6.8 Time to Severe Cracking

In case of chloride induced corrosion, cracking results from the internal stresses within concrete which is developed due to the increasing expansive force exerted by the corrosion products on surrounding concrete (Etman, 2012; Wang et al., 2010). As discussed in literature, time to severe cracking induced by corrosion is the summation of two different times-crack initiation time and crack propagation time. The following sections will discuss the effect of different parameters such as-compressive strength, concrete cover, rebar diameter and corrosion rate on the time of crack initiation and propagation for the types of concrete mixes considered for this study.

6.9 Time to Crack Initiation

Time to crack initiation is usually considered to be the time from corrosion initiation by depassivation of protective layer to the initiation of first crack (Wang et al., 2010). For this research venture, crack initiation time was calculated based on the model suggested by El Maaddawy and Soudki (2007). The effects of different variables-compressive strength,

concrete cover, bar diameter and exposure class (corrosion current density) on the initiation time are discussed as follows:

6.9.1 Effect of Compressive Strength and Concrete Cover

As per the equation of El Maaddawy and Soudki (2007), the value of concrete tensile strength is required to calculate initiation time for certain type of concrete. In this study, the tensile strength was computed from the compressive strength, determined in the laboratory for different types of mixes considered, based on the empirical relation as suggested by Mirza et al. (1979). Furthermore, 5 different types of concrete cover – 25mm for exposure class-XD1 and XS1 and 37.5 mm, 50mm, 62.5 mm and 75 mm for exposure classes XD2 and XS2 were considered for each concrete mix with a constant rebar diameter of 16 mm. Effects of these variations on crack initiation time are shown in Figures 6.4.1.1-6.4.1.4.

Figure 6.4.1.1: Effect of compressive strength and concrete cover for exposure class XD1

Figure 6.4.1.2: Effect of compressive strength and concrete cover for exposure class XS1

Figure 6.4.1.3: Effect of compressive strength and concrete cover for exposure class XD2

Figure 6.4.1.4: Effect of compressive strength and concrete cover for exposure class XS2

All figures show that crack initiation time remains constant for increasing value of compressive strength of various types of concrete mixes regardless of the concrete cover and exposure class considered. Crack initiation time principally depends on the amount of corrosion product formed to cause the cracking of cover (Liu and Weyers, 1998; El Maaddawy and Soudki, 2007) which in turn mainly depends on the concrete cover, corrosion current density and the rebar to be corroded. Thus, concrete strength has no significant impact on the crack initiation time.

However, concrete cover has a noteworthy effect on the crack initiation time. From Figure 6.4.1.1, it can be seen that, for exposure class XD1, 12.5 mm increase in concrete cover results in an increase in crack initiation time by 1.25 years on average. On the other hand, for other exposure categories XS1, XD2, XS2, the increase in crack initiation time are found to be insignificant for 12.5 mm increase in concrete cover. This is because the higher the concrete cover the more time will be required for the Cl- ions to reach rebar surface to initiate corrosion and also for the formation of require amount of corrosion products to initiate cracking.

6.9.2 Effect of Exposure Classes

Figure 6.4.2 shows the effect of different exposure classes on the crack initiation time for different concrete mixes with particular concrete cover (37.5mm and 50mm) and rebar diameter (16 mm).
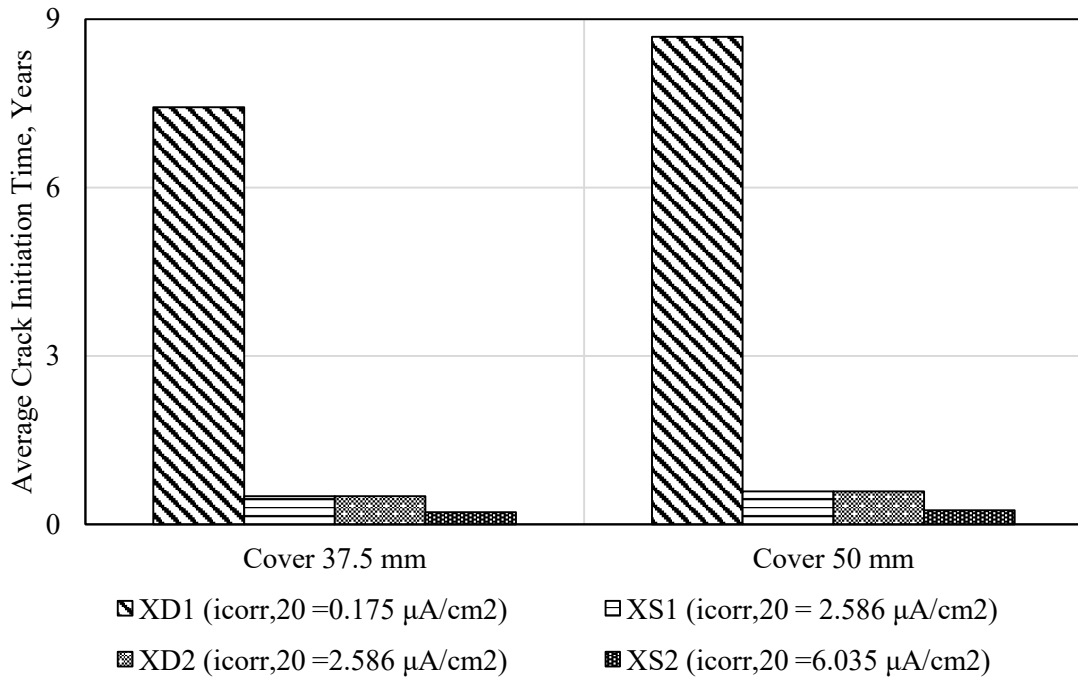
Figure 6.4.2: Effect of Exposure Classes on Initiation Time

The main impact of the exposure classes is on the corrosion rate which is represented by the term corrosion current density, $i_{corr,20}$. As the severity increases the corrosion rate increases and the crack initiation time decreases. Considering corrosion rate, exposure class XS2 has severe impact on reduction of crack initiation time with respect to that of classes XD2 and XS1. Numerically, the impact is 57.1% and 57.3% severe as compared to XS1 and XD2 exposure, for concrete cover value of 37.5mm and 50 mm, respectively. Exposure class XD2 and XS1 have similar intensity of corrosion rate ($i_{corr,20}$=2.586 $\mu A/cm^2$) and thus show negligible difference in crack initiation time. However, XD1 shows least severe impact which result in crack initiation time as high as about 7.4 years and 8.7 years for 37.5 mm and 50 mm cover, respectively (bar diameter is constant).

6.9.3 Effect of Bar Diameter

Figure 6.4.3 shows the effect of different bar diameter on the crack initiation time for different concrete mixes with particular concrete cover (50mm).
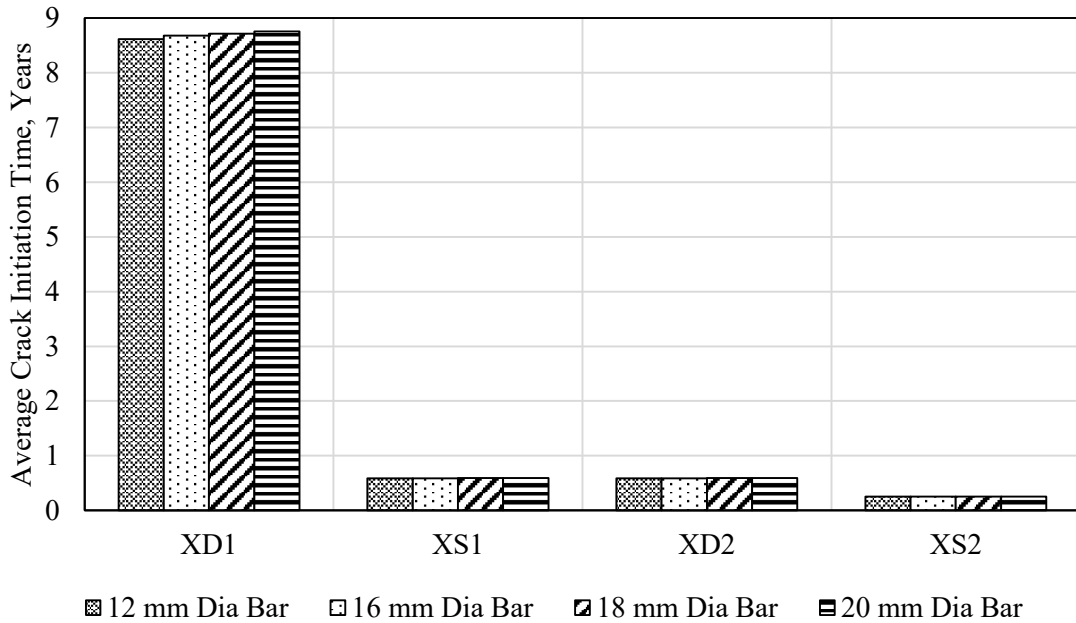
Figure 6.4.3: Effect of Bar Diameter on Initiation Time

For a particular exposure class and cover, diameter of embedded rebar does not seem to have significant effect on crack initiation time. However, higher diameter of rebar produces a slight increase in the crack initiation time. In case of exposure class XD1 and concrete cover 50 mm, the increase in crack initiation times are 0.064, 0.1 and 0.14 years for 16mm, 18mm and 20mm dia bar, respectively, as compared to 12 mm dia bar whereas for exposure XS2, the values are 0.004, 0.007 and 0.0095 years, respectively. Moreover, in case of exposure classes XD2 and XS1, the increase in crack initiation times are 0.002, 0.003 and 0.004 years for 16mm, 18mm and 20mm dia bar, respectively, as compared to 12 mm diameter bar. It seems from the data trend that for same corrosion current intensity, rebar with lager cross section endures slow corrosion to form rust and thus delays the crack initiation time to minute extent.

6.10 Time to Crack Propagation

As mentioned before, time to severe corrosion damage is the total of crack initiation time and crack propagation time. Therefore, the time required for the crack propagation spans from the time since corrosion initiation to the time to reach a limit crack width (in this case 1 mm) (Wang et al., 2010; Mullard and Stewart, 2009). For this particular research, the time from corrosion cracking initiation to the time required to reach a certain crack width for constant corrosion rate ($i_{corr-20}$) is evaluated based on the model suggested by Mullard and Stewart (2009).

6.10.1 Effect of Compressive Strength and Concrete Cover

As per the equation of Mullard and Stewart (2009), crack propagation time depends on the crack propagation rate (mm/hr) which in turn is a function of cover cracking parameter (Ψ). With high cover cracking parameter value, crack propagation rate decreases exponentially and hence, the crack propagation time increases. The cover cracking parameter is in turn depends on the concrete tensile strength, bar diameter and concrete cover. Concrete with high tensile strength (high compressive strength) for a constant rebar diameter and concrete cover will results in lower cracking parameter value and thus higher cracking rate. However, for increasing value of concrete cover will produce higher value of cracking parameter and lower value of crack propagation rate (mm/hr).

The following figures show the effect of concrete compressive strength on crack propagation time for various cover and exposure classes. Five different types of concrete cover – 25mm for exposure class-XD1 and XS1 and 37.5 mm, 50mm, 62.5 mm and 75 mm for exposure classes XD2 and XS2 were considered for each concrete mix with a constant rebar diameter of 16 mm.
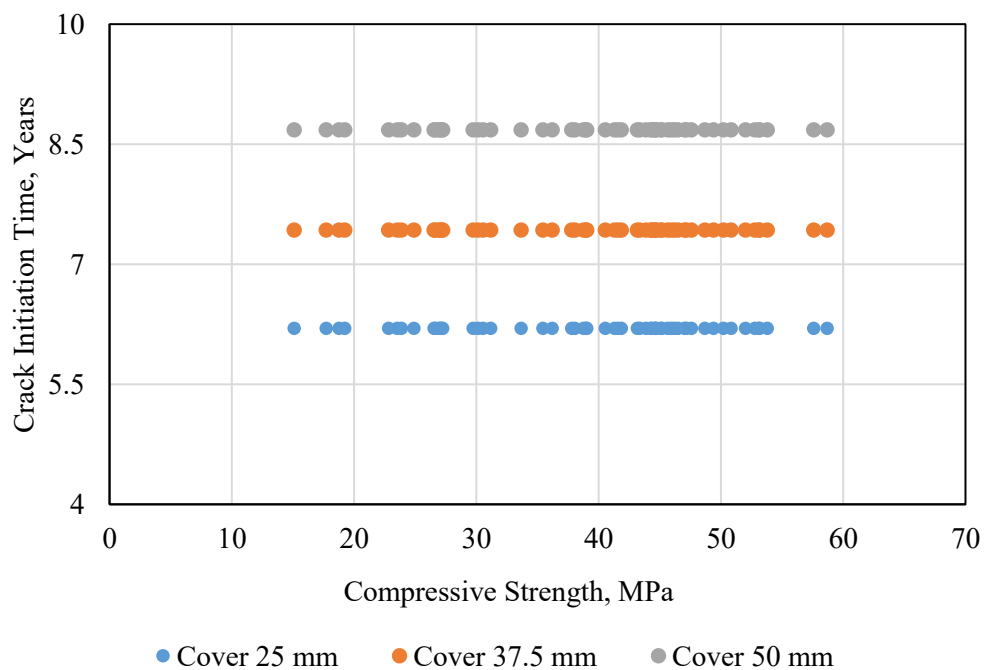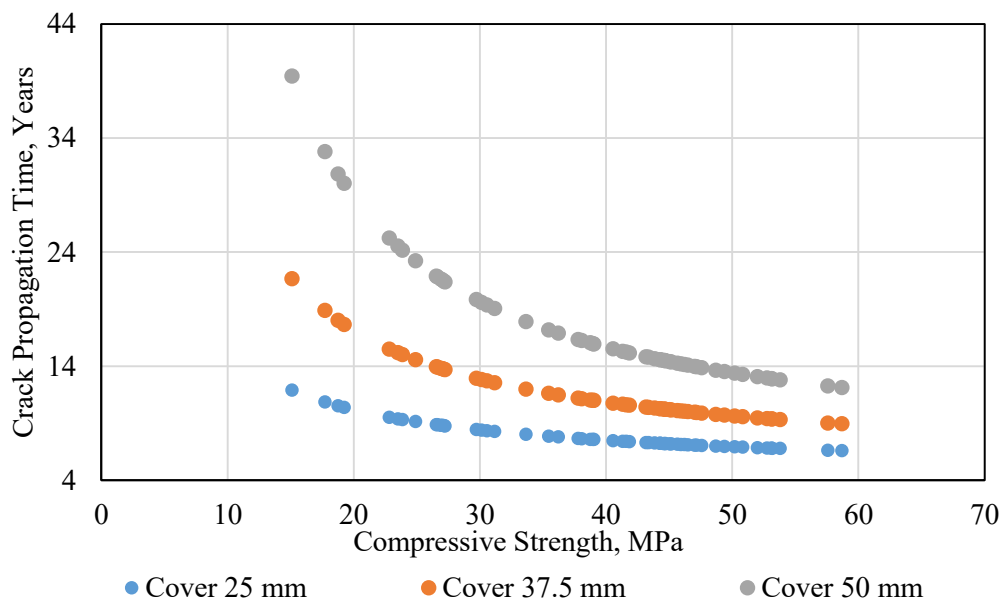

Figure 6.5.1.1: Effect of compressive strength and concrete cover for exposure class XD1
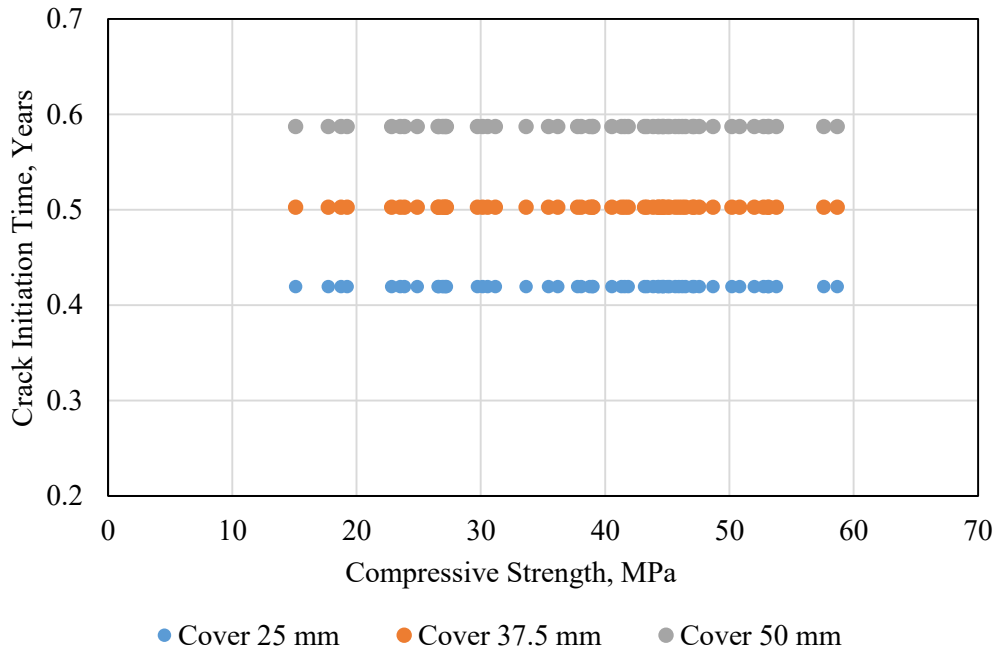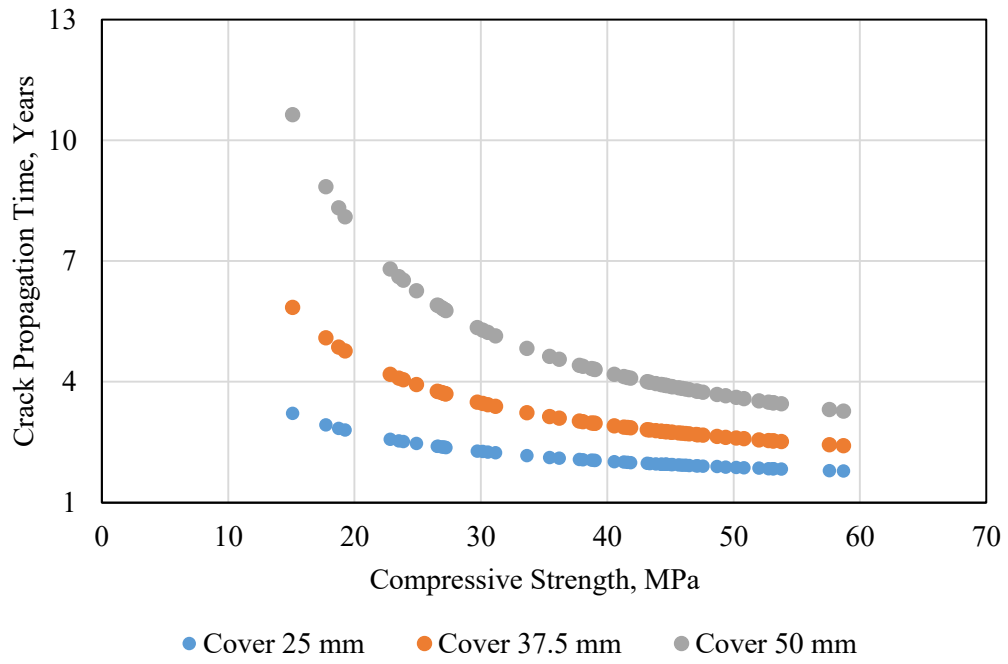
Figure 6.5.1.2: Effect of compressive strength and concrete cover for exposure class XS1
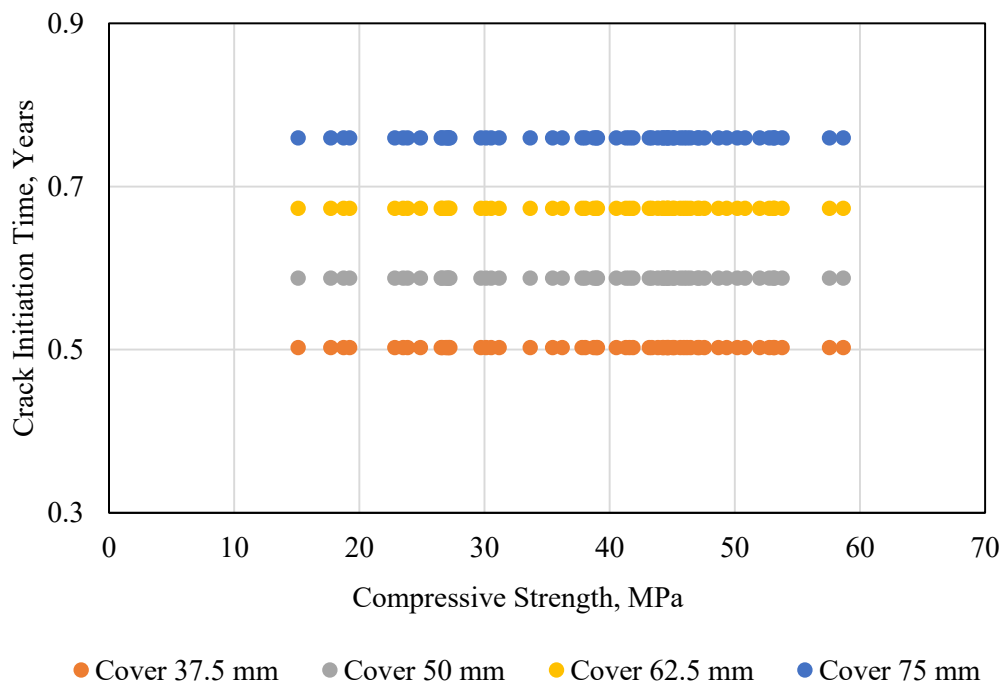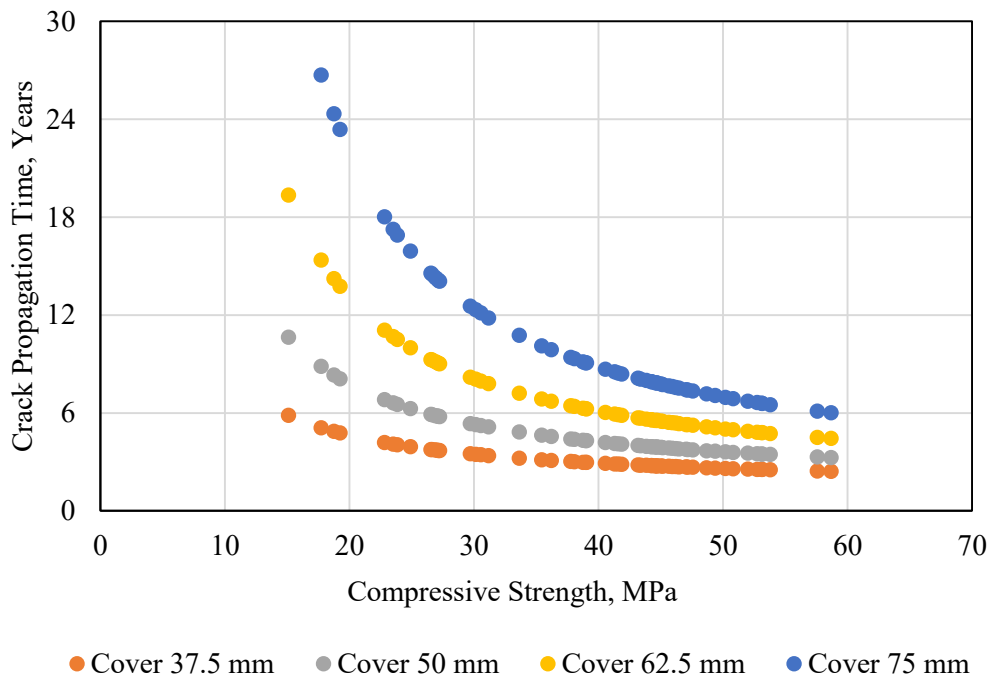

Figure 6.5.1.3: Effect of compressive strength and concrete cover for exposure class XD2
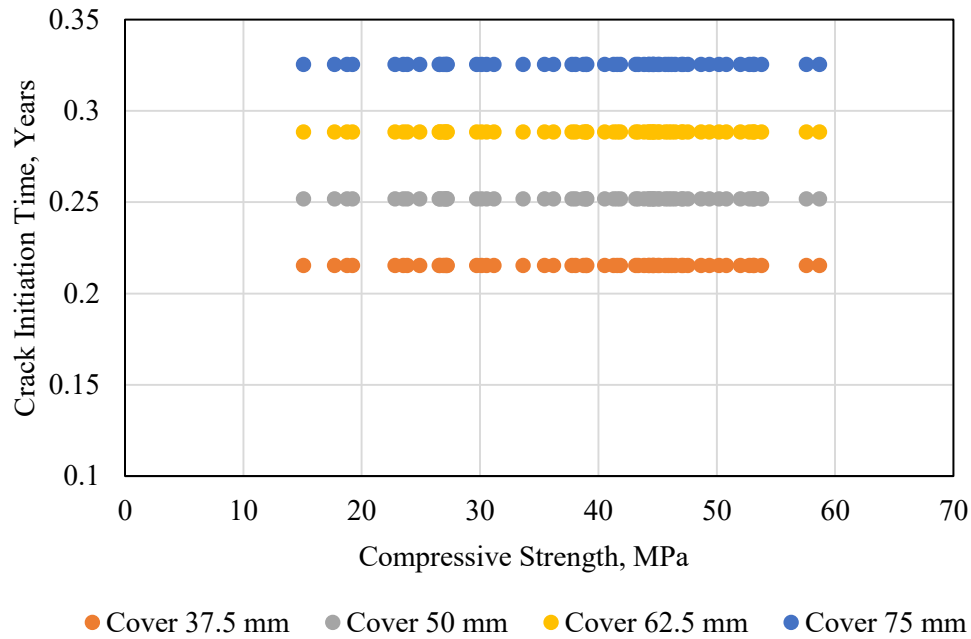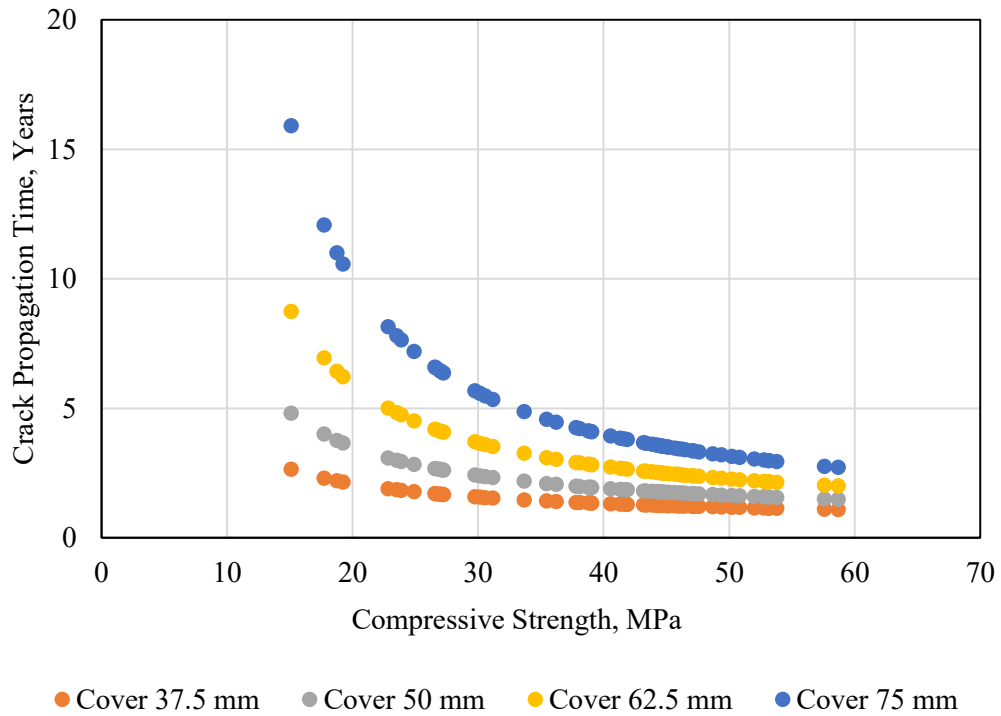
Figure 6.5.1.4: Effect of compressive strength and concrete cover for exposure class XS2

All figures (Figures 6.5.1.1 to Figure 6.5.1.4) are the graphical representation of the crack propagation time vs compressive strength of the concretes with different cover for exposure classes XD1, XS1, XD2, and XS2.

From Figure 6.5.1.1, it can be depicted that in case of exposure XD1, concrete with compressive strength varying in the range of 15 MPa to 60 MPa shows decreasing crack propagation time to be from 12 years to 6.8 years, from 21.6 years to 9.4 years and 39.5 years to 12.9 years for cover value of 25mm, 37.5 mm and 50 mm, respectively. For exposure class XS1 (shown in Figure 6.5.1.2), the values are observed to be 3.2 years to 1.8 years, 5.8 years to 2.4 years and 10.6 years to 3.3 years for cover 25mm, 37.5mm and 50mm, respectively. Based on these observations, it can be surmised that higher cover value results in higher crack propagation time. Moreover, larger cover (50mm) imparts high rate of decrease in crack propagation with increasing compressive strength from 15 MPa to 60MPa, as compared to the smaller cover (37.5mm and 25mm).

Figures 6.5.1.3 and 6.5.1.4 show similar trend in case of exposure classes XD2 and XS2, respectively. In case of XD2, increase in compressive strength from 15MPa to 60MPa shows exponential decrease in crack propagation time to be from 5.9 years to 2.4 years, from 10.6

years to 3.3 years, from 19.3 years to 4.5 years and from 35.2 years to 6.1 years for cover values of 37.5mm, 50mm, 62.5mm and 75mm, respectively. Exposure XS2 class structures, however, shows, the exponential decrease to be from 2.6 years to 1.1 years, from 4.8 years to 1.2 years, from 8.8 years to 2 years and from 15.9 years to 2.8 years for similar cover values. It can also be observed that as the severity increases from class XD1 to XS2, the crack propagation time decreases.

6.10.2 Effect of Bar Diameter

As per the model proposed by Mullard and Stewart (2009), bar diameter has a decreasing effect on the cover cracking parameter (Ψ) similar to that of concrete compressive strength. Therefore, like compressive strength, bar diameter variation has exponential decreasing effect on the crack propagation time. In order to investigate the effect of bar size variation on crack propagation time, rebar diameter of 12mm, 16mm, 18mm and 20mm were chosen for each exposure class and concrete cover of 50mm.
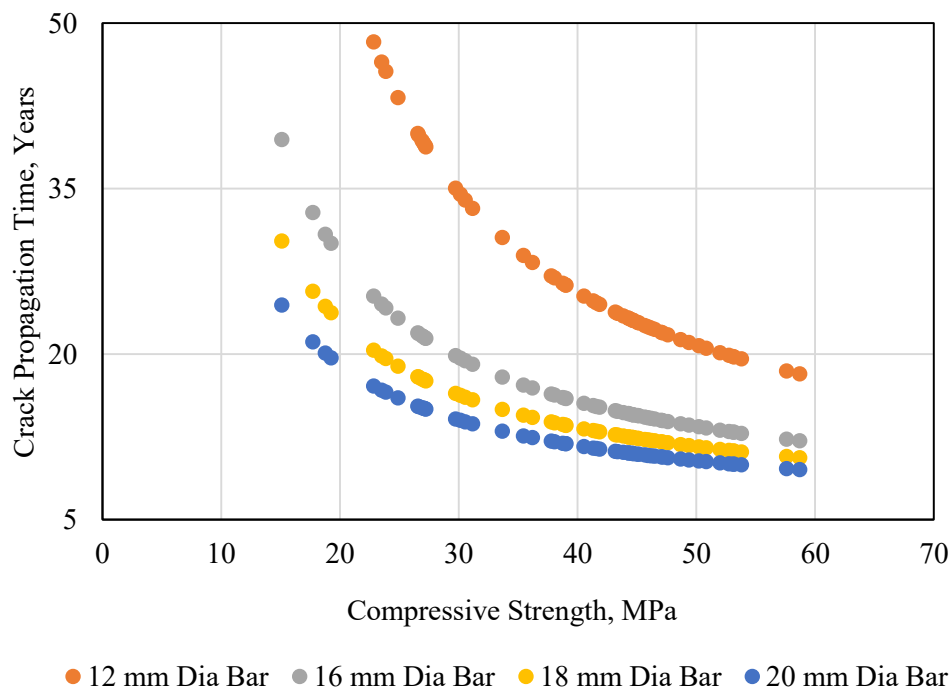
Figure 6.5.2.1: Effect of rebar diameter for exposure class XD1
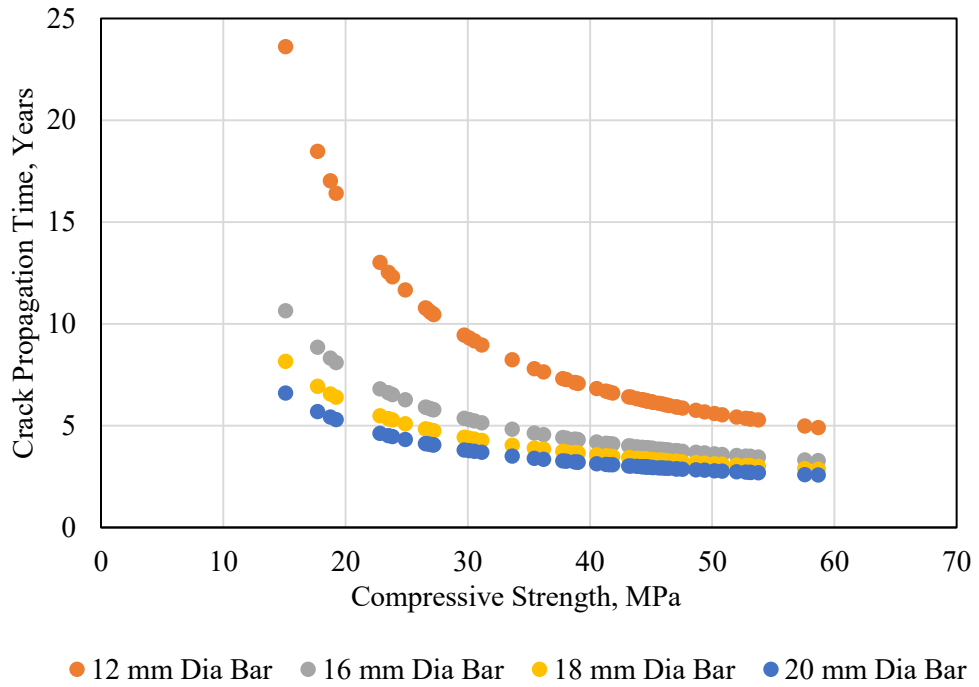
Figure 6.5.2.2: Effect of rebar diameter for exposure class XS1
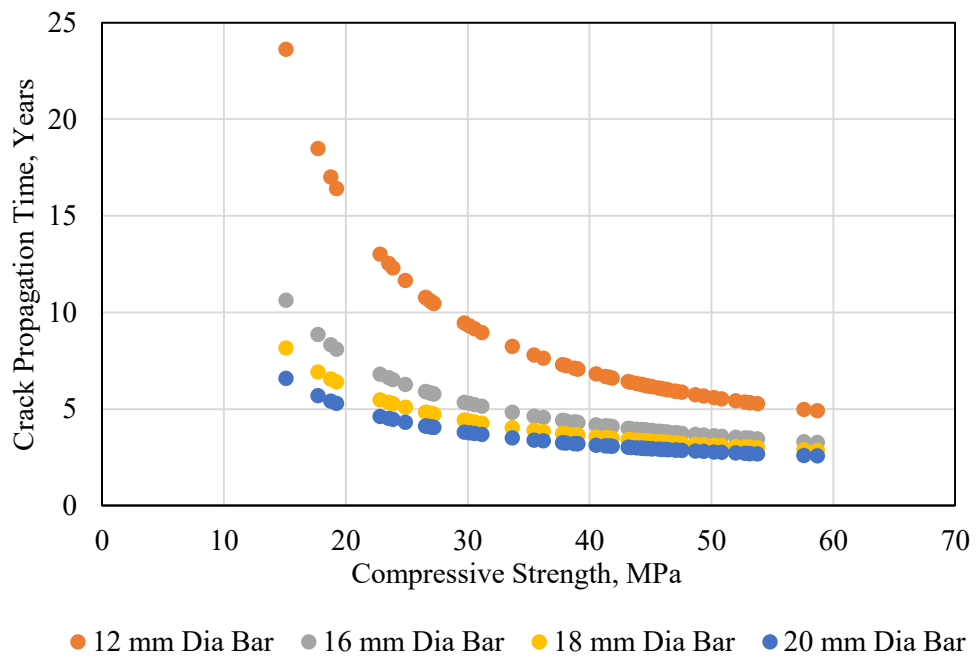
Figure 6.5.2.3: Effect of rebar diameter for exposure class XD2
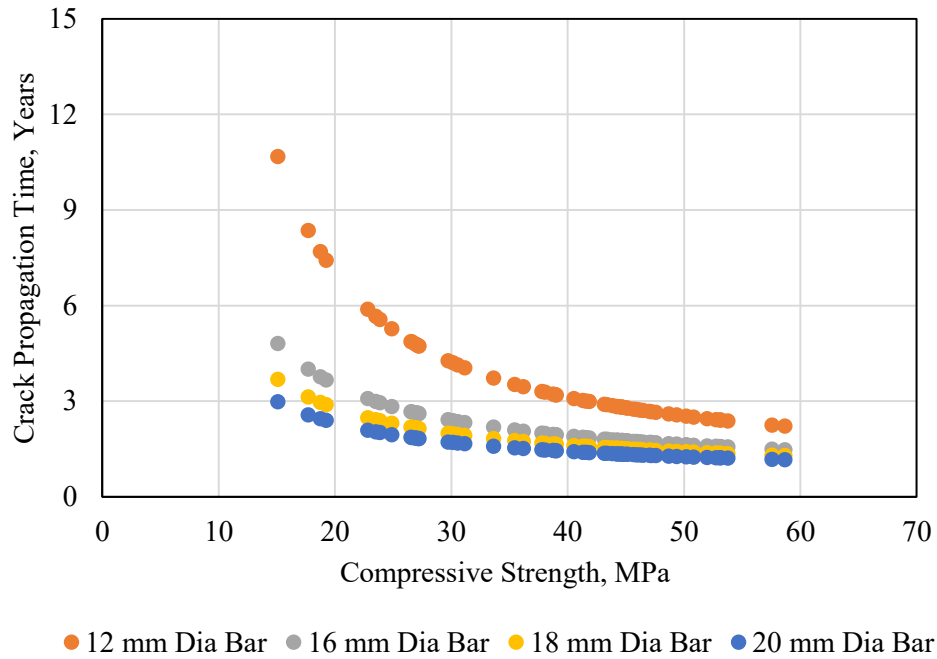
Figure 6.5.2.4: Effect of rebar diameter for exposure class XS2

Figures 6.5.2.1 to 6.5.2.4 show relation between crack propagation time vs compressive strength of the concretes for different bar diameter for exposure classes XD1, XS1, XD2, and XS2, respectively. It can be seen from these figures that larger bar diameter results in lower crack propagation time due to its inverse effect on the cover cracking parameters.

From Figure 6.5.2.1, it can be described that in case of exposure XD1, concrete with compressive strength increasing in the range from 15 MPa to 60 MPa shows exponentially decreasing crack propagation time to be from 87.6 years to 18.5 years, from 39.5 years to 12.3 years, from 30.2 years to 10.7 years and 24.4 years to 9.6 years for rebar diameter of 12mm, 16mm, 18mm and 20mm, respectively. Both exposure classes XS1 (shown in Figure 6.5.2.2) and XD2 (shown in Figure 6.5.2.3) shows similar pattern of decrease in crack propagation time because of the similar corrosion severity (similar corrosion rate). The crack propagation time values, observed for both these cases, are found to be decreasing from 23.6 years to 5.0 years, from 10.6 years to 3.3 years, from 8.2 years to 2.9 years and 6.6 years to 2.6 years for rebar diameter of 12mm, 16mm, 18mm and 20mm, respectively. In case of XS2 type of exposure (Figure 6.5.2.4), however, the exponential decreases in crack propagation time with increase in compressive strength (from 15MPa to 60MPa) are from 10.7 years to 2.3 years, from 4.8 years to 1.5 years, from 3.7 years to 1.3 years and 3.9 years to 1.2 years for rebar diameter of 12mm, 16mm, 18mm and 20mm, respectively. Based on these observations, it can be

concluded that lower value of rebar diameter imparts high decreasing rate on crack propagation time with increasing compressive strength. Comparison between exposure classes also show the trend of increase in crack propagation time due to decrease in corrosion rate or severity.

6.11 Service Life Prediction Result

The main objective of this study was to evaluate service life of different types concrete mixes based on the diffusion coefficient value of the particular mix. In order to achieve this objective, diffusion coefficient obtained through rapid migration test of 58 types of concrete mixes were utilized. Based on these diffusion coefficient values, corrosion initiation time was evaluated. Crack initiation and propagation time was also evaluated based on the chosen parametric value as suggested by codes and literature and some from testing results. Then total service life was determined by adding the corrosion initiation time, crack initiation time and crack propagation time for each mix. For exposure type XD1, the cover increment up to 37.5 mm seems to be enough to provide desirable serviceability whereas for type XS1, it is observed to be 50mm. For other two types of exposure, at least 75 mm cover may be required to obtain adequate service life of RC elements, in come case. Analysis of the observed pattern in service life variation shows similarity with the anticipated trend. However, one of the main reasons behind this research venture is to provide quantification of those established trends.
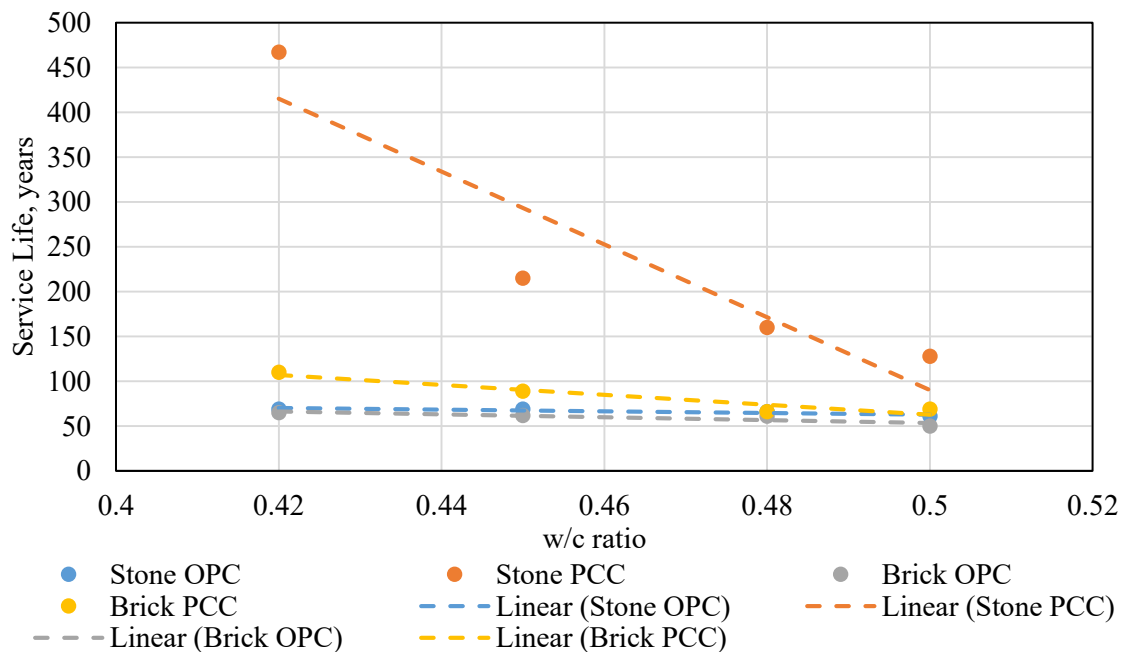
Figure 6.6.1: Effect of Aggregate and Cement Type on Service Life of RC Elements with Cover 37.5mm and Exposure XS1 Type

Figure 6.6.1 shows effect of variation in aggregate type and cement type on service life of RC element with 37.5mm cover and XS1 type of exposure. It can be observed from the graph that service life varies inversely with increasing w/c ratio. As for variation due to aggregate type, stone with OPC shows about 6-7 years increase, on average, in service life as compared to that of brick with OPC. In case of concrete with PCC, stone aggregate shows on average 159 years increase than brick aggregate. It can also be presumed that usage of PCC increases the service life about 4~5 times, on average, with respect to OPC, in case of stone aggregate concrete. For brick aggregate concrete the increase is of about 1.5~2 times, on average than OPC. This similar pattern can be observed for other exposure categories as well, as shown in Figure 6.6.2. Figure 6.6.2 also demonstrates the decrease in service life trends with the increasing intensity of corrosion severity as in order of XD1, XS1, XD2 and XS2.
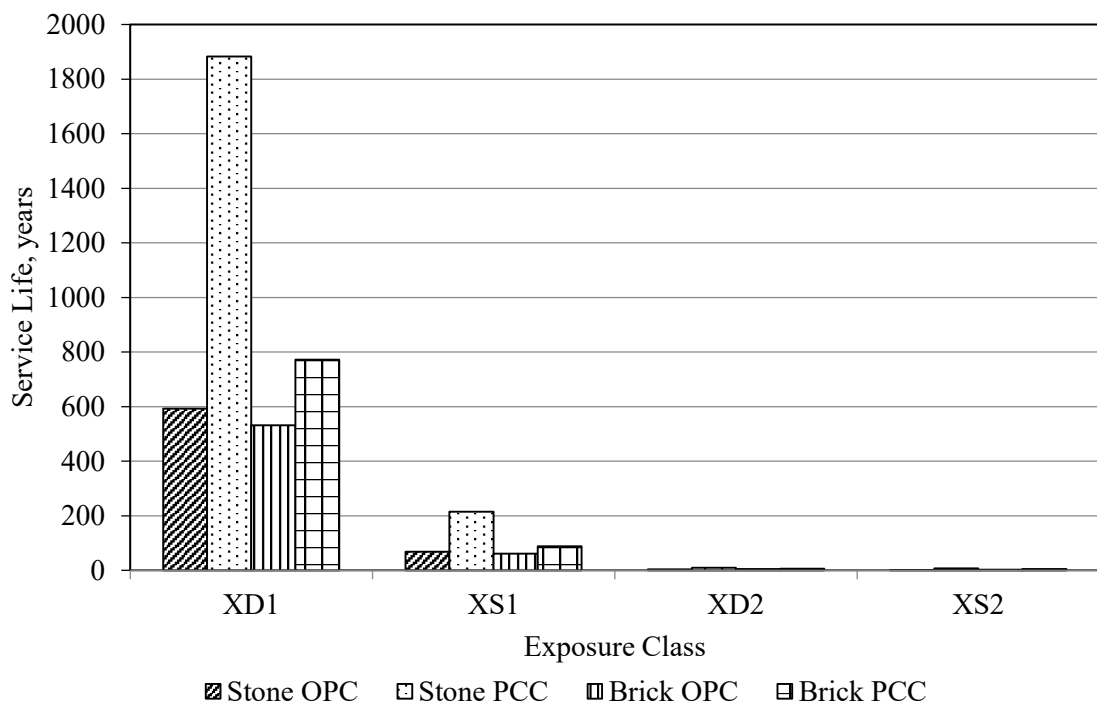
Figure 6.6.2: Effect of Aggregate and Cement Type on Service Life of RC Elements with Cover 37.5mm for varying Exposure

Moreover, change in cover also has profound impact on variation in service life of a RC element. Figure 6.6.3 portrays the trend of such variation for a particular w/c ratio 0.45 and exposure class XS1. It can be seen that in all cases, increase in cover results in higher service life. In almost all case, increase in cover value from 25mm to 37.5mm yields about 10 times better service life whereas from 37.5mm to 50mm it is 3-4 times. Figures 6.6.4 and 6.6.7 also

show increase in service life with increase in cover value for different exposure classes and mix variations.
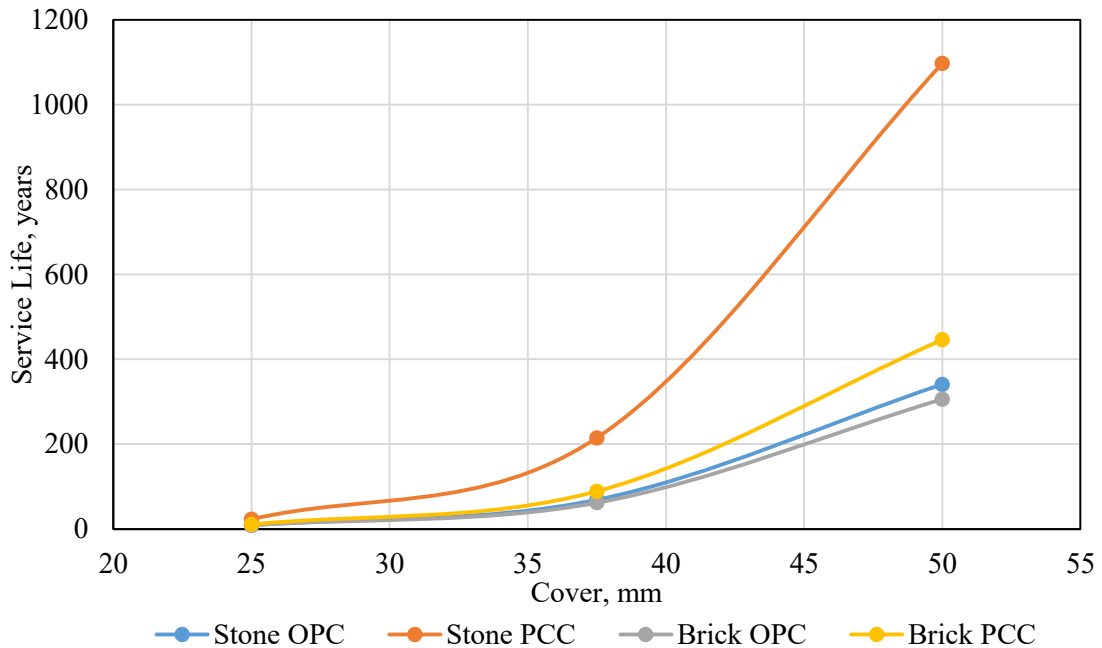
Figure 6.6.3: Effect of Cover Variation

For this research, stone aggregate concrete was prepared for a wide variation w/c ratio ranged from 0.33-0.55. In case of lower w/c ratio (0.33-0.38), water reducing admixture MGlenium ACE 30II was used with the intention of attaining high workability. Figure 6.6.4 displays the impact of admixture on serviceability of concrete mixes prepared using stone aggregate with OPC and PCC for varying cover value. Concretes with admixture and without admixture, considered here, are of w/c ratio 0.35 and 0.45, respectively and are supposed to endure XS1 type of exposure. It can be inferred from the graph that usage of admixture in mixes of low w/c ratio (0.35) results in about 2-5 times higher service life as compared to the mixes without admixture and of high w/c ratio (0.45). Similar pattern can be observed for other exposure classes as shown in Figure 6.6.5 and 6.6.6. In the extreme condition, PCC shows better performance for w/c ratio 0.45 as compared to mixes with w/c ratio of 0.35 and OPC. This is because in case of exposure classes XD1 and XS1, the aging coefficient (a) were chosen 0.65 for both types of cement while for XD2 and XS2 the values considered here are 0.3 and 0.6 as per FIB Bulletin 34 (2006).

Figure 6.6.7 shows change in service life for six different mix variations (Mix No. 41, 44, 47, 50, 53 and 56) of w/c ratio 0.35 exposed to XS1 type environment. Mix 41, 44 and 47 were prepared with stone aggregate (of size 19mm downgraded) and varying admixture content.

While, mix 50, 53 and 56 were prepared to replicate similar slump situations of mix 41, 44 and 47 by using higher water and cement content instead of using admixture. It can be observed from the figure that usage of higher water and cement (mixes 50, 53 and 56) cannot attain similar level of serviceability as that of mixes with admixture. However, increase in cement content from 514 Kg/m^3 to 557 Kg/m^3 has positive impact on the service life improvement.
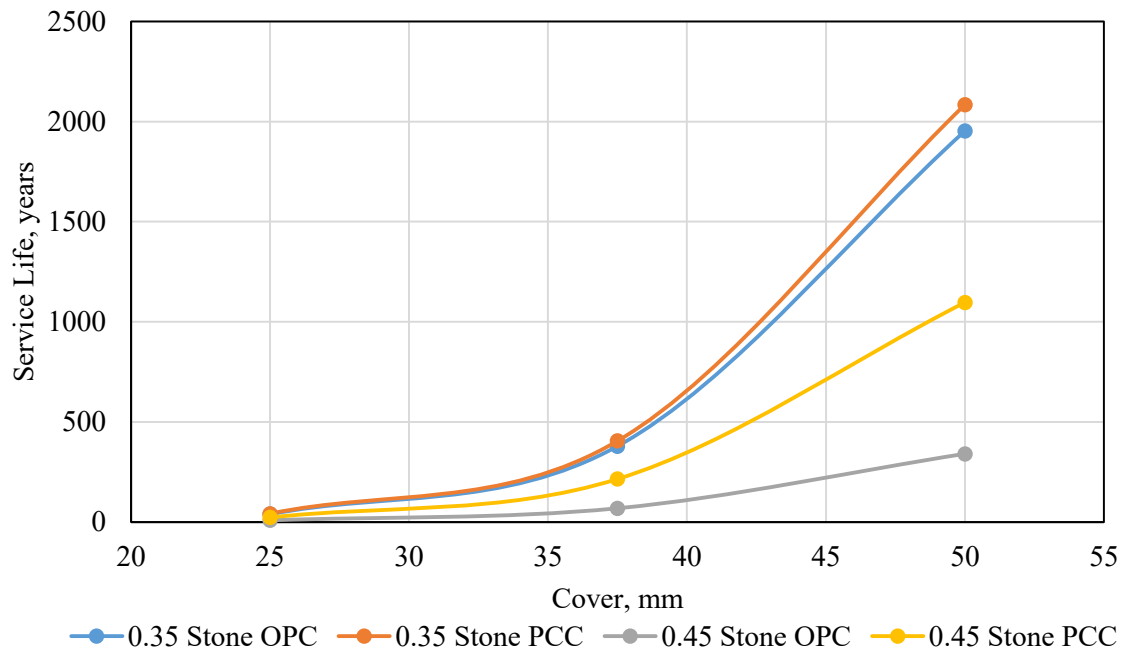
Figure 6.6.4: Variation in Service Life for Mixes with and without Admixture (XS1 Exposure)
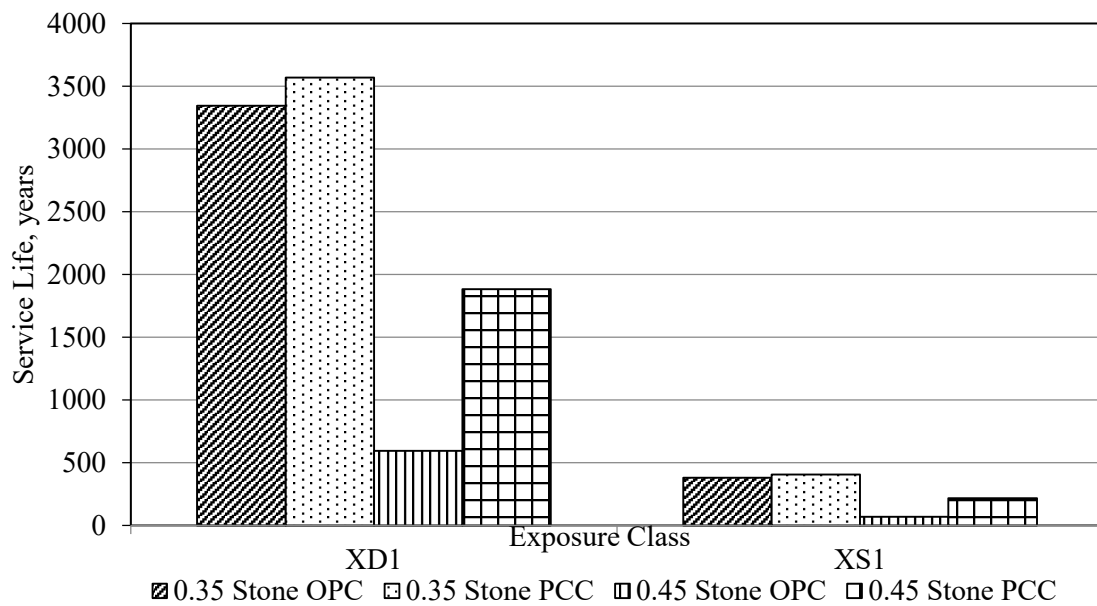
Figure 6.6.5: Impact of Admixture for Exposure XD1 and XS1
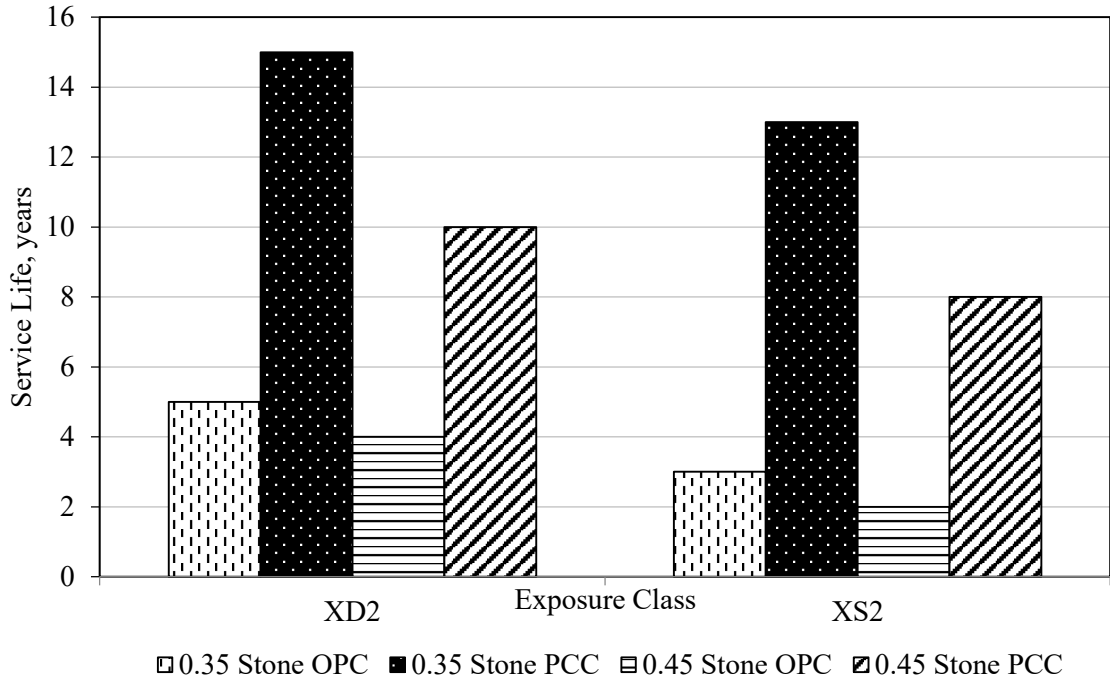
Figure 6.6.6: Impact of Admixture for Exposure XD2 and XS2
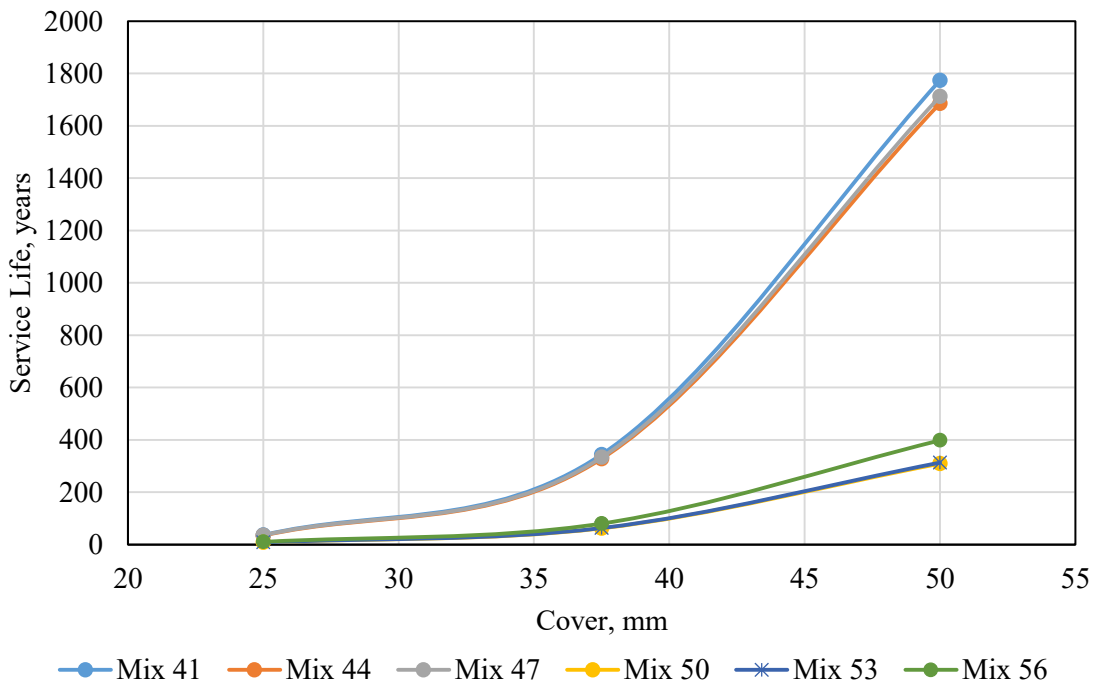
Figure 6.6.7: Service Life Variation for Mixes with Varying Admixture and Higher
Cement and Water Content

Now, the total service life from corrosion initiation to crack propagation time, for all mixes
considered are given in the following tables (Tables 6.1 to 6.4) as per the exposure category

and chosen concrete cover for further understanding. The values shown were calculated using the aging exponent value, in case of XD1 and XS1 of 0.65 for OPC and PCC both and in case of XS2 and XD2, 0.3 for OPC and both 0.6 and 0.45 for PCC.

Table 6.1 Service Life for Exposure Class XD1

Mix No.	25mm Cover Service Life, (years)	37.5 mm Cover Service Life, (years)	50 mm Cover Service Life, (years)
1	406	4006	14280
2	667	6656	23753
3	434	4353	15521
4	488	3345	17247
5	500	3430	17689
6	597	4113	21221
7	250	1671	8582
8	306	2073	10661
9	288	1949	10018
10	455	3115	16054
11	1072	7441	38448
12	492	3376	17408
13	520	3568	18398
14	809	5595	28886
15	727	5022	25924
16	379	2582	13293
17	734	5072	26179
18	321	2172	11175
19	96	603	3054
20	96	593	2998
21	93	570	2872
22	86	518	2607
23	57	315	1559
24	599	4123	21269
25	280	1883	9677
26	210	1397	7155
27	171	1113	5686
28	194	1281	6555
29	92	561	2825
30	87	532	2675
31	87	520	2610
32	74	424	2107
33	148	956	4871
34	122	772	3916
35	93	568	2861
36	96	585	2937

Mix No.	25mm Cover Service Life, (years)	37.5 mm Cover Service Life, (years)	50 mm Cover Service Life, (years)
37	64	365	1808
38	69	394	1956
39	61	334	1635
40	50	253	1209
41	445	3038	15655
42	803	5552	28671
43	628	3584	18483
44	423	2883	17453
45	621	4278	22072
46	473	3240	16704
47	429	2933	15110
48	635	4375	22577
49	489	3351	17281
50	88	537	2709
51	123	782	3977
52	320	2169	11156
53	89	544	2745
54	128	817	4158
55	121	774	3940
56	109	685	3471
57	204	1356	6950
58	143	928	4737

Table 6.2 Service Life for Exposure Class XS1

Mix No.	25mm Cover Service Life, (years)	37.5 mm Cover Service Life, (years)	50 mm Cover Service Life, (years)
1	33	315	1617
2	53	522	2690
3	36	342	1758
4	39	379	1953
5	40	389	2003
6	48	467	2403
7	21	190	973
8	25	236	1208
9	24	222	1136
10	37	354	1819
11	85	843	4353
12	40	383	1972
13	42	405	2084
14	65	634	3270
15	58	570	2936
16	31	293	1506
17	59	575	2965
18	26	247	1267
19	9	69	347
20	9	69	341
21	9	66	328
22	8	61	298
23	6	37	179
24	48	467	2409
25	23	215	1097
26	18	160	812
27	15	128	646
28	17	147	745
29	9	65	323
30	9	62	306
31	9	61	299
32	8	50	243
33	13	110	554
34	11	89	446
35	9	66	327
36	10	69	337

Mix No.	25mm Cover Service Life, (years)	37.5 mm Cover Service Life, (years)	50 mm Cover Service Life, (years)
37	7	43	208
38	7	47	227
39	7	41	191
40	6	32	144
41	36	344	1774
42	64	630	3249
43	50	491	2530
44	34	328	1686
45	50	485	2501
46	46	444	2289
47	35	333	1712
48	51	496	2558
49	39	381	1958
50	8	62	309
51	11	90	453
52	26	246	1264
53	8	63	313
54	11	93	474
55	11	89	450
56	10	80	398
57	17	154	790
58	13	106	538

Table 6.3 Service Life for Exposure Class XD2

Mix No.	37.5 mm Cover Service Life, (years)		50 mm Cover Service Life, (years)		62.5 mm Cover Service Life, (years)		75 mm Cover Service Life, (years)	
	a=0.3; a=0.6	a=0.45	a=0.3; a=0.6	a=0.45	a=0.3; a=0.6	a=0.45	a=0.3; a=0.6	a=0.45
1	5		9		15		25	
2	5		9		17		29	
3	5		9		15		25	
4	5		9		16		27	
5	5		9		16		27	
6	5		9		17		28	
7	5		8		14		23	
8	4		8		14		23	
9	4		8		14		23	
10	14	6	72	17	270	39	775	79
11	25	9	150	25	572	63	1654	131
12	14	6	77	17	288	40	830	82
13	15	7	81	18	303	42	872	86
14	21	8	118	22	447	53	1290	111
15	19	7	107	21	407	50	1174	105
16	12	6	62	15	230	35	658	72
17	19	7	108	21	410	51	1184	105
18	11	6	54	14	198	32	567	65
19	4		6		10		16	
20	4		7		11		18	
21	5		8		13		21	
22	5		8		14		22	
23	4		7		12		19	
24	17	7	91	19	344	46	989	93
25	10	6	49	14	177	31	503	63
26	9	6	39	13	138	28	389	55
27	8	5	33	12	114	25	321	49
28	9	6	37	13	130	28	364	54
29	5		8		14		22	
30	5		8		14		22	
31	5		9		15		25	
32	6		10		18		31	
33	8	6	30	12	102	25	284	48
34	7	6	26	12	87	24	238	45
35	7	6	22	11	69	22	186	41
36	8	7	25	14	75	27	199	51

Mix No.	37.5 mm Cover Service Life, (years)		50 mm Cover Service Life, (years)		62.5 mm Cover Service Life, (years)		75 mm Cover Service Life, (years)	
	a=0.3; a=0.6	a=0.45	a=0.3; a=0.6	a=0.45	a=0.3; a=0.6	a=0.45	a=0.3; a=0.6	a=0.45
37	5		8		13		21	
38	5		9		15		25	
39	6		10		18		31	
40	7		12		23		41	
41	5		9		17		28	
42	5		10		19		31	
43	5		9		17		29	
44	5		9		16		27	
45	5		10		18		29	
46	5		9		17		28	
47	5		9		16		26	
48	5		9		17		29	
49	5		9		15		26	
50	4		7		11		18	
51	4		7		11		18	
52	5		8		14		23	
53	4		7		11		18	
54	4		7		11		18	
55	4		7		11		18	
56	4		7		12		19	
57	4		8		13		21	
58	4		7		11		18	

Table 6.4 Service Life for Exposure Class XS2

Mix No.	37.5 mm Cover Service Life, (years)		50 mm Cover Service Life, (years)		62.5 mm Cover Service Life, (years)		75 mm Cover Service Life, (years)	
	a=0.3; a=0.6	a=0.45	a=0.3; a=0.6	a=0.45	a=0.3; a=0.6	a=0.45	a=0.3; a=0.6	a=0.45
1	3		6		12		21	
2	3		7		14		25	
3	3		6		12		21	
4	3		7		13		23	
5	3		7		13		23	
6	3		7		14		24	
7	3		5		10		18	
8	3		6		11		19	
9	3		6		11		18	
10	12	4	70	14	266	35	770	74
11	24	7	147	23	568	59	1650	127
12	13	5	74	15	285	37	825	78
13	13	5	78	15	300	38	867	81
14	19	6	115	20	443	50	1285	106
15	17	6	105	18	404	47	1169	100
16	10	4	59	13	226	31	653	67
17	17	6	106	19	407	47	1180	100
18	9	4	51	12	195	29	562	60
19	2		4		7		12	
20	2		4		7		12	
21	2		5		8		14	
22	3		5		8		14	
23	2		4		7		12	
24	15	5	89	17	340	42	984	88
25	8	4	46	11	172	27	496	56
26	7	4	36	10	133	23	383	48
27	6	3	30	9	110	21	314	42
28	7	4	34	10	124	23	356	46
29	3		5		8		14	
30	3		5		8		14	
31	3		5		9		15	
32	3		6		10		17	
33	6	3	27	9	97	20	275	40
34	5	3	23	8	81	18	229	36
35	4	3	18	7	63	16	176	31
36	5	4	19	8	66	18	184	36

Mix No.	37.5 mm Cover Service Life, (years)		50 mm Cover Service Life, (years)		62.5 mm Cover Service Life, (years)		75 mm Cover Service Life, (years)	
	a=0.3; a=0.6	a=0.45	a=0.3; a=0.6	a=0.45	a=0.3; a=0.6	a=0.45	a=0.3; a=0.6	a=0.45
37	2		4		8		13	
38	3		5		9		15	
39	3		5		10		17	
40	3		6		12		21	
41	3		7		13		22	
42	3		8		16		27	
43	3		7		14		25	
44	3		7		13		22	
45	3		7		14		25	
46	3		7		14		24	
47	3		6		12		21	
48	3		7		14		25	
49	3		6		13		22	
50	2		4		7		12	
51	2		4		8		13	
52	3		6		11		19	
53	2		4		7		12	
54	2		4		8		13	
55	2		4		8		13	
56	2		4		8		13	
57	2		5		9		16	
58	2		4		8		14	

6.12 Overview

The corrosion initiation time of RC elements, determined using the diffusion coefficients of the concrete mixes used, show variations with changes in mix parameters. This corrosion initiation time is followed by time to severe cracking which is a function of concrete and rebar property of RC element and corrosion severity of the surrounding environment. Using the corrosion initiation and severe cracking time, the total service life of different concrete types were evaluated and the obtained outcomes were analyzed for existing pattern. The analysis show better performance of stone aggregate and PCC in case of severe corrosion susceptibility. In contrast, concretes with brick aggregate and OPC show least service life values. Usage of water reducing admixture with low water content seems to improve service life to great extent.

Furthermore, higher values of concrete cover impart better serviceability, especially in case of severe environmental exposure. All observed patterns discussed above, show compliance with the expected trend. However, quantification of the effect of different important parameters on service life of a wide range of common concrete mixes has been presented. Such quantification can be considered as the primary significance of this research endeavor.

7.1 General

The main objectives of this research attempt was to evaluate service life of various concrete mix types based on their chloride diffusion coefficient values and observe variation in its pattern due to changes in concrete mix parameters. Effects of multiple factors – aggregate type and gradation, cement type, mix proportions, W/C ratio, admixture content, concrete cover, bar diameter and exposure class on different components of service life of a wide variety of concrete mixes, prepared using locally available material, were studied in depth. An attempt to quantify the effects of those variables on serviceability has been made based on these study findings. This chapter includes an overall summary of the major outcomes obtained from this research work with several recommendations for future research works to be conducted on this domain.

7.2 Conclusions

In this study, chloride diffusion coefficients of different concrete mixes were determined from a non-steady state migration experiment. The obtained values can be considered as key durability parameters as they signify the measure of the resistance of concrete mixes to the chloride ingress. All the evaluated results were studied for variation with changes in the mix parameters and the following conclusions were reached:

   i. Stone aggregate concrete with low w/c ratio (0.33-0.38) and admixture shows lower coefficient values and therefore, lower chloride susceptibilities as compared to stone aggregate concrete with high w/c ratio (0.42~0.55) and no admixture. In case of stone aggregate concrete containing OPC, mix with w/c ratio of 0.45 shows diffusion coefficient value of 23.77×10^{-12} m^2/s which is about 1.85 times higher than the value of mix with 0.35 w/c ratio and admixture. Similar pattern can be observed in case of mixes with PCC.For mixes with w/c ratio of 0.45, diffusion coefficient value is of 20.665×10^{-12} m^2/s whereas for w/c ratio of 0.35 it is 12.57×10^{-12} m^2/s. The reason that can be attribute to these observations is the formation of better hydration product due to lower water content.

ii.   Use of PCC as an alternative to OPC, in case of stone aggregate concrete, provides better resistance to chloride ion penetration with lower values of diffusion coefficient. In case of stone aggregate concrete mixes containing PCC and w/c ratio of 0.45, a diffusion coefficient value of 15.75×10^{-12} m^2/s was obtained while its OPC counterpart showed a diffusion coefficient value of as high as 23.77×10^{-12} m^2/s.

iii.   Among three gradation type of stone aggregate, mix type 2 (60% 0f ¾ and 40% of ½) exhibits about 12% and 9% better performance, on average, as compared to the gradation type 1(100% of ¾) and type 3 (100% of ½), in case of mixes with OPC. However, for PCC mixes, these values are about 23~24% and 21~22%, respectively.

iv.   Mixes with higher water and cement content, prepared with the intention of achieving similar slump values for w/c ratio 0.35 without admixture, yields relatively poor result as compared to similar mix with admixture. This is because, a higher water content leads to presence of greater free water content in the cement mix which results in a higher permeability due to development of poorly oriented hydration products. This is the same reason that contributes to the increase in permeability thus in diffusion coefficient values with the increase in w/c ratio, regardless of the cement or aggregate type used.

v.   Between two aggregate types, stone aggregate demonstrates better performance in resisting chloride penetration than brick aggregate, irrespective of the w/c ratio and cement type used. The test results show, on average, about 5~6% higher diffusion coefficients of brick aggregate concrete with OPC and w/c ratio range 0.42~0.5 than the stone aggregate concrete with similar composition of w/c ratio and cement. Use of PCC in brick aggregate concrete improves its durability performance to an extent (such as for w/c ratio of 0.45, 12% reduction as compared to OPC) but still, brick aggregate yields concrete with unacceptable or very poor resistance to chloride ingress.

vi.   In case of brick aggregate concrete, two commonly used mix proportions- 1:1.5:3 and 1:2:4 were considered to study their effects on durability aspects. The results show, between these two mix variations, concretes with 1:2:4 perform the least in resisting chloride penetration, regardless of the w/c ratio used. The mixes with 1:1.5:3 volumetric

ratio show diffusion coefficient values ranging from 24×10^{-12} to $27 \times 10^{-12} m^2/s$ while the mixes with mix proportion 1:2:4 exhibits coefficient values from 28×10^{-12} to $32.9 \times 10^{-12} m^2/s$.

Based on these diffusion coefficient values, the corrosion initiation times of various concrete mixes were determined for four different exposure classes (XD1, XD2, XS1 and XS2) and five concrete cover values of 25mm, 37.5mm, 50mm, 62.5mm and 75mm. Corrosion initiates when the chloride level within concrete reaches a critical value. The accumulated corrosion products start exerting expansive force and eventually cracking occurs. The time required to severe cracking was measured from compressive strength value of the mixes for the exposure classes and concrete cover selected. Ultimately, the total service life of all the concrete mixes were calculated from their respective corrosion initiation, crack initiation and crack propagation time. The findings of service life evaluation can be summarized as follows:

i. The variation in corrosion initiation time follows similar pattern as that of discussed in case of variation in diffusion coefficient. This is because the corrosion initiation time is directly proportional to the diffusion coefficient values. However, other factors such as concrete cover, aging exponent and the exposure class also have significant impacts on the variation of corrosion initiation time.

ii. As for crack initiation and propagation time, higher concrete cover provides longer severe cracking time to reach the limiting crack width of 1.0 mm. In case of exposure class XS2, the cover increase from 62.5mm to 75mm shows increase in severe cracking time (crack initiation + crack propagation) from 3~8 years to 4~13 years.

iii. As for compressive and rebar diameter value, both have decreasing effect on the cover cracking parameter thus on severe cracking time.

iv. In case of least severe exposure condition XD1, all concrete mixes perform well with the typical concrete cover. As for medium exposure of XS1 in saline environment, the cover typically provided are also found to be satisfactory for attaining service life for both OPC and PCC concrete.

v.   In extreme exposure condition, OPC mixes with both stone and brick aggregates perform the least. It appears that usage of OPC and brick aggregate needs to be avoided for extreme exposure condition unless significantly higher cover is provided.

vi.   Although usage of PCC improves the service life of both brick and stone aggregate concrete to a considerable extent, use of stone aggregate in conjunction with PCC can be used for enhanced service life, in extreme exposure condition of XD2 and XS2. It appears that brick aggregate concrete with PCC can also provide satisfactory service life. This is because of the higher aging exponent considered for PCC on which service life value is significantly dependent. However, it would be prudent to determine aging exponent for brick aggregate concrete through proper experimentation in order to provide conclusive comment on service life of such concrete.

vii.   The inclusion of water reducing admixture with low w/c ratio also proves to be effective in improvement of service life, especially under severe exposure conditions.

7.3 Suggestions for Future Study

The research is one of the fresh attempts in Bangladesh to evaluate the serviceability of different types of concrete with moderate to extreme exposure. The concept of using migration coefficient of concrete mixes in determining the total service life of a RC element is still new in the context of Bangladesh. Hence, the prospect of further improvement and extensive research is also immense. This study considered the effects of variations in diffusion coefficient for different mixes, concrete cover, aging exponent and exposure classes for service life assessment of RC structures. The observations show significant impact of diffusion coefficient, cover and aging exponent on the variations of service life values. However, this study has utilized aging exponent from fib 34 (2006) code. Moreover, the test results obtained were based on relatively small sample size. Hence, it is suggested to include following directives for future research endeavor:

i.   Effect of varying cement content and supplementary cementitious material on the service life of concrete structure should be studied with statistically significant sample size to quantify any possible degree of enhancement.

ii.   The service life modelling of the existing structures is of immense importance. The diffusion coefficient, chloride level and the aging exponent can be determined from the migration test on samples from existing structures. A range of cover value can be selected from a comprehensive survey data, performed on such structures all over the country.

iii. Certain parameter values considered in determining corrosion initiation time were adopted from codes which were developed considering environmental condition of certain countries. Therefore, future research should include study and suggest values for the environmental conditions of Bangladesh.

iv.   The corrosion initiation time is found to be significantly affected by the aging exponent value in conjunction with diffusion coefficient. However, the available code does not include specification of any aggregate type in determining the aging exponent value. Moreover, the available data does not include values for lower w/c ratio and PCC cement types usually used in this country. Therefore, valuation of aging exponent for such locally used mix variations can be made, especially for brick aggregate concrete.

v.   For this study the effect of carbonation on chloride induced corrosion was not considered. So, future study considering effect of carbonation on the chloride induced corrosion is recommended for thorough understanding of this phenomena.

Afroz, S., Rahman, F., Iffat, S., and Manzur, T. (2015). "Sorptivity and Strength Characteristics of Commonly Used Concrete Mixes of Bangladesh." International Conference on Recent Innovation in Civil Engineering for Sustainable Development (IICSD)

Almusallam, A. A., Al-Gahtani, A. S., Aziz, A. R., and Rasheeduzzafar,(1996). "Effect of reinforcement corrosion on bond strength." *Constr. Build. Mater.,* 10(2), 123–129. DOI: 10.1016/0950-0618(95)00077-1.

Alonso, C., Andrade, C., Castellote, M. and Castro, P., (2000). "Chloride threshold values to depassivate reinforcing bars embedded in a standardized OPC mortar." *Cem. Concr. Res.,* 30(7), pp. 1047–1055.

Alonso, C., Andrade, C., Rodriguez, J., and Diez, J. M. (1998). "Factors controlling cracking of concrete affected by reinforcement corrosion." *Mater. Struct.,* 31(7), 435–441. DOI: 10.1007/bf02480466.

Al-Sulaimani, G. J., Kaleemullah, M., Basunbul, I. A., and Rasheeduzzafar, (1990). "Influence of corrosion and cracking on bond behavior and strength of reinforced concrete members." *ACI Struct. J.,* 87(2), 220–231. DOI: 10.14359/2732.

Altoubat, S., Maalej, M., and Shaikh, F. (2016). "Laboratory Simulation of Corrosion Damage in Reinforced Concrete." *International Journal of Concrete Structures and Materials,* 10(3), 383-391. DOI: 10.1007/s40069-016-0138-7.

Angst, U. (2011). "Chloride induced reinforcement corrosion in concrete: Concept of critical chloride content – methods and mechanisms." Ph.D. thesis, Department of Structural Engineering, Norwegian University of Science and Technology.

ASTM C.143 / C143M, (2015). " Standard Test Method for Slump of Hydraulic-Cement Concrete." ASTM International, West Conshohocken, PA.

ASTM C29 (2009), "Standard Test Method for Bulk Density ("Unit Weight") and Voids in Aggregate," ASTM International, West Conshohocken, PA, DOI: 10.1520/C0029, http://www.astm.org/.

ASTM C39 – 14a, (2014). "Standard Test Method for Compressive Strength of Cylindrical Concrete Specimens," ASTM International, West Conshohocken, PA, DOI: 10.1520/C0039_14a, http://www.astm.org/.

ASTM C127 (2007), "Standard test method for Density, Relative Density (Specific Gravity) and Absorption of Coarse Aggregate," ASTM International, West Conshohocken, PA, DOI: 10.1520/C0127, http://www.astm.org/.

ASTM C128 (2009), "Standard test method for Density, Relative Density (Specific Gravity) and Absorption of Fine Aggregate," ASTM International, West Conshohocken, PA, DOI: 10.1520/C0128, http://www.astm.org/

ASTM C136 / C136M-14 (2014), "Standard Test Method for Sieve Analysis of Fine and Coarse Aggregates," ASTM International, West Conshohocken, PA, DOI: 10.1520/C0136_C0136M-14, http://www.astm.org/

Bajaj, S. (2012). "Effect of corrosion on physical and mechanical properties of reinforced concrete." M.S. thesis, Univ. of Akron, Akron, OH.

Baten, B. and Hasan, M. J. (2017). "Evaluation of Corrosion Damage of Indigenous Concrete Mixes in Bangladesh using Half-Cell Potential." B. Sc. Thesis in Civil Engineering, Department of Civil Engineering, Bangladesh University of Engineering and Technology, Dhaka, Bangladesh.

Bertolini, L., Bolzoni, F., Pastore, T., and Pedeferri, P. (1996). "Behaviour of stainless steel in simulated concrete pore solution." *Br. Corros. J.,* 31(3), 218–222. DOI: 10.1179/bcj.1996.31.3.218.

Browne, R. D. (1980). "Mechanisms of corrosion of steel in concrete in relation to design, inspection, and repair of offshore and coastal structures." *Performance of concrete in marine environment, ACISP-65.* Detroit, Michigan: American Concrete Institute. pp. 169-204.

Bungey, J. H. (1989). *Testing of concrete in structures*, 2nd Ed. New York: Chapman & Hall,

Carino, N. J. (1999). "Nondestructive Techniques to Investigate Corrosion Status in Concrete Structures." *Journal of Performance of Constructed Facilities,* 13(3), 96-106. DOI: 10.1061/(asce)0887-3828(1999)13:3(96).

Clifton, J. (1993). "Predicting the service life of concrete." *ACI Materials Journal,* 90(6), 611–617.

DARTS (2004). "Durable and Reliable Tunnel Structures: Deterioration Modelling, European Commission, Growths 2000," Contract G1RD-CT-2000-00467, Project GrD1-25633.

Das, B. B., Singh, D. N., and Pandey, S. P. (2012). "Rapid chloride ion permeability of OPC- and PPC-based carbonated concrete." *Journal of Materials in Civil Engineering,* 24(5), 606-611. DOI: 10.1061/(ASCE)MT.1943-5533.0000415.

DuraCrete (1998). "Modelling of Degradation, DuraCrete - Probabilistic Performance based Durability Design of Concrete Structures, EU - Brite EuRam III," Contract BRPR-CT95-0132, Project BE95-1347/R4-5, December 1998, pp. 174.

DuraCrete (2000a). "Statistical Quantification of the Variables in the Limit State Functions, DuraCrete - Probabilistic Performance based Durability Design of Concrete Structures. EU - Brite EuRam III," Contract BRPR-CT95-0132, Project BE95-1347/R9, January 2000, pp. 130.

Elfmarkova, V., Spiesz, P. and Brouwers, H.J.J. (2015). "Determination of the Chloride Diffusion Coefficient in Blended Cement Mortars," *Cem. And Conc. Res.,* 78(2015):190-199.

El Maaddawy, T. and Soudki, K.A. (2007). "A Model for Prediction of Time from Corrosion Initiation to Corrosion Cracking." *Cement & Concrete Composites*, 29(3): 168-175.

Elsener, B. (2002). "Macrocell corrosion of steel in concrete – implications for corrosion monitoring." *Cement and Concrete Composites,* 24(1):65-72. DOI:10.1016/s0958-9465(01)00027-0.

Ervine, C. and Cooper, T. (2010). *Longer Lasting Products: alternatives to the throwaway society*, 1st ed., Farnham, Surrey: Gower.

Etman, Z. A. (2012). "Reinforced Concrete Corrosion and Protection." *Concrete Research Letters*, 3(1).

Farhat, R. (2010). "Thickness of Concrete Cover for Corrosion Protection of Steel Reinforcement and Crack Control." *Advanced Materials Research,* 95:61-68. DOI: 10.4028/www.scientific.net/AMR.95.61.

Feliu, S., González, J., Feliu, S., and Andrade, C. (1989). "Relationship between conductivity of concrete and corrosion of reinforcing bars." *British Corrosion Journal,* 24(3):195-198. DOI:10.1179/000705989798270027.

Feliu´, S., Gonza´lez, J. A., Andrade, C., and Feliu´, V. (1989). ''Polarization resistance measurements in large concrete specimens: Mathematical solution for unidirectional current distribution.'' *Materials and structures: Research and testing (RILEM),* 22(129):199–205.

Feliu´, S., Gonza´lez, J. A., and Andrade, C. (1996). ''Electrochemical methods for on-site determinations of corrosion rates of rebars.'' *Techniques to assess the corrosion activity of steel reinforced concrete structures, ASTM STP 1276,* N. Berke, E. Escalante, C. Nmai, and D. Whiting, ed. West Conshohocken, Pa.: ASTM. pp.107–118.

FIB Bulletin 34 (2006). "Model Code for Service Life Design." Fib. Lausanne.

GEMITE Technical Memorandum (2005). "Corrosion of Steel in Concrete due to Carbonation." Available at:
http://gemite.com/tech_bulletin/Tech_Bulletin_Concrete_Corrosion_due_to_Carbonation_04_05.pdf.

Heiyantuduwa, R., Alexander, M. G., and Mackechnie, J. R. (2006). "Performance of a penetrating corrosion inhibitor in concrete affected by carbonation-induced corrosion." *J. Mater. Civ. Eng.,* 18 (6), 842–850. DOI: 10.1061/(ASCE)0899-1561(2006)18:6(842).

Hong, K., and Hooton, D. (1999). "Effects of Cyclic Chloride Exposure on Penetration of Concrete Cover." *Cement and Concrete Research,* 29(9):1379-1386. DOI: 10.1016/S0008-8846(99)00073-3.

Hou, T.C., Nguyen, V.K., Su, Y.M., Chen, Y.R., and Chen, R. J. (2017). "Effects of coarse aggregates on the electrical resistivity of Portland cement concrete," *Const. and Build. Mater.,* 133:397-408.

Langford, P & Broomfield, J. (1987). "Monitoring the corrosion of reinforcing steel." *Constr. Repair,* 1:32-36.

Leber, I., and Blakey, F. A. (1956). "Some effects of carbon dioxide on mortars and concrete." *ACI Mater. J.,* 28(3), 295–308. DOI: 10.14359/11515.

Lee, S., Won, J., Park, D., Lee, M., & Moon, K. (2013). "The Effect of Cover Thickness to Corrosion Characteristics of Reinforced Steel Bar Emedded in Mortar Specimen (W/C:0.6) Aged 5 Years in Seawater." *Advanced Materials Research,* 785-786, 1176-1180. DOI: 10.4028/www.scientific.net/amr.785-786.1176.

Lizarazo-Marriaga, J. and Claisse, P. (2009). "Determination of the concrete chloride diffusion coefficient based on an electrochemical test and an optimization model." *Materials Chemistry and Physics,* 117(2-3):536-543.

LNEC E 465 (2005). "Methodology for Estimating the Concrete Performance Properties Allowing to Comply with the Design Working Life of the Reinforced or Prestressed Concrete Structures under the Environmental Exposures XS and XC." LNEC Specification, Portugal.

Mart´ın-P´erez, B., Zibara, H., Hooton, R., and Thomas, M. (2000). "A study of the effect of chloride binding on service life predictions." *Cement and Concrete Research,* 30(8):1215-1223.

Manzur, T., Baten, B., Hasan, M.J., Akter, H., Tahsin, A., and Hossain, K. M. A. (2018). "Corrosion Behaviour of Concrete Mixes With Masonry Chips," *Cons. And Build. Mate.,* 185: 20-19.

Mindess, S., Young, JR., and Darwin, D. (2003). *Concrete.* New Jersey: Pearson Prentice Hall, 495p.

Millard, S. G., Harrison, J. A., and Edwards, A. J. (1989). ''Measurement of the electrical resistivity of reinforced concrete structures for the assessment of corrosion risk.'' *The British J. Non-Destructive Testing,* 31(11), 617–621. DOI: 10:49:21 2016 BST.

Millard, S. G., Ghassemi, M. H., and Bungey, J. H. (1990). ''Assessing the electrical resistivity of concrete structures for corrosion durability studies.'' *Corrosion of reinforcement in concrete*, C. L. Page, K. W. J. Treadway, and P. B. Bamforth, ed. New York: Elsevier Science. p.303–313.

Miyazato, S., and Otsuki, N. (2010). "Steel Corrosion Induced by Chloride or Carbonation in Mortar with Bending Cracks or Joints." *Journal of Advanced Concrete Technology,* 8(2), 135-144. DOI: 10.3151/jact.8.135.

Mirza, S.A., Hatzinikolas, M., MacGregor, J.G. (1979). "Statistical Descriptions of Strength of Concrete." *Journal of the Structural Division,* 105(ST6): 1021-1037.

Montemor, M. F., Simões, A. M. P., and Ferreira, M. G. S. (2003). "Chloride-induced corrosion on reinforcing steel: From the fundamentals to the monitoring techniques." *Cem. Concr. Compos.,* 25(4–5):491–502. DOI: 10.1016/s0958-9465(02)00089-6.

Moreno, M., Morris, W., Alvarez, M. G., and Duffo, G. S. (2004). "Corrosion of reinforcing steel in simulated concrete pore solutions—Effect of carbonation and chloride content." *Corros. Sci.,* 46:2681–2699. DOI: 10.1016/j.corsci.2004.03.013.

Mullard, J.A. and Stewart, M.G. (2009). "Corrosion-Induced Cover Cracking of RC Structures: New Experimental Data and Predictive Models." Research Report No. 275.01.2009, Centre for Infrastructure Performance and Reliability, The University of Newcastle, NSW, Australia.

Neville, A. (1995). "Chloride attack of reinforced concrete: an overview." *Materials and Structures,* 28 (2):63-70. DOI: 10.1007/bf02473172.

Neville, A. M., and Brooks, J. J. (2002). *Concrete Technology,* 2nd ed. Harlow: Pearson.

NT BUILD 355 (1997). "Concrete, mortar and cement-based repair materials: Chloride diffusion coefficient from migration cell experiments," Ed. 2, Nordtest, Espoo, Finland.

NT BUILD 492 (1999). "Concrete, Mortar and Cement Based Repair Materials: Chloride Migration Coefficient from Non-Steady State Migration Experiments." NORDTEST, Finland.

OVBB-Richtlinie (2003). "Enhaltung und Instandsetzung Von Bauten aus Beton und Stahlbeton." Austrian Society for Construction Technology, Austria. (in german)

Palumbo, N. (1991). "Accelerated Corrosion Testing of Steel Reinforcement in Concrete." M. Engg. thesis in Civil Engineering, Departrnent of Civil Engineering and Applied Mechanics, McGill University.

Polder, R. B. (2001). "Test Methods for on Site Measurement of Resistivity of Concrete-a RILEM TC 154 Technical Recommendation." *Construction and Building Materials,* 15(2001):125-131.

Pradhan, B. and Bhattacharjee, B., (2009). ""Half-Cell Potential as an Indicator of Chloride-Induced Rebar Corrosion Initiation in RC. *Journal of Materials in Civil Engineering,* 21(10):543-552.

Presuel-Moreno, F. (2013). *Analysis and Estimation of Service Life of Corrosion Prevention Materials Using Diffusion, Resistivity and Accelerated Curing for New Bridge Structures.* Tallahassee, Florida: Florida Department of Transportation Research Center.

Rasheeduzzafar, Al-Saadoun, S. S., & Al-Gahtani, A. S. (1992). "Corrosion Cracking in Relation to Bar Diameter, Cover, and Concrete Quality." *Journal of Materials in Civil Engineering,* 4(4):327-342. DOI: 10.1061/(asce)0899-1561(1992)4:4(327).

Real, S., Bogas, J.A., and Ferrer, B. (2017). "Service Life of Reinforced Structural Lightweight Aggregate Concrete Under Chloride Induced Corrosion." *Materials and Structures,* 50:101.

Recommendations of RILEM TC 154-EMC: Electrochemical techniques for measuring metallic corrosion (2000). "Test Methods for on Site Measurement of Resistivity of Concrete." *Materials and Structures,* 33:603-611.

Rosenberg, A., Hansson, C., and Andrade, C. (1989). "Mechanisms of corrosion of steel in concrete." *Materials science of concrete I*, J. P. Skalny, ed. Westerville, Ohio: The American Ceramic Society. 285–313p.

Rumman, R., Kamal, M. R., Manzur, T., and Noor, M. A. (2015). "Durability Performance of Locally Produced OPC and PCC Cement Concretes." International Conference on Recent Innovation in Civil Engineering for Sustainable Development. DOI: 10.13140/RG.2.1.2463.1128.

Samson, E., Marchand, J. and Snyder, K. A. (2003). "Calculation of ionic diffusion coefficients on the basis of migration test results." *Materials and Structures,* 36:156-165.

Sengul, O. (2014). "Use of Electrical Resistivity as an indicator for durability," *Cons. And Build. Mater.* 73: 434-441.

Sindelar, R. L., Duncan, A. J., Dupont, M. E., Lam, P.-S., Louthan, M. R., and Skidmore, J. T. E. (2011). "Materials aging issues and aging management for extended storage and transportation of spent nuclear fuel." *NUREG/CR-7116, SRNL-STI-2011-00005,* Savannah River National Laboratory, Aiken, SC.

Song, H. –W., and Saraswathy, V. (2007). "Corrosion Monitoring Reinforced Concrete Structures- A Review." *International Journal of Electrochemical Science,* 2(2007):1-28.

Smith, C. O. (1977). "Effects of environment," Chapter 13. *The science of engineering materials,* 2nd ed. Englewood Cliffs, N.J.: Prentice-Hall.

Stanish, K. D., Hooton, R. D., and Thomas, M. D. A. (1997). *Testing the chloride penetration resistance of concrete: A literature review.* DTFH61-97-R-00022, Toronto, ON, Canada: Univ. of Toronto, Canada.

Tuutti, K. (1982). *Corrosion of steel in concrete,* Stockholm: Swedish Cement and Concrete Research Institute, 469 pp.

Tuutti, K. (1993). The effect of individual parameters on chloride induced corrosion. In L.-O. Nilsson (Ed.), Chloride Penetration Into Concrete Structures (pp. 18–25). G¨oteborg, Sweden.

Tuutti, K. (1980). "Service life of structures with regard to corrosion of embedded steel," *Performance of Concrete in Marine Environment, ACI SP-65.* Detroit, Michigan: American Concrete Institute. p. 223-236.

Verbeck, G. J. (1975). "Mechanisms of Corrosion in Concrete." *In Corrosion of metals in concrete, ACI SP-49.* Detroit, Michigan: American Concrete Institute, p. 21-28.

Verma, S. K., Bhadauria, S. S., and Akhtar, S. (2014). "Monitoring Corrosion of Steel Bars in Reinforced Concrete Structures." *The Scientific World Journal*, 2014:1-9. DOI: 10.1155/2014/957904.

Wang, X., Nguyen, M., Stewart, M.G., Syme, M. and Leitch, A. (2010). "Analysis of Climate Change Impacts on the Deterioration of Concrete Infrastructure – Part 1: Mechanisms, Practices, Modelling and Simulations – A review." *CSIRO,* Canberra.

Webster, P. M. (2000). "The assessment of corrosion-damaged concrete structures." Ph.D. thesis, School of Civil Engineering, Univ. of Birmingham, Birmingham, U.K.

Wenner, F. (1915). ''A method of measuring earth resistivity.'' *Journal of the Franklin Institute,* 180(3), 373-375. DOI: 10.1016/s0016-0032(15)90298-3.

Yoon, I.-S., Copuroglu, O., and Park, K.-B. (2007). "Effect of global climatic change on carbonation progress of concrete." *Atmos. Environ.*, 41(34):7274–7285. DOI: 10.1016/j.atmosenv.2007.05.028.

Yunovich, M., Thompson, N. G., Balvanyos, T., and Lave, L. (2002). "Highway Bridges, Appendix D, Corrosion Cost and Preventive Strategies in the United States," by G.H. Koch, M. H. Broongers, N.G. Thompson, Y.P. Virmani, and J.H. Payer." *FHWA-RD-01-156,* McLean, VA.

Zhou, Y., Gencturk, B., Willam, K. and Attar, A., (2015). "Carbonation-Induced and Chloride-Induced Corrosion in Reinforced Concrete Structures." *Journal of Materials in Civil Engineering,* 27(9).